UNIVERSITY OF CALIFORNIA
RIVERSIDE

Biogeochemistry of Carbon Dynamics in Furrow Irrigated Soils

A Dissertation submitted in partial satisfaction
of the requirements for the degree of

Doctor of Philosophy

in

Environmental Sciences

by

Claudia Christine Escobar Avila

September 2021

Dissertation Committee:
Dr. Samantha Ying, Chairperson
Dr. Peter Homyak
Dr. Ying-Hsuan Lin

The Dissertation of Claudia Christine Escobar Avila is approved:

_____

_____

_____

Committee Chairperson

University of California, Riverside

Acknowledgements

I would like to thank the following scientists for assisting in the technical aspects of this work, very notably Dr. Ying Lin (UCR Environmental Dynamics and GeoEcology, EDGE Institute), Alyssa Duro, Abdi Garniwan, Michael Schaefer, Thomas Haensel, Aral Greene, Benjamin Maki, Danielle Stevenson, Miranda Aiken, Macon Abernathy, Eric Dubinsky, Holly Andrews, Darrel Jenerette, Robert Johnson, David Lyons (UCR Environmental Sciences Research Lab), Dr. Alexander Frie-Vliet, Dr. Marilyn Fogel, and each member of the dissertation committee, Dr. Peter Homyak, Dr. Ying-Hsuan Lin, and Dr. Samantha Ying.

Funding sources for this work include the UCR Department of Environmental Sciences, the Eugene Cota Robles Fellowship, the University of California Office of the President Research Catalyst Award, the Hilda and George Liebig Fellowship, and the Frank T. Bingham Memorial Fellowship in Soil Science.

Dedication

I would like to thank the countless family, friends, and programs that encouraged, supported, and allowed me to be in a position to pursue this degree. First, I'd like to thank the Adolfo's. The first is my wonderful husband, Adolfo Avila, whom has been the love of my life for the past 13 years. Adolfo has always been the voice of encouragement, who helped me get through the lows and helped in celebrating the highs these past 6 years. If it was not for his love, his comedic genius, and his support, I am very certain that I would not have made it. He is an amazing father and gave me the most beautiful and precious gift, our son, Adolfo Valentín Avila. I may not have started this journey with him, but I am most definitely finishing this for him. My curious and kind child, Valentín, *eres mi vida y mi alegria.*

I'd like to also thank the past, current, and extended members of the Dirty Lab. I feel so fortunate to have been surrounded by wonderful lab mates that made our lab feel like a family—from the beers to the babysitting. I love and appreciate every single one of you. I'd like to especially thank my wonderful friend and lab mate, Miranda Aiken, for her frequent lovely meals, treats, and babysitting that she has done for my family, most notably the assistance she has provided us the past two years. The Avila's are forever in her debt. Next, I'd like to thank the wonderful Herr Frau Professor Dr. Samantha Ying, who holds a B.S., B.S., and PhD from The Stanford. Sam is my advisor, mentor, and friend, and over the past six years, has helped shape me as a mother and scientist. She helped build my confidence and gave me the necessary tools to use my voice and pursue the things that I

didn't think were possible. As a mother, I am so appreciative of the wisdom, encouragement, and the times that Sam has said "go mama" and "I will take baby."

And lastly, I'd like to thank the many family members that have celebrated me and been my guiding light my entire life. My mamá, Margarita Escobar, who taught me to work hard and to apply myself, and my brothers, Chris, Alex, and Kenny for being the first group of people to recognize that I was a major nerd and for making a point to let me know that I was and am smarter than them. I'd like to also thank my cousin Ana, who has been a sister to me my whole life and whose family is so close to ours, Lou, Janine and Sergio—you all mean so much to me. You all center me and remind me that life with family is what matters. To the rest of my large and wonderful families, my ancestors that forged this path, and those that we will be blessed with in the future, the Escobar's, Marin's, Avila's, Rivera's, Mulari's, Rodriguez's, Reveles', Ruiz's—*gracias*!

ABSTRACT OF THE DISSERTATION

Biogeochemistry of Carbon Dynamics in Furrow Irrigated Soils

by

Claudia Christine Escobar Avila

Doctor of Philosophy, Graduate Program in Environmental Sciences
University of California, Riverside, September 2021
Dr. Samantha Ying, Chairperson

Drying-rewetting cycles are ubiquitous across natural and managed ecosystems. These cycles are known to mobilize carbon (C) in soils producing dramatic pulses in microbial respiration. While many factors contribute to these pulses, how the drying-rewetting history of soils affects these emissions remains unclear, especially in irrigated soils where soil moisture fluctuations are much more repetitive than natural, seasonally influenced soils, and where the volume of soil that water dominates is on much smaller spatiotemporal scales.

To understand the controls of repeated wet-up and dry-down effects on agricultural soils, in the first study, we took a systems-level approach to examine the cross section of a furrow irrigated orchard in a semi-arid Mediterranean climate to delineate the C dynamics in the two contrasting regions of water availability: in furrows used to deliver water to tree crops where soils are temporarily but repeatedly inundated versus in berms where trees

are planted and soils only receive water during infrequent rain events. Overall, our findings show that the high degree of heterogeneity in soil moisture across the landscape of a furrow-irrigated field results in contrasting gaseous release of C as CO_2, microbial selectivity of substrates, and dominant mechanisms for C stabilization.

In the same heterogenous landscape, we characterized the temporal variation in composition and concentration of soil C pools over the course of a year. We found that within this timeframe, soils that are typically dry but have large amount of litter and root inputs did not vary significantly in total C concentrations but exhibited increase in the active C pool after seasonal rain events. We also found that sustained anoxic conditions that dominate furrow soils throughout the year limit decomposition, regardless of season. The seasonal trends captured in this study can inform ecological models of semi-arid irrigated soils to better predict C sequestration.

Lastly, in the third study, we estimated the potential changes to CO_2 flux and soluble C chemistry if a legacy furrow-irrigated soil was converted to precision irrigation, hypothesizing that large releases of C would occur when lower-volume irrigation method is adopted. However, we found that low-volume irrigation leads to water limitations that inhibit CO_2 pulse release from berm soils.

Table of Contents

List of Figures

List of Tables

List of Equations

Chapter 1: Introduction to Carbon Dynamics in Managed Soils

1.1 California agriculture and current threats

California is a global producer of fruits, vegetables, and nuts, with more than a quarter of the state considered farmland. With a profit of $50.1 billion in 2019, California remains the number one producer in the United States far exceeding all other states with nearly half of revenue generated from exports (California Department of Food and Agriculture 2020). The combined factors of the wide range of ecosystems, lengthened growing seasons, and water import infrastructure in California has allowed the state to prosper in the agricultural industry. Any challenges affecting the state's agricultural sector can impact global food security as California dominates many crop and livestock commodities and is the sole producer of over a dozen fruits, vegetables, and nuts.

The effects of climate change are a potential threat to California's economy, where recurring and extended droughts in recent decades have negatively impacted agricultural production (Howitt et al. 2015), which are expected to not only increase in frequency, but in intensity (Marvel et al. 2019). Many growers have responded to limited and uncertain water resources by switching methods of irrigation, which has also been encouraged by and incentivized by policymakers (California Natural Resources Agency 2021). Across the United States, irrigation accounted for over a third of total water withdrawals, with more than half of that water being applied as surface irrigation, while only accounting for 37% of the total irrigated land acreage (Maupin 2018). In California, it is estimated that anywhere between 40-80 % of water used is for irrigation, where a total of 9 million acres

of croplands depends on irrigation (Dieter et al. 2018; Painter et al. 2021). In the Colorado River and South Coast watersheds of California, which are predominantly surface irrigated, a shift towards more precise, water-saving irrigation methods (i.e. drip and micro-sprinkler irrigation) have been observed (Johnson and Cody 2015). The decision to make these shifts in irrigation method, although beneficial in terms of water savings, typically do not consider biogeochemical processes that occur in soils which have the potential to have lasting effect on soil carbon (C) and overall soil health.

1.2 Importance of soil carbon

Soil C is an important component of productive and natural landscapes. Increased soil C is a proxy for "soil health" with benefits including improved soil structure, increased nutrient cycling, increased microbial diversity, and reduced erosion (Lal 1997; Quinton et al. 2010; Reicosky 2003; Lal 2004). Soils have historically been overlooked as a resource to mitigate climate change, though it is the largest terrestrial C sink. It is estimated that managed lands have the highest potential to increase soil C stocks (Chen et al. 2019) and this is largely dependent on how soils are managed. Efforts to estimate the societal value of sequestering soil organic C (SOC) found that the value (or cost if removed from soil) is \$0.133 USD kg^{-1} (Lal 2014)—where soils in North America are estimated to have lost 20 – 75% of their original SOC stock through conversion to agricultural lands (Lajtha et al. 2018), which can be further degraded if agricultural soils are mismanaged (Lal 2004).

1.3 Soil carbon and water

Soils are very complex media where minerals, microbes, organic matter, and water interact. The addition of water to previously dry soils catalyzes the well-documented "Birch effect", where C is lost as CO_2 as microbial communities metabolize available substrate (Birch 1958). Understanding and predicting the magnitude and duration of the Birch effect varies widely across ecosystems but it is well understood that as dry soils are wet up, carbon is lost. This process is termed C mineralization or soil organic matter (SOM) decomposition, where available organic C substrates are oxidized by microbes and released as CO_2.

The mechanisms that can affect SOM mineralization include severity and length of the dry period both of which impact the rate of microbial turnover (Fierer and Schimel 2002; Lundquist, Jackson, and Scow 1999), microbial access to substrates as a function of pore connectivity (Lopez-Sangil et al. 2018; Xiang et al. 2008), and disruption of soil aggregates which can release of previously occluded SOM (Lopez-Sangil et al. 2018; Lundquist, Jackson, and Scow 1999; Xiang et al. 2008). The master variable controlling the extent to which each of these mechanisms are at play in the soil matrix is soil moisture content.

The C cycle is largely controlled by microbially-mediated processes. Soil organic C that enters soil systems as large complex polymers must first be cleaved into smaller monomers before microbes can metabolize them (Fenchel, Blackburn, and King 2012). Exoenzymes produced and excreted by microbes can aid in this rate-limiting step toward C mineralization; however, mineral-associations can prevent enzymatic degradation of

organic C compounds, leading to an accumulation of SOC. The physical and chemical limitations in terrestrial ecosystems make bacterial metabolisms particularly dependent on the presence of liquid water, where activity is frequently limited to aqueous films (Fenchel, Blackburn, and King 2012). Under water stress conditions, bacteria can produce spores or cysts as anti-desiccation measures to prevent cell lysis. Fungi, on the other hand, can be active in gas-filled pore spaces and can decompose complex polymers even when bacteria are inactive to due water limitations.

In addition to the need for liquid water for most microbial activity, the redox status of the soil solution also limits metabolisms at play. Microbial communities have been observed to shift as redox status fluctuates, showing distinct molecular profiles of physiologies of the microbial communities better suited to each soil condition (Pett-Ridge and Firestone 2005). Plasticity, or the ability of microbes to withstand and proceed with normal physiological processes under a wide spectrum of redox conditions is generally not the case in soil. The major metabolic pathways active in redox fluctuating soils are more often tolerant aerobes or anaerobes, which are competitive with the presence (aerobes) or absence (anaerobes) of O_2 and are inactive during periods when redox status is incompatible with their metabolic needs. Facultative organisms on the other hand are most competitive when redox conditions are not static. In agricultural soils, where redox status is driven by volume and frequency of precipitation and irrigation, and resultant drying and rewetting extents, can lead to divergent microbial communities in parts of the field that have contrasting soil moisture input.

Wet-dry cycles and their effect on soil carbon dynamics are often investigated in natural soils with prolonged wet and dry seasons such as in tropical soils. These extended wet and dry periods can lead to distinct reducing and oxidizing conditions that can influence multiple elemental cycles (e.g., Fe and C) (Thompson et al. 2018) and microbial metabolisms (DeAngelis et al. 2010) that can strongly influence carbon sequestration or release. The mineralizability, or how easily C can be transformed into a substrate for microbial respiration, is typically associated with the degree of mineral protection within the soil matrix (K. Kaiser and Guggenberger 2003). In soils with extended periods of low redox potential (E_h), the dissolution and reprecipitation of metal oxides such as Fe (oxyhydr)oxides and Al hydroxides can aid in the formation of mineral-organic complexes (Oades 1988) and slow soil organic carbon (SOC) turnover (Porras et al. 2017; Kögel-Knabner et al. 2008). However, in irrigated managed soils particularly within semi-arid landscapes, soil moisture oscillations can occur on smaller spatial and shorter temporal scales, where reduced species are not necessarily accumulating, and carbon sequestration mechanisms are dependent on management factors.

1.4 Assessing soil carbon dynamics

Previous studies have focused upon the resultant fate of C as CO_2 and/or methane emissions to describe overall carbon balance; however, the transformation of C between aqueous, solid, and gaseous phases in soil systems is not well understood. Chemical speciation of dissolved organic carbon in porewater and solid phase carbon associated with organo-mineral complexes are rarely coupled with gas phase measurements or are limited

in scope. Porewater C chemistry typically presented as total dissolved organic carbon (DOC) concentrations can provide helpful insight into the maximum potential aqueous carbon mass that can be respired or mineralized within a soil matrix. However, lack of information on aqueous and solid phase C speciation precludes characterization of the energetics of the system; the thermodynamic quality of available C for microbial respiration have not typically been accounted for in previous studies. Previous studies have mainly determined thermodynamic favorability of redox processes based upon the energetics of available terminal electron acceptors. For example, the energy gain from oxidizing a specific organic molecule using O_2 as an electron acceptor is greater than using SO_4^{2-} as electron acceptor, therefore favoring aerobic metabolisms in the presence of oxygen. However, recently an increasing number of studies are demonstrating the need to consider the thermodynamic quality of the electron donor, in this case the organic C substrate, as an additional threshold on whether it is thermodynamically favorable for an organic compound to be respired or preserved (Boye et al. 2017). The consideration of the nominal oxidation state of C (NOSC): $NOSC = 4 - (4C + H - 2O - 3N - 2S + 5P - z)/C$ (stoichiometry of each element in substrate) (LaRowe and Van Cappellen 2011) can lead to thermodynamic preservation of C if the NOSC value is below the thermodynamic limit of the soil solution in anoxic soils. In irrigated soils, the anaerobic periods are often short-lived, however, anaerobic microsites found in soil aggregates could exhibit the same thermodynamic preservation of C that could be a dominant pathway for C sequestration on the field scale (Keiluweit et al. 2017).

Recent studies on pore water chemistry have indicated that DOC composition, as opposed to DOC concentration, influences mineral-organic complex formation (Young et al. 2018). The DOC in solution can co-precipitate or adsorb onto mineral surfaces (Kaiser and Kalbitz 2012) but the assemblages are self-organized depending on functional groups, which can provide insight on the stability and microbial accessibility of organic compounds associated with mineral surfaces (Kleber, Sollins, and Sutton 2007). Previous work examining the soluble carbon species in pore water associated with a range of pore diameters showed that more complex C compounds (i.e., aromatic and condensed) are associated with finer pore throats (~20 μm diameter), while larger pore domains (~200 μm) are dominated by lipids, proteins, and carbohydrates. These findings add to the observation that when fine pore space is saturated, respiration increases, and C stabilization is largely dependent on microbial inaccessibility to fine pores (Bailey et al. 2017). Additionally, recent studies have shown that porewater chemistry analyses done on the same soil can be significantly different depending on whether the original soil structure is maintained or if the soils are homogenized; it was reported that dissolved organic C content is increased when pore networks are removed, showing a need to accurately characterize field conditions by maintaining soil structure (Smith et al. 2017).

Solid phase soil C characterization has focused primarily on determining total soil C (TC) content, SOC concentrations, and presence or concentration of humic and fulvic acids. While TC and SOC concentrations provide baseline information on soil C stock, how C is associated with mineral surfaces alters C turnover rates and, in that way, will change a soil's C storage capacity (Torn et al. 1997). Humic and fulvic fractions of C,

which were traditionally thought to be the recalcitrant C pools in soil, have been shown to be operationally defined and not necessarily indicators of stable C pools in soil (Lehmann and Kleber 2015; Schmidt et al. 2011). Chemical extractions used to measure humic and fulvic acid concentrations alters the soil matrix resulting in products that are not necessarily representative of native carbon species (Schmidt et al. 2011). Recent studies using C 1s near-edge X-ray absorption fine structure spectroscopy (C NEXAFS) on soil have shown to provide more accurate understanding of C chemistry via nondestructive techniques (Solomon et al. 2005). This method can provide information on C speciation (e.g., aromatic, phenolic, aliphatic, carboxyl and alkyl functional groups) on bulk and discrete fractions of soil, which can give information on the energetics required to use that C as an energy source and where that C is associating within different density or water stable aggregate fractions.

1.5 Drought and carbon management

An understanding of how the carbon cycle will change as water becomes more limiting in managed soils in semi-arid landscapes has large socio-economic implications (Howitt et al. 2015). The change in the volume, rate, and method of water application on agricultural soils can greatly influence the carbon budget. However, a multi-phase approach to characterize C dynamics in solid, aqueous, and gas phases as a function of irrigation method in managed semi-arid land has not previously been investigated.

In the greenbelt of Riverside, California, USA, furrow irrigation has been utilized and maintained on orange orchards for over a century, presenting a valuable opportunity

to examine long-term furrow irrigation on soil carbon biogeochemistry. A furrow irrigated orchard provides a single landscape with contrasting soil moisture environments where soils can be temporarily inundated within furrows, while water delivery to berms only occur during rainfall events (Figure 1.1). Typically, the methods of capturing carbon dynamics in this type of system include field scale measurements of soil gas flux, but inputs and transformations of C in aqueous and solid forms within the soil are not accounted for which fails to capture the heterogeneity of the landscape.

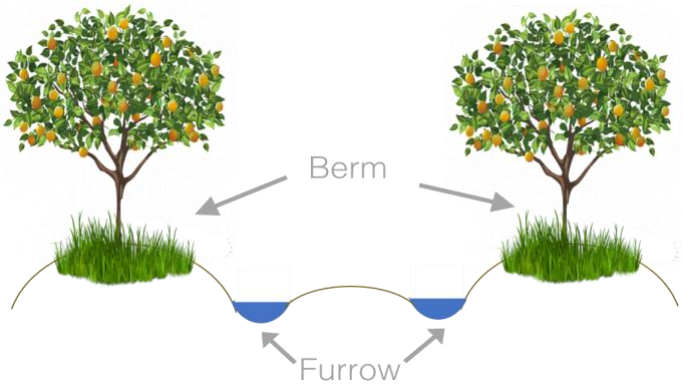

Figure 1.1: Simplified illustration of berm and furrow at field site.

Johnson et al. (2007) compiled the many opportunities in agricultural soil management to decrease greenhouse gas emissions but fails to associate any benefits or drawbacks to emissions based on irrigation method, which is an important land management decision. Previous investigations on C dynamics following wet-dry cycles in irrigated soils have been done on row crops, which present high variability to C flux due to high soil disturbance (Lundquist, Jackson, and Scow 1999). The drying and rewetting of irrigated agricultural soils have been shown to increase background levels of DOC by up to a 2.5-fold increase in field experiments. However, this DOC increase has not been

conclusively linked to subsequent increases in microbial respiration, which suggests that more stable C likely remains in the soil following repeated wet-dry cycles (Lundquist, Jackson, and Scow 1999). Under certain settings, the benefits of increased SOC can be negated by increased emissions, resulting in agricultural soil being GHG sources (Gao et al. 2018). How soil moisture fluctuations brought on by irrigation in semi-arid landscapes affect the C cycle have not previously been explored.

In Chapter 2, I describe a systems-level approach to characterizing C dynamics exhibited in a legacy furrow irrigated orchard, by exploring gaseous release of C as CO_2, solid phase chemistry, and aqueous C chemistry. In Chapter 3, I characterize the spatiotemporal variation in the solid phase of various C pools. And lastly, in Chapter 4, I explore the possible changes to C dynamics if furrow irrigated soils are switched to micro-sprinkler irrigation.

1.6 References

Bailey, V. L., A. P. Smith, M. Tfaily, S. J. Fansler, and B. Bond-Lamberty. 2017. "Differences in Soluble Organic Carbon Chemistry in Pore Waters Sampled from Different Pore Size Domains." *Soil Biology and Biochemistry* 107 (April): 133–43. https://doi.org/10.1016/j.soilbio.2016.11.025.

Birch, H. F. 1958. "The Effect of Soil Drying on Humus Decomposition and Nitrogen Availability." *Plant and Soil* 10 (1): 9–31. https://doi.org/10.1007/BF01343734.

Boye, Kristin, Vincent Noël, Malak M. Tfaily, Sharon E. Bone, Kenneth H. Williams, John R. Bargar, and Scott Fendorf. 2017. "Thermodynamically Controlled Preservation of Organic Carbon in Floodplains." *Nature Geoscience* 10 (6): 415–19. https://doi.org/10.1038/ngeo2940.

California Department of Food and Agriculture. 2020. "California Agricultural Statistics Review 2019-2020."

California Natural Resources Agency. 2021. "Report to the Legislature on the 2012-2016 Drought." March 2021. https://water.ca.gov/-/media/DWR-Website/Web-Pages/Water-Basics/Drought/Files/Publications-And-Reports/CNRA-Drought-Report-final-March-2021.pdf.

Chen, Songchao, Dominique Arrouays, Denis A. Angers, Manuel P. Martin, and Christian Walter. 2019. "Soil Carbon Stocks under Different Land Uses and the Applicability of the Soil Carbon Saturation Concept." *Soil and Tillage Research*, Soil Carbon and Climate Change: the 4 per Mille Initiative, 188 (May): 53–58. https://doi.org/10.1016/j.still.2018.11.001.

DeAngelis, Kristen M., Whendee L. Silver, Andrew W. Thompson, and Mary K. Firestone. 2010. "Microbial Communities Acclimate to Recurring Changes in Soil Redox Potential Status: Fluctuating Redox Microbial Communities." *Environmental Microbiology* 12 (12): 3137–49. https://doi.org/10.1111/j.1462-2920.2010.02286.x.

Dieter, Cheryl A., Molly A. Maupin, Rodney R. Caldwell, Melissa A. Harris, Tamara I. Ivahnenko, John K. Lovelace, Nancy L. Barber, and Kristin S. Linsey. 2018. "Estimated Use of Water in the United States in 2015." USGS Numbered Series 1441. Circular. Reston, VA: U.S. Geological Survey. http://pubs.er.usgs.gov/publication/cir1441.

Fenchel, Tom, Henry Blackburn, and Gary M. King. 2012. *Bacterial Biogeochemistry: The Ecophysiology of Mineral Cycling*. Academic Press.

Fierer, Noah, and Joshua P. Schimel. 2002. “Effects of Drying–Rewetting Frequency on Soil Carbon and Nitrogen Transformations.” *Soil Biology and Biochemistry* 34 (6): 777–87. https://doi.org/10.1016/S0038-0717(02)00007-X.

Gao, Bing, Tao Huang, Xiaotang Ju, Baojing Gu, Wei Huang, Lilai Xu, Robert M. Rees, David S. Powlson, Pete Smith, and Shenghui Cui. 2018. “Chinese Cropping Systems Are a Net Source of Greenhouse Gases despite Soil Carbon Sequestration.” *Global Change Biology* 24 (12): 5590–5606. https://doi.org/10.1111/gcb.14425.

Howitt, Richard, Duncan MacEwan, Josué Medellín-Azuara, Jay Lund, and Daniel Sumner. 2015. “Economic Analysis of the 2015 Drought For California Agriculture,” August, 31.

Johnson, Jane M. -F., Alan J. Franzluebbers, Sharon Lachnicht Weyers, and Donald C. Reicosky. 2007. “Agricultural Opportunities to Mitigate Greenhouse Gas Emissions.” *Environmental Pollution* 150 (1): 107–24. https://doi.org/10.1016/j.envpol.2007.06.030.

Johnson, Renée, and Betsy A Cody. 2015. “California Agricultural Production and Irrigated Water Use,” June, 28.

Kaiser, K., and G. Guggenberger. 2003. “Mineral Surfaces and Soil Organic Matter.” *European Journal of Soil Science* 54 (2): 219–36. https://doi.org/10.1046/j.1365-2389.2003.00544.x.

Kaiser, Klaus, and Karsten Kalbitz. 2012. “Cycling Downwards – Dissolved Organic Matter in Soils.” *Soil Biology and Biochemistry* 52 (September): 29–32. https://doi.org/10.1016/j.soilbio.2012.04.002.

Keiluweit, Marco, Tom Wanzek, Markus Kleber, Peter Nico, and Scott Fendorf. 2017. “Anaerobic Microsites Have an Unaccounted Role in Soil Carbon Stabilization.” *Nature Communications* 8 (1): 1771. https://doi.org/10.1038/s41467-017-01406-6.

Kleber, M., P. Sollins, and R. Sutton. 2007. “A Conceptual Model of Organo-Mineral Interactions in Soils: Self-Assembly of Organic Molecular Fragments into Zonal Structures on Mineral Surfaces.” *Biogeochemistry* 85 (1): 9–24. https://doi.org/10.1007/s10533-007-9103-5.

Kögel-Knabner, Ingrid, Georg Guggenberger, Markus Kleber, Ellen Kandeler, Karsten Kalbitz, Stefan Scheu, Karin Eusterhues, and Peter Leinweber. 2008. “Organo-Mineral Associations in Temperate Soils: Integrating Biology, Mineralogy, and Organic Matter Chemistry.” *Journal of Plant Nutrition and Soil Science* 171 (1): 61–82. https://doi.org/10.1002/jpln.200700048.

Lajtha, Kate, Vanessa Bailey, Karis Mcfarlane, Kieth Paustian, Dominique Bachelet, Rose Abramoff, Denis Angers, et al. 2018. *Chapter 12: Soils. In Second State of the Carbon Cycle Report (SOCCR2): A Sustained Assessment Report.* https://doi.org/10.7930/SOCCR2.2018.Ch12.

Lal, R. 1997. "Residue Management, Conservation Tillage and Soil Restoration for Mitigating Greenhouse Effect by CO2-Enrichment." *Soil and Tillage Research*, XIVth ISTRO Conference on Agroecological and Economical Aspects of Soil Tillage, 43 (1): 81–107. https://doi.org/10.1016/S0167-1987(97)00036-6.

———. 2004. "Soil Carbon Sequestration Impacts on Global Climate Change and Food Security." *Science* 304 (5677): 1623–27. https://doi.org/10.1126/science.1097396.

———. 2014. "Societal Value of Soil Carbon." *Journal of Soil and Water Conservation* 69 (6): 186A-192A. https://doi.org/10.2489/jswc.69.6.186A.

LaRowe, Douglas E., and Philippe Van Cappellen. 2011. "Degradation of Natural Organic Matter: A Thermodynamic Analysis." *Geochimica et Cosmochimica Acta* 75 (8): 2030–42. https://doi.org/10.1016/j.gca.2011.01.020.

Lehmann, Johannes, and Markus Kleber. 2015. "The Contentious Nature of Soil Organic Matter." *Nature* 528 (7580): 60–68. https://doi.org/10.1038/nature16069.

Lopez-Sangil, Luis, Iain Hartley, Pere Rovira, Pere Casals, and Emma J. Sayer. 2018. "Drying and Rewetting Conditions Differentially Affect the Mineralization of Fresh Plant Litter and Extant Soil Organic Matter." June 7, 2018. https://doi.org/10.1016/j.soilbio.2018.06.001.

Lundquist, E. J, L. E Jackson, and K. M Scow. 1999. "Wet–Dry Cycles Affect Dissolved Organic Carbon in Two California Agricultural Soils." *Soil Biology and Biochemistry* 31 (7): 1031–38. https://doi.org/10.1016/S0038-0717(99)00017-6.

Marvel, Kate, Benjamin I. Cook, Céline J. W. Bonfils, Paul J. Durack, Jason E. Smerdon, and A. Park Williams. 2019. "Twentieth-Century Hydroclimate Changes Consistent with Human Influence." *Nature* 569 (7754): 59–65. https://doi.org/10.1038/s41586-019-1149-8.

Maupin, Molly A. 2018. "Summary of Estimated Water Use in the United States in 2015," June, 2.

Painter, Jaime A., Justin T. Brandt, Rodney R. Caldwell, Jonathan V. Haynes, and Amy L. Read. 2021. "Documentation of Methods and Inventory of Irrigation Information Collected for the 2015 U.S. Geological Survey Estimated Use of Water in the United States." USGS Numbered Series 2020–5139. *Documentation of Methods*

and Inventory of Irrigation Information Collected for the 2015 U.S. Geological Survey Estimated Use of Water in the United States. Vol. 2020–5139. Scientific Investigations Report. Reston, VA: U.S. Geological Survey. https://doi.org/10.3133/sir20205139.

Pett-Ridge, J., and M. K. Firestone. 2005. "Redox Fluctuation Structures Microbial Communities in a Wet Tropical Soil." *Appl. Environ. Microbiol.* 71 (11): 6998–7007. https://doi.org/10.1128/AEM.71.11.6998-7007.2005.

Porras, Rachel C., Caitlin E. Hicks Pries, Karis J. McFarlane, Paul J. Hanson, and Margaret S. Torn. 2017. "Association with Pedogenic Iron and Aluminum: Effects on Soil Organic Carbon Storage and Stability in Four Temperate Forest Soils." *Biogeochemistry* 133 (3): 333–45. https://doi.org/10.1007/s10533-017-0337-6.

Quinton, John N., Gerard Govers, Kristof Van Oost, and Richard D. Bardgett. 2010. "The Impact of Agricultural Soil Erosion on Biogeochemical Cycling." *Nature Geoscience* 3 (5): 311–14. https://doi.org/10.1038/ngeo838.

Reicosky, D. C. 2003. "Conservation Agriculture: Global Environmental Benefits of Soil Carbon Management." In *Conservation Agriculture: Environment, Farmers Experiences, Innovations, Socio-Economy, Policy*, edited by Luis García-Torres, José Benites, Armando Martínez-Vilela, and Antonio Holgado-Cabrera, 3–12. Dordrecht: Springer Netherlands. https://doi.org/10.1007/978-94-017-1143-2_1.

Schmidt, Michael WI, Margaret S. Torn, Samuel Abiven, Thorsten Dittmar, Georg Guggenberger, Ivan A. Janssens, Markus Kleber, et al. 2011. "Persistence of Soil Organic Matter as an Ecosystem Property." *Nature* 478 (7367): 49–56.

Smith, A. Peyton, Ben Bond-Lamberty, Brian W. Benscoter, Malak M. Tfaily, C. Ross Hinkle, Chongxuan Liu, and Vanessa L. Bailey. 2017. "Shifts in Pore Connectivity from Precipitation versus Groundwater Rewetting Increases Soil Carbon Loss after Drought." *Nature Communications* 8 (1): 1335. https://doi.org/10.1038/s41467-017-01320-x.

Solomon, Dawit, Johannes Lehmann, James Kinyangi, Biqing Liang, and Thorsten Schäfer. 2005. "Carbon K-Edge NEXAFS and FTIR-ATR Spectroscopic Investigation of Organic Carbon Speciation in Soils." *Soil Science Society of America Journal* 69 (1): 107. https://doi.org/10.2136/sssaj2005.0107dup.

Thompson, Aaron, Diego Barcellos, Christine O'Connell, Whendee L. Silver, and Christof Meile. 2018. "Hot Spots and Hot Moments of Soil Moisture Explain Fluctuations in Iron and Carbon Cycling in a Humid Tropical Forest Soil." November 1, 2018. https://www.mdpi.com/2571-8789/2/4/59.

Torn, Margaret S., Susan E. Trumbore, Oliver A. Chadwick, Peter M. Vitousek, and David M. Hendricks. 1997. "Mineral Control of Soil Organic Carbon Storage and Turnover." *Nature* 389 (6647): 170–73. https://doi.org/10.1038/38260.

Xiang, Shu-Rong, Allen Doyle, Patricia A. Holden, and Joshua P. Schimel. 2008. "Drying and Rewetting Effects on C and N Mineralization and Microbial Activity in Surface and Subsurface California Grassland Soils." *Soil Biology and Biochemistry* 40 (9): 2281–89. https://doi.org/10.1016/j.soilbio.2008.05.004.

Young, Robert, Shani Avneri-Katz, Amy McKenna, Huan Chen, William Bahureksa, Tamara Polubesova, Benny Chefetz, and Thomas Borch. 2018. "Composition-Dependent Sorptive Fractionation of Anthropogenic Dissolved Organic Matter by Fe(III)-Montmorillonite." *Soil Systems* 2 (14). https://www.mdpi.com/2571-8789/2/1/14/htm.

Chapter 2: A Multi-Phase Approach to Characterizing Carbon Dynamics as a Function of Soil Moisture Within a Semi-Arid Furrow Irrigated Orchard

2.0 Abstract

Drying-rewetting cycles are ubiquitous across natural and managed ecosystems. These cycles are known to mobilize C in soils producing dramatic pulses in microbial respiration. While many factors contribute to these pulses, how the drying-rewetting history of soils affects these emissions remains unclear, especially in irrigated soils where soil moisture fluctuations are much more repetitive than natural, seasonally influenced soils, and where water dominates much smaller spatiotemporal scales. To understand the controls of repeated wet-up and dry down effects on agricultural soils, we took a systems-level approach to examine the cross section of a furrow irrigated orchard to delineate the C dynamics in the two contrasting regions of water availability, where soils can be temporarily but repeatedly inundated where water is delivered (i.e., furrows) while the base of trees (i.e., berms) only receive water during rainfall events in a semi-arid Mediterranean climate. Overall, our findings show that the highly heterogenous landscape of a furrow irrigated field results in differences in gaseous release of C as CO_2, microbial selectivity of substrates, and mechanisms for C stabilization. By monitoring soil moisture as a function of depth for over two years, our results reveal that furrow soils undergo dramatic wet-dry cycles, while moisture within the berm is relatively constant. We were able to capture the contrasting response to soil moisture changes within the furrow and berm soils by continuously monitoring CO_2 flux throughout water input events. Carbon respiration results show that berm soils are soil moisture limited, where maximum flux is achieved

after rainfall events, while CO_2 flux is suppressed within furrows upon irrigation and highest CO_2 flux results upon drying. Solid phase soil C speciation determined by C 1s NEXAFS demonstrated C of higher aromaticity remained in furrow soil as compared to berm soils. Microbial community analysis shows significantly different communities reside within berm and furrow soils, where furrow soils support more anaerobic metabolisms and spore-formers while berm soils have relatively higher abundance of aerobic microbes capable of degrading larger, more complex C compounds. Porewater C chemistry Our findings show that the types of water input and rewetting history can greatly differentiate C respiration within managed soils.

2.1 Introduction

Drying-rewetting cycles are very common across natural and managed ecosystems. It has been well documented that as soils wet up, a sudden pulse of C mineralization (i.e., Birch effect) occurs due to a combination of physical, chemical, and biological processes. However, many studies that have coupled the effects of wet-dry cycles on soil carbon dynamics focused upon natural landscapes with prolonged wet and/or dry seasons, such as in tropical forests (Brown and Lugo 1982; Bhattacharyya et al. 2018) or in desert ecosystems (Cable and Huxman 2004; Schimel 2018). In natural ecosystems, wet and dry periods can fluctuate over large spatiotemporal scales, where extended wet and dry periods can lead to distinct oxic and anoxic conditions that can simultaneously influence multiple elemental cycles (e.g., Fe and C) (Thompson et al. 2018; Zhao et al. 2020) and microbial metabolisms (DeAngelis et al. 2010; Kakumanu, Ma, and Williams 2019; Pérez Castro et

al. 2019). Unlike natural landscapes, however, soil moisture oscillations in irrigated managed soils, particularly within semi-arid landscapes, usually occur on much smaller spatiotemporal scales. In these ecosystems, the boundaries where irrigation water is or isn't applied can lead to a highly heterogenous landscape where carbon sequestration is dependent on management factors. The drying and rewetting of irrigated agricultural soils have been shown to increase background levels of dissolved organic carbon (DOC) by up to a 2.5-fold increase in field experiments (Lundquist, Jackson, and Scow 1999). However, this DOC increase has not been conclusively linked to subsequent increases in microbial respiration, which suggests that more stable C likely remains in the soil following repeated wet-dry conditions present in irrigated soils (Lundquist, Jackson, and Scow 1999; Guo et al. 2014).

Some of the mechanisms that can account for this release in C as soils wet up is due increased accessibility of organic C to microbes within smaller pores (Lopez-Sangil et al. 2018; Xiang et al. 2008), mineralization of microbial necromass that has been accumulated during the dry period (Fierer and Schimel 2002; Lundquist, Jackson, and Scow 1999), and activation of exoenzymes (Schimel and Weintraub 2003). However, aside from the need to co-locate microbial communities and their carbon food sources to result in observable C mineralization during soil wet up, the magnitude of C mineralization is partially determined by carbon quality. Pore-water C chemistry typically presented as dissolved organic carbon (DOC) concentrations can provide helpful insight into the maximum potential aqueous carbon mass that can be respired or mineralized within a soil matrix. However, an increasing number of studies have demonstrated that assessing the organic carbon

composition informs the thermodynamic favorability of a carbon substrate when assessing C mineralizability, as an additional threshold on whether it is energetically favorable for an organic compound to be respired or preserved (LaRowe and Van Cappellen 2011; Boye et al. 2017). These studies demonstrate the need to characterize not only the quantity of C present in soil, but the quality of the C that could be used to fuel microbial respiration. Simultaneously, the carbon that is not respired and remains in soil is determined in part by the conditions that favor aerobic versus anaerobic respiration.

How easily soil organic carbon (SOC) can be transformed into a substrate for microbial respiration is typically associated with the degree of mineral protection within the soil matrix (K. Kaiser and Guggenberger 2003; Torn et al. 1997a; Jastrow 1996). For example, soils with extended periods of low redox potential (E_h) can lead to the dissolution and reprecipitation of metal oxides such as Fe (oxyhydr)oxides and Al hydroxides which can form mineral-organic complexes (Oades 1988) and inhibit SOC turnover (Porras et al. 2017; Kögel-Knabner et al. 2008). However, in irrigated soils, reduced species are likely not accumulating to the degree that would give rise to a stabilization pathway for organic C. In agricultural soils, wet-dry cycles induced by irrigation can influence the water stable aggregate fractions, where increased aggregate stability is preferred for water infiltration, reduced soil erosion, and root growth. Slaking, which occurs as aggregates are destabilized, can contribute to large pulses of labile substrates that can then be metabolized by microbes (Navarro-García, Casermeiro, and Schimel 2012).

Increasingly, researchers examining soil C dynamics conclude that there is a need to evaluate dominant controls on C mineralization using an integrated systems approach to

evaluate the contribution of biological, chemical and physical processes simultaneously (Bailey et al. 2017; Homyak et al. 2018). To do this, it is necessary to characterize C flux dynamics, aqueous and solid phase C dynamics, water flow and transport, and microbial community composition at the same time. This approach provides a framework to build integrated mechanistic models that can complement larger scale studies.

Previous investigations following wet-dry cycles in irrigated soils have been performed on row crops, which present high variability to C flux due to frequent soil disturbances (Lundquist, Jackson, and Scow 1999; Kallenbach, Rolston, and Horwath 2010). Under certain settings, the benefits of increased SOC can be negated by increased emissions, resulting in agricultural soil being GHG sources (Gao et al. 2018). In sum, the effects of irrigation-induced soil moisture fluctuations in semi-arid landscapes on soil C is not fully understood. In this study, we ask 1) how does rewetting history influence C release in managed semi-arid landscapes? 2) Where and how is C associating within the soil matrix under repeated drying-rewetting? And 3) how are microbial community compositions shaped by available substrate?

In the Greenbelt of Riverside, CA, furrow irrigation has been utilized and maintained on orange orchards for over a century, presenting a valuable opportunity to examine long-term effects of wet-dry cycling furrow irrigation on soil carbon biogeochemistry. A furrow irrigated orchard provides a single landscape with contrasting soil moisture environments where soils can be temporarily inundated within furrows, while water delivery to berms only occurs during rainfall events. Typically, the methods used to characterize carbon dynamics in this type of system include field-scale measurements of

soil gas flux, but C inputs and transformation in aqueous and solid phases within the soil matrix are not necessarily accounted for and fail to capture the heterogeneous biogeochemical processes at play across the landscape. Here we used a multi-phase approach to unravel the dominant mechanisms that determine how C is transformed in soils with contrasting soil moisture regimes.

2.2 Materials and Methods

2.2.1 Field description

Field measurements were performed, and samples were taken from a furrow irrigated orange grove located in the Greenbelt region of Riverside, CA, USA (33.9086 N, 117.4295 W). This historic orchard has been in operation since circa 1915 and has maintained furrow irrigation, as this is the typical irrigation strategy of the region. Approximately 400 Washington navel orange trees are planted within 4 acres of the property. The soil at the grove is a coarse-loamy, mixed, active, thermic Haplic Durixeralfs (surface pH 7.0, < 1% $CaCO_3$, 1 dS/m EC). The climate is semi-arid (BSh) with hot, dry summers and cooler, wet winters. The mean annual air temperature is 17 °C and annual precipitation is 305 mm occurring predominantly in the winter months (October through April). The furrows are constructed and tilled five times per year via furrow ridgers and maintained by shovel. Wild vegetation dominated by Cirsium arvense (Canadian thistle) is not cleared on berms; berm soils also seasonally receive litter from leaf fall. Irrigation water is sourced from the Gage Canal, which brings water from the nearby Santa Ana river, and watering occurs twice monthly on the 3rd and 18th of every month where furrows are

flooded for 48 hours. The farm is organic certified where the only additions made to the soil are horse manure and fish fertilizer. Hourly precipitation data recorded from a nearby CIMIS station (CIMIS, UC Riverside, Station 044) was referenced throughout the duration of the CO_2 flux measurements in both winter and summer with rainfall only occurring during the winter measurements.

2.2.2 Field measurements

Soil CO_2 flux was measured using a Licor 8100 IR analyzer (Li-cor, Lincoln, NE, USA) and multiplexer with 20 cm diameter chambers (Li-Cor 8100-104). PVC collars were installed into the berm and furrow soils (n = 3 each) within a 15 m radius and allowed to equilibrate for 10 days prior to measurements. Carbon dioxide concentrations were measured over 3 min with pre- and post-purge lengths of 30 s and a dead band time of 15 s per measurement. Flux was calculated using Soil Flux Pro software (v4.0; Li-COR, Lincoln, Nebraska). Measurements were taken over several weeks to capture both irrigation events per month during winter (February 2018) and summer (September 2018). With the 6 total chambers connected to a single multiplexer and IR analyzer, the set time interval per chamber resulted in CO_2 flux measurements every 22 min. Chambers remained open when not measuring flux to allow for rainfall to enter and allow for typical drying and wetting within the chambers as well as allowing for gas to freely equilibrate with the atmosphere. Soil moisture and temperature were measured within 10 cm of the outside edge of each chamber (Decagon EC5, Decagon Devices, Pullman, WA, USA). For summer flux measurements, berm soils were watered to simulate a precipitation event at the end of

the dry season (September) by applying equal quantities of water to the berm soil collars to achieve a volumetric water content of 0.15 cm^3 cm^{-3}, which is the approximate minimum moisture content observed in the furrow. Continuous soil moisture and temperature measurements were taken using sensors placed at four depths within the furrow (10, 40, 70, and 100 cm) and at 10 cm depth in the berm in triplicate and measured at 5-minute intervals (Decagon 5TM and EM50 Datalogger, Decagon Devices, Pullman, WA, USA).

2.2.3 Soil sample collection and solid phase analysis

Soil sample collection for chemical analyses

Soil was collected from the berm and furrow (0 - 10 cm depth) and the equivalent depth of the furrow surface within the berm (30 - 40 cm) using a trowel and auger on 5/16/18 (n = 12 for each location). The average water content at the time of sampling was 0.11 g g^{-1} for the furrow and 0.01 g g^{-1} for the berm. Subsamples were air-dried for several days then ground and sieved to <2 mm. Detailed chemical analyses were focused on surface soil samples from the A horizon (0 – 10 cm). Additionally, a yearlong bimonthly survey of surface soils taken from the berm and furrow was conducted to capture seasonal variation, if any, in total C, N, $\delta^{13}C$, and $\delta^{15}N$ (total n = 85 for each).

Solid phase analysis

Bulk samples were analyzed for total elemental concentrations using X-ray fluorescence spectrometry (Spectro XEPOS) and total carbon and nitrogen (%) and $\delta^{13}C$ and $\delta^{15}N$ (Costech ECS4010 Elemental Analyzer coupled through Thermo Scientific Conflo IV to Thermo Scientific Delta V Advantage Isotope Ratio Mass Spectrometer). On

subsamples of berm and furrow soils not ground or sieved (n = 3), water-stable aggregate size distribution in berm and furrow soils was determined using wet sieving technique described previously by Six et al. (Six et al. 2000). Briefly, soils from the berm and furrow were wet-sieved at a consistent agitation of 25 beats per minute for two minutes by hand into >2000 µm, 250- 2000 µm, 53-250 µm, and <53 µm particle fractions and a free light fraction that remained suspended at the start of the agitation. Saturated hydraulic conductivity (K_{sat}) of unprocessed berm and furrow soil (n = 3) was measured using the constant head method and Darcy's equation (see Appendix 1 for details).

`Berm and furrow soils (n = 3) were density fractionated using a sodium polytungstate solution of two densities (1.65 and 2.4 g mL^{-1}) to divide the soil into particulate organic matter (POM) (<1.65 g mL^{-1}), co-precipitated mineral and organic matter (1.65 – 2.4 g mL^{-1}), and organic matter coating on minerals (>2.4 g mL^{-1}), hereafter referred to as light (POM), intermediate (co-precipitates), and heavy (mineral coating) fractions (Moni et al. 2012) to determine the distribution of carbon associated with mineral fractions.

Carbon NEXAFS spectra were collected at the Canadian Light Source High Resolution Spherical Grating Monochromator (SGM) Beamline 11ID-1 on bulk, intermediate density, and heavy density fractions of the berm (0-10 cm and 30-40 cm samples) and furrow (0-10 cm). Soils were ground and sieved and suspended in DI water. Samples were wet mounted on gold-coated Si wafers and allowed to dry then mounted on an Al holder with carbon tape. Spectra were collected from 270-320 eV in slew scanning mode with 60 s scans. Typically, 30 scans were collected per sample with each scan using

a fresh spot to reduce beam damage. Spectra were binned into discrete energy points with a resolution of 0.1 eV, and spectral deconvolution peak fitting were performed in Athena (Gillespie et al. 2015; Ravel and Newville 2005). The aromaticity, or ratio of the aromatic peak to the carboxylic functional group peak, was calculated to determine which samples contained more complex aromatic C structures in the solid phase.

Water extractions were conducted on berm and furrow soils by mixing 10 mL of DDI water with 10 g of soil and shaking on a rotary shaker (90 rpm) for 16 hours. The slurry was then centrifuged for 30 minutes (2,000 x g) and solution was filtered (0.2 μm) and acidified with trace metal grade HNO_3 to a final acid concentration of 2% by volume to prevent metal precipitation. Samples were then analyzed for aqueous Fe, Al, Ca, Mg, Mn, P, and Na via inductively coupled plasma optical emission spectroscopy (ICP-OES, Optima 7300 DV, PerkinElmer Inc.). Water extractions were performed in triplicate. To quantify the amount of poorly-crystalline Fe (oxyhydr)oxides ($Fe_{(AO)}$) in berm and furrow soils, ground and sieved soils were treated with oxalate buffered to a pH of 3.0 with 0.2 M ammonium oxalate/0.2 M oxalic acid following a modified procedure adapted from Poulton and Canfield (2005). A citrate-bicarbonate-dithionite (CBD) extraction method was used to quantify free crystalline Fe oxide (Fe_{CBD}), (Mehra and Jackson 2013). Exchangeable calcium and magnesium were quantified following a modified ammonium acetate extractions method by Reeuwijk, LP van (2002), using 1.0 g of soil and 10 ml of NH_4OAc. Each chemical extraction was performed in triplicate and analyzed using ICP-OES.

2.2.4 Intact core collection and pore water analysis

Intact soil cores (n = 5 for the berm and n=4 for the furrow) were collected by pressing a 15 cm length of 4-inch diameter PVC pipe into the soil using a wood block. Cores were then extracted by removing the surrounding soil and a fine mesh cloth was secured to the bottom of each core. Each end was then capped for transport. Cores collected in both the berm and furrow showed minimal compaction using this method. Each core was partially submerged in DDI water to promote capillary rise. After each core was saturated, it was then placed in a DDI-saturated plastic-lined ceramic pressure plate chamber at wilting point pressure (-0.29 MPa). The effluent was collected, and carbon speciation was determined using the gas chromatography/electron ionization-mass spectrometry (GC/EI-MS) technique as described in Chen et al. (2019). In situ active pore water extractions were also collected in the field via lysimeters placed in the berm and furrow (n = 5 for each) at a depth of 15 cm (SSAT-A-6, Irrometer Co, Riverside, CA) using a handheld vacuum pump with extraction pressure ranging from 10-25 kPa. Lysimeter extraction from the berm was after an intense rain event and extraction from the furrow was done on a subsequent outing during an irrigation period.

To perform GC/EI-MS on pore water from cores and lysimeter samples, pore water samples were frozen immediately after collection and freeze-dried in 20 mL aliquots to concentrate pore water C compounds. Samples were then reacted with N,O-Bis(trimethylsilyl)trifluoroacetamide (BSTFA) + TMCS, 99:1 (Sylon BFT) to promote silylation to target hydroxyl groups. Derivatized samples were run on a GC/MS (Agilent 6890N GC coupled with 5975 MSD, Agilent) for aqueous carbon species characterization.

species were identified by comparing the retention time of the species in the samples to spectral data from the NIST library (J. Y. Chen et al. 2019). Once identified, the parent compounds were estimated by accounting for the derivatization that reacted -OH functional groups with -$Si(CH_3)_3$ using the following equation:

Parent compound: $C = C_{GC} - 3X, H = H_{GC} - 9X + X$ (1.1)

where subscript GC is the number of C or H present In the derivatized compound and X is the number of $Si(CH_3)_3$ identified in the GC/EI-MS.

2.2.5 Soil sample collection for microbial analysis

Methods for 16S rRNA and ITS, data analysis/collection and statistical analysis.

Microbial communities were sampled from depths corresponding to and within one meter from long-term soil moisture sensors within the berm and furrow (Berm: 0-10 cm, 30-40 cm, Furrow: 0-10cm, 40-50cm, 60-70cm, and 90-100cm) using an auger. Sub-samples for microbial analyses were removed from the auger with pre-cut sterile syringes. Triplicate samples were taken for each depth and kept in separate sterile plastic containers and immediately placed on dry ice and stored at -80 ^{o}C prior to analysis. Samples were shipped on dry ice overnight to Lawrence Berkeley National Laboratory and analyzed for 16S rRNA (bacterial) and ITS (fungal) analysis.

Genomic DNA was extracted from triplicate samples from each sampled location and depth using the DNeasy PowerSoil DNA Extraction Kit (QIAGEN). DNA extracts were sent to the Vincent J. Coates Genomics Sequencing Laboratory at the University of California, Berkeley for library preparation and sequencing of the V4 region of the 16S

rRNA gene for bacteria and archaea (515f forward primer, 806r reverse primer) and the internal transcribed spacer region (ITS) for fungi (ITS1f forward primer, ITS2 reverse primer). Sequencing was performed on an Illumina MiSeq v3 yielding 300-bp paired-end reads.

Forward and reverse reads were aligned and paired using usearch [v8.1.1861 (Edgar 2010)] fastq_mergepairs command (maximum diff = 3). The aligned reads were quality filtered (command fastq_filter with -fastq_trunclen = 230, -fastq_maxee = 0.1), concatenated into a single fasta file, and singletons were removed (command sortbysize with minsize = 2). These filtered sequences were used for operational taxonomic unit (OTU) clustering with the uparse pipeline (Edgar 2013) (setting the OTU cut-off threshold to 97%. Chimeric sequences were filtered with uchime (Edgar et al. 2011) with reference to the ChimeraSlayer database downloaded from http://drive5.com/uchime/gold.fa. OTU abundances across individual samples were calculated by mapping chimera-filtered OTUs against the quality-filtered reads (command usearch_global with -strand plus -id 0.97).

Taxonomy was assigned to each OTU by a Naïve Bayes classifier using the assign_taxonomy.py command in QIIME (Wang et al. 2007) with reference to the SILVA database accessed from mothur (Schloss et al. 2009)s release 119: For phylogenetic inference of bacterial and archaeal OTUs, representative sequences for each bacterial OTU were aligned to a SILVA SEED sliced alignment using the PyNAST algorithm (Caporaso et al. 2010) and archaeal and bacterial phylogeny was inferred using FastTree (Price, Dehal, and Arkin 2010). This workflow resulted in 51 archaeal, 9,020 bacterial, and 2,208 fungal OTUs.

Statistical analyses of OTU data were conducted in R v3.6.1. Alpha and beta diversity metrics were calculated using the 'phyloseq' package v1.28.0. Taxa in differential abundance among depths and treatments were identified using the 'DESeq2' package (Love, Huber, and Anders 2014) v1.24.0 with test = "wald"and fitType = "parametric". We performed two-sample t-test statistical comparison (IGOR Pro, R) on the solid phase analysis of the year-long survey samples taken from the berm and furrow (0 – 10 cm).

2.2.6 Statistical analyses

The annual survey data were tested for normality using a Shapiro-Wilk test. Those that did exhibit normal distribution ($\delta^{15}N$ and elemental concentrations Na, Ca, and Fe) where then compared (berm vs furrow) using a t-test. Those measured values that did not meet the criteria for parametric statistical analyses (total C, total N, $\delta^{13}C$, C/N, and elemental concentrations Mg, Al, Si, P, and S) were then compared using a Wilcoxon Signed-rank test.

2.3 Results

2.3.1 Soil Moisture and Temperature Fluctuations

Volumetric water content of the furrow ranged from 0.15 to 0.35 $m^3\,m^{-3}$ at four depths within the furrow soil (10, 40, 70, 100 cm; Figure 2.1A and Figure A1.2) and 0.07 to 0.11 $m^3\,m^{-3}$ in the berm (10 cm) soil, with the exception of large pulses from a rain event, which peaked in the winter months at 0.20 $m^3\,m^{-3}$ (Figure 2.1A). Within the furrow, the greatest daily moisture fluctuations were observed near the surface with fluctuations

dampening with depth. In contrast, moisture in berm soils at 10 cm depth was unaffected by water delivered via irrigation and only increases after precipitation events. Soil temperature follows a seasonal trend typical of Mediterranean climates (warm summers and cool winters) with daily soil temperature fluctuations being more drastic in the berm soils than furrow soils due to relatively drier conditions (Figure 2.1B). Soil CO_2 flux measurements were conducted during the hottest (summer; July-September) and coldest (winter; December-February) months of the year when the highest CO_2 fluxes is expected in the summer and lowest CO_2 fluxes are expected in the winter (Eric A. Davidson and Janssens 2006; Fang and Moncrieff 2001).

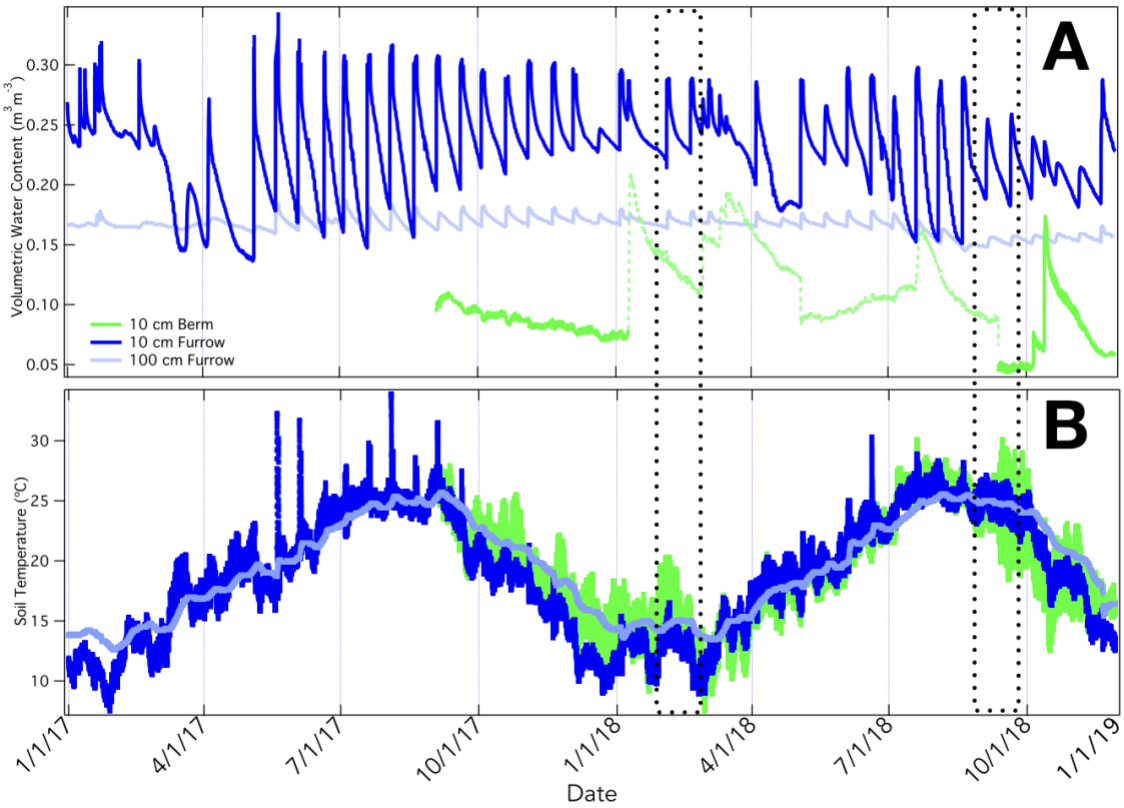

Figure 2.1. Volumetric water content and soil temperature from a depth of 10 cm in the berm and furrow and at a depth of 100 cm in the berm over a two-year period (n = 3). The time periods delineated by dotted boxes correspond to when the flux measurements were taken, one in the summer season (dry) and one in the winter season (wet).

2.3.2 Soil CO_2 flux from furrow soils

Soil CO_2 flux in the furrow is suppressed at the onset of irrigation and nearly completely inhibited within the first 24 hours after irrigation begins (Figure 2.2 and 2.3). During both seasons, soil CO_2 flux increases ~24 hours after the 48-h irrigation ends which corresponds with decrease in surface ponding as water infiltrates into the subsurface. The gradual increase in CO_2 flux is reflective of the rate of drainage of water from soil pores, which is evidenced in part by soil moisture decrease in the upper 10 cm of the soil. During the wet season, the CO_2 flux rates increase daily with diurnal peaks corresponding to the warmest times of the day until the next wetting event suppresses flux (Figure 2.2). In the dry season, the highest flux corresponds to 3-5 days after irrigation has ceased then begins to decrease as soil moisture conditions drop to pre-wetting conditions (~0.08 $m^3 m^{-3}$ VWC; Figure 2.3). Greater maximum flux was reached during the summer than winter within dried furrow soils likely due to higher soil temperatures.

2.3.3 Soil CO_2 flux from berm soils

In contrast to furrow soils, water is only delivered to berm surface soils via precipitation events which are restricted to the wet season (winter). During the winter months multiple precipitation events occurred with varying intensity. Prior to a major rain event at the end of February, soil CO_2 flux was sustained at approximately 1.5 μmol m^{-2} s^{-1} with minor daily variations. Immediately after the rain event, CO_2 flux from berm soils

approximately doubled and the magnitude of daily fluctuations subsequently increased (Figure 2.2).

Throughout the summer months, there was no water delivered to berm surface soils and soil moisture in the top 10 cm remained low (Figure 2.3). We hypothesized that prolonged dry conditions caused accumulation of organic C substrates within berm soils that would be quickly respired once water became available. To test this hypothesis, an artificial rainfall event was simulated near the end of the dry summer months and CO_2 flux was measured. The magnitude of soil CO_2 flux after wetting was 11 times greater than the average baseline flux measurement prior to wetting.

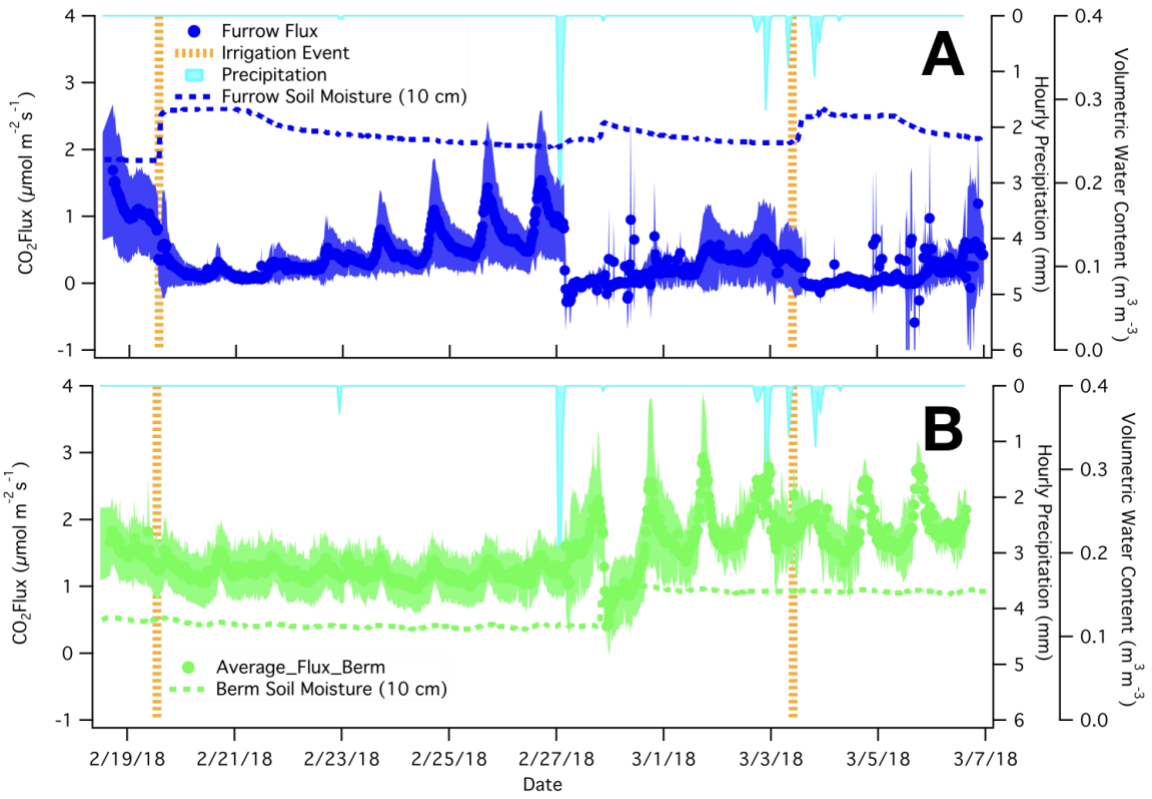

Figure 2.2. Soil CO_2 flux and soil moisture measured in furrow (A) and berm (B) soils during the wet season (winter) over two consecutive irrigation events. The same hourly precipitation data is provided in both panels. CO_2 flux data is displayed with filled circles indicating the average flux of triplicate chambers with the range of flux measurements within the same timeframe shown in the shaded vertical lines.

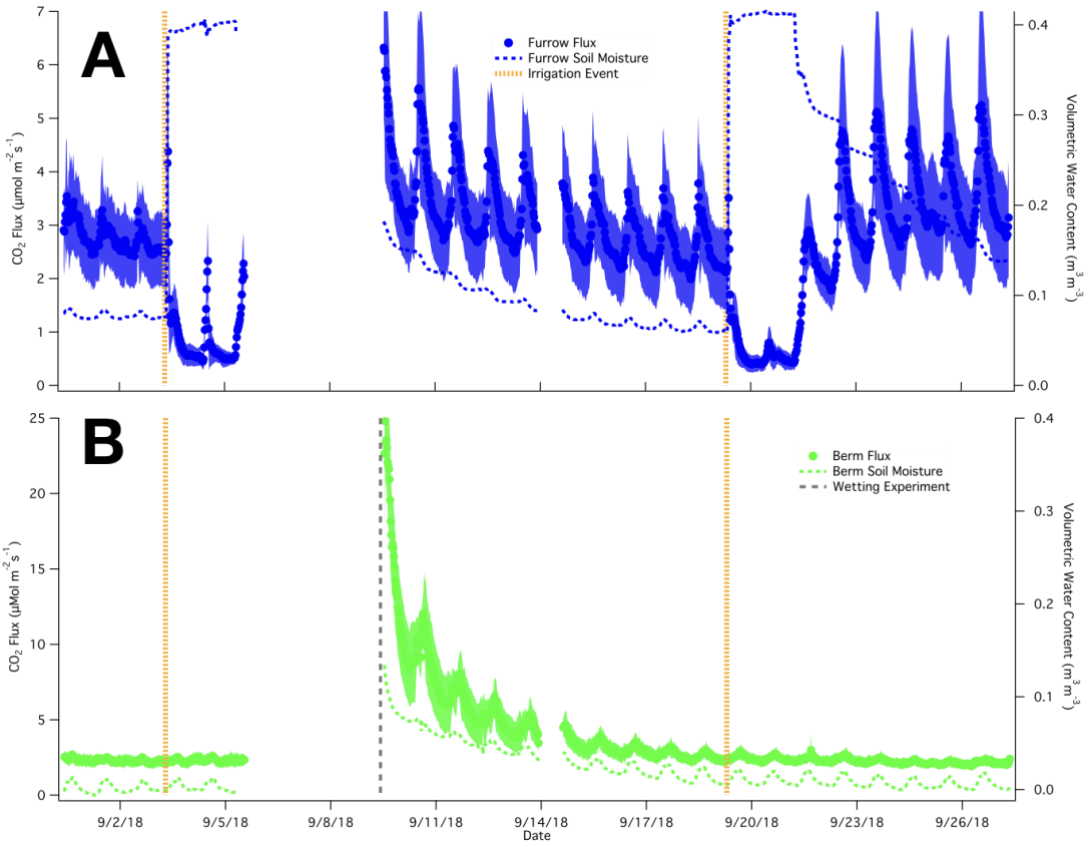

Figure 2.3. CO_2 flux and soil moisture measured in furrow (A) and berm (B) soils during the dry season (summer) over two consecutive irrigation events. CO_2 flux data is displayed with filled circles indicating the average flux of triplicate chambers with the range of flux measurements within the same timeframe shown in the shaded vertical lines. Gray dashed line in panel (B) indicates a simulated rain event applied to berm soils. Power outage prevented data collection from 9/6/18 to 9/9/18 and on 9/14/18.

2.3.4 Bulk Soil C, N, and metals composition

Soils from the top 10 cm of the berm and furrow were collected twice per month for 12 months to determine whether the average C and N content are significantly different between the two locations. Results show that average C content in berm surface soils is 2.4±0.4 wt. % , which is higher than the average C content of furrow soils (1.2±0.5 wt. % C; $p < 0.001$) (Figure A1.3). Carbonates measured in both berm and furrow soils showed an average content of < 0.02 %, with a slightly higher amount present in the furrow, so total C is assumed to be organic. Stable C isotopic composition in furrow soils also shows

significantly greater enrichment of ^{13}C (-25.96 ±0.54‰ $\delta^{13}C$) than in berm soils (-24.76 ±0.82‰ $\delta^{13}C$; $p < 0.001$). Similarly, total N content of berm soils were significantly higher than furrow soils and ^{15}N was enriched within furrow soils as compared to the berm (Figure A1.4). Total concentration of Fe (~4.5%), Al (~6%), and Ca (~2.5%) were comparable between the berm and furrow soils (Figure A1.5).

2.3.5 Water stable aggregates

Soils were divided into water stable aggregate fractions to assess the physical stability of soil structure within the berm and furrow environments. In both soils, the largest proportion of soil mass was associated with 53-250 μm sized aggregates (Figure 2.4). The larger portion of microaggregates of the smallest in the furrow is likely due to deposition of clay particles from suspended sediments within irrigation water and from physical disruption of aggregates in the furrow during tillage. Correspondingly, a lower saturated hydraulic conductivity (K_{sat}) was also measured in furrow soil as compared to the berm, even when the furrow soil was tilled (Figure 2.5). The furrow soil shows more positive $\delta^{13}C$ values (Figure A1.6) in each of the water stable aggregate fractions compared to the berm aggregate fractions, indicating the presence of more processed or decomposed C relative to berm soil. In both the berm and furrow aggregate fractions, there is an increase in $\delta^{13}C$ values as the aggregate size decreases, indicating that more microbially processed C is being incorporated in the microaggregates (Moni et al. 2012). More C and N is associated with 53-250 μm aggregate fraction in the furrow while greater proportion of C and N is associated in the 250-2000 μm size fraction of the berm soil (Figure 2.4).

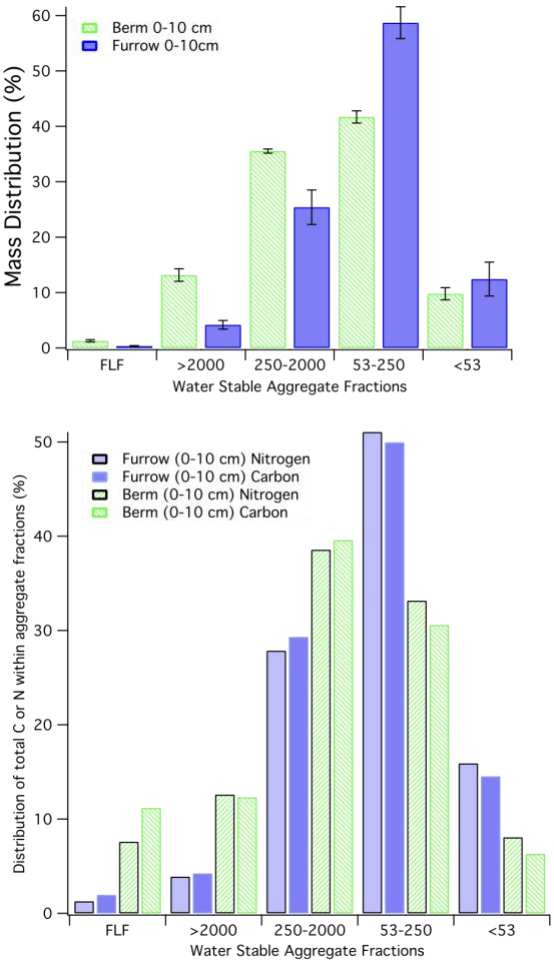

Figure 2.4. (Top) Mass distribution of the water stable aggregate fractions in berm and furrow soils. (Bottom) Distribution of total C and N within each water stable aggregate fraction in the berm and furrow soils.

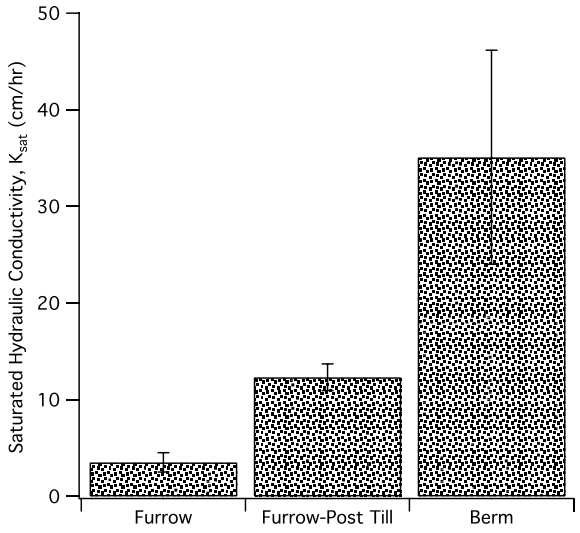

Figure 2.5. The saturated hydraulic conductivity of surface furrow and berm soils and surface soil taken immediately after tilling in the furrow. Triplicate samples were analyzed bulk soils; average values are presented along with standard error displayed with error bars.

2.3.6 Iron oxide and exchangeable calcium

Sequential Fe extractions were performed to determine the percentage mass of soil composed of crystalline, poorly-crystalline, and clay Fe minerals, in surface soils from berm and furrow. Results show that there may be a slightly higher proportion of poorly crystalline Fe in the furrow soil than the berm soils, though difference between berm and furrow are not statistically significant (Figure 2.6). The ammonium acetate extractions resulted in 9.66 ± 0.07 % exchangeable calcium in the furrow and 7.25 ± 0.06 % in the berm soils.

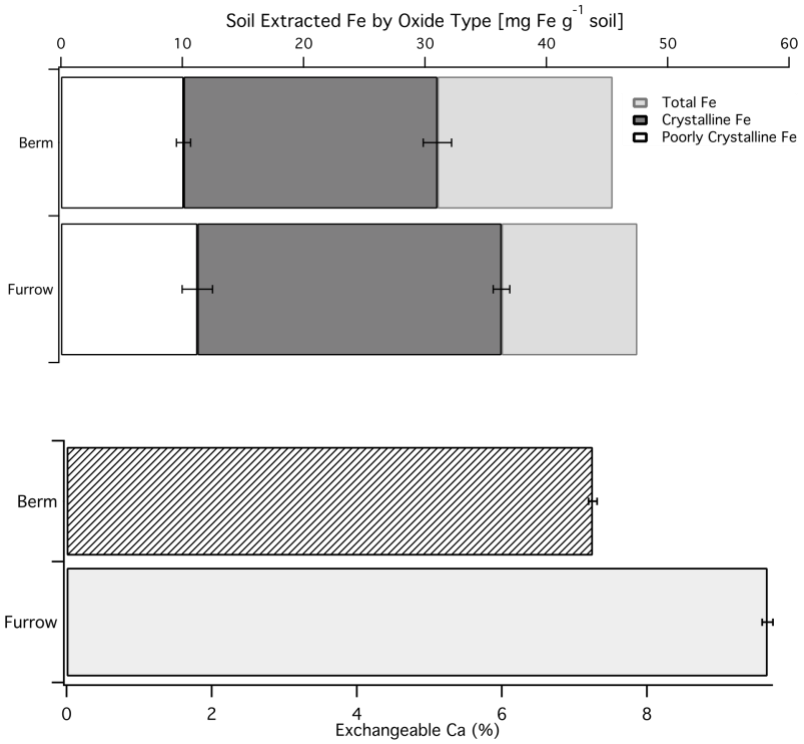

Figure 2.6. (Top) Fe-oxide type determined by ED-XRF of berm (top) and furrow (bottom) soils in bulk soils and through sequential extractions. (Bottom) Exchangeable calcium percentage determined through extraction in the berm and furrow soils. Triplicate samples were analyzed bulk soils; average values are presented along with standard error displayed with error bars.

2.3.7 Density fractionations

Between the furrow and berm surface soil, the mass distribution of each density fraction was relatively similar, with the majority of the overall soil mass attributed to the heavy fraction and a small difference observed in the mass percentage in the light fraction of the furrow (Table 2.1). Due to the light fraction being mostly particulate organic matter (POM), the increased leaf litter and fine root material in the berm is likely responsible for the higher relative mass in the light fraction compared to the furrow soil. Isotopic δ^{13} C values indicate that C associated with the heavy fractions are more microbially processed (i.e. more positive δ^{13}C values), with a larger proportion of microbially derived C observed

in the furrow (Moni et al. 2012) (Figure 2.7). These results show that relatively more C is associated with the heavy fraction of furrow soil as compared to soil from the berm. This is likely due to leaf litter input to berm soils which leads to a greater relative proportion of C mass associated with the light fraction. Although total C due the POM was highest in the light fraction, when accounting for the overall mass, more C was associated with the intermediate density fraction in both the berm and furrow (Figure 2.8B).

Table 2.1. Mass distribution of each density in the berm and furrow soils.

Sample	Density Fractions		
	Light	Intermediate	Heavy
Furrow	0.70%	5.78%	93.51%
Berm	0.89%	5.80%	93.31%

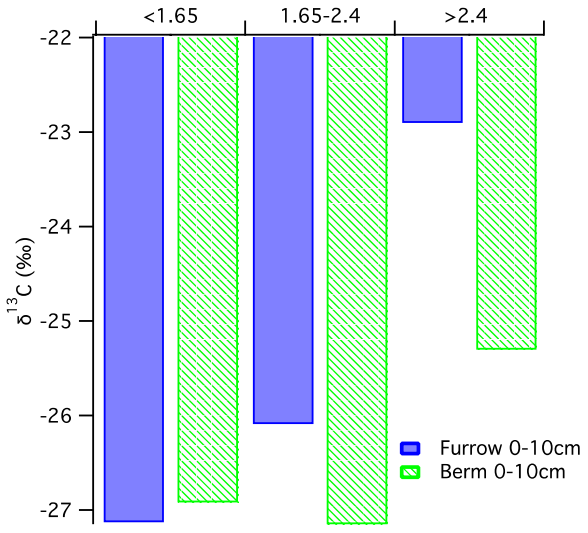

Figure 2.7. The δ^{13} C values of both soils and their associated densities.

2.3.8 Carbon speciation in solid phase

Carbon NEXAFS spectra of bulk soil and density fractions was used to determine differences in C bound in co-precipitates (intermediate fraction) and mineral coatings (dense fraction). Due to the C in the light fraction being predominantly particulate organic matter, C NEXAFS spectra was only collected on the intermediate and heavy fractions of the berm and furrow soil (Figure 2.8A). Across samples spectra exhibit prominent aromatic (~285 eV) and carboxyl (~288.5 eV) peaks consistent with previously published spectra of soil organic C (Solomon et al. 2005).

To provide a semi-quantitative comparison of C chemistry, aromaticity was calculated by normalizing the aromatic peak (284-285.5 eV) to the carboxyl peak (287.7-288.6 eV) in each spectrum (Lehmann et al. 2005). Higher aromaticity generally implies that the C compounds associated with the solid phase require a higher redox potential environment to be degraded (Fiedler and Kalbitz 2003). Solid phase C in furrow soil has higher aromaticity in both the intermediate and heavy fractions compared to the same fractions in the berm. Additionally, higher aromaticity was associated with mineral coatings in the furrow while more aromatic carbon compounds were abundant in the co-precipitated fraction in the berm.

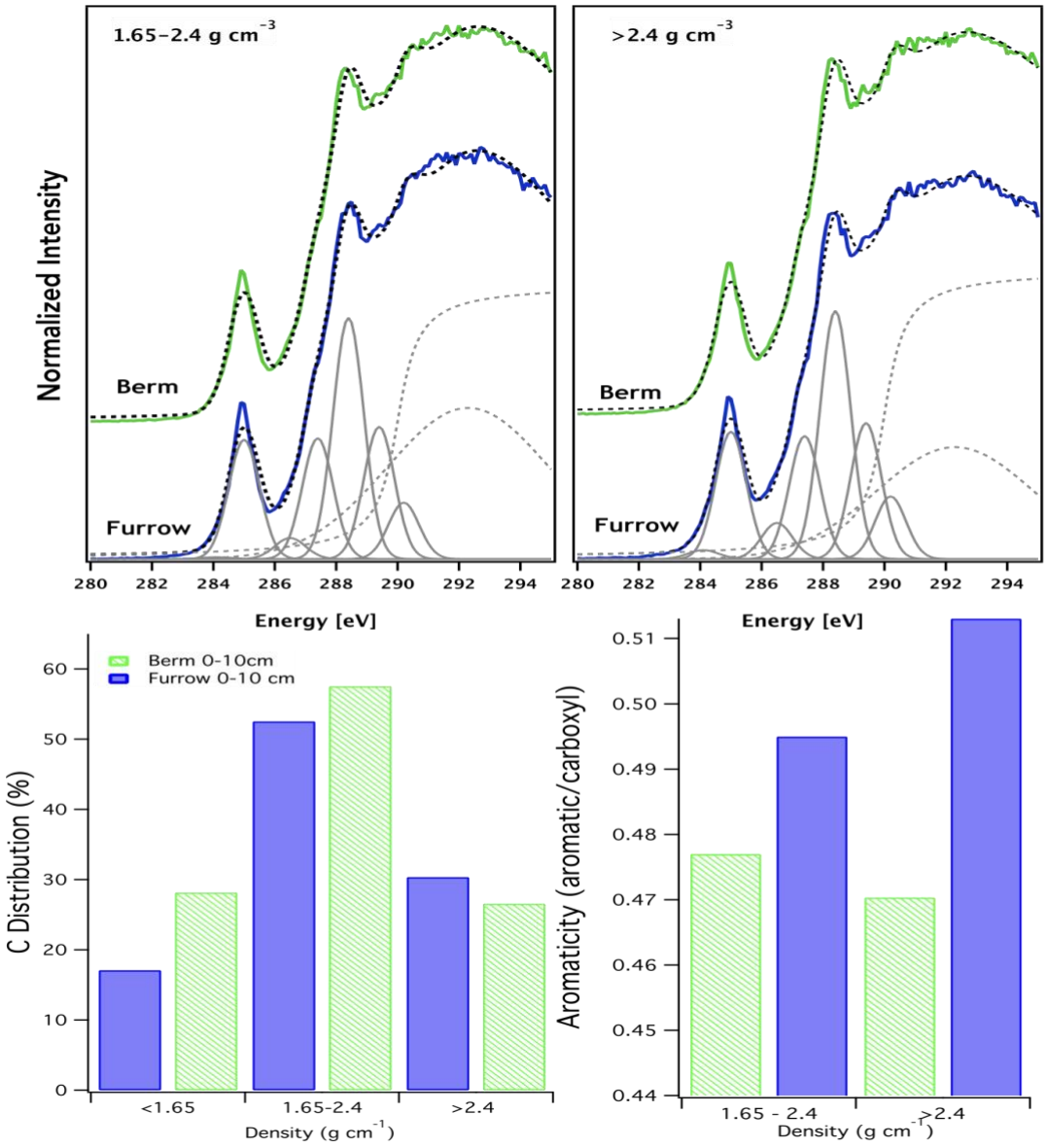

Figure 2.8. Carbon NEXAFS spectra of the intermediate and heavy fractions of the berm and furrow (top), total C by weight percent of each fraction (bottom left), and aromaticity of furrow and berm soil (bottom right).

2.3.9 Substrate chemistry of porewater

Analysis of soil porewater extracted using both a pressure plate extraction in the lab with intact soil cores and also in situ extraction using lysimeters show that the majority of C substates is composed of complex hydrocarbons, lignin, and lipids with low C nominal

oxidation state (NOSC) in berm soils (Figure 2.9). In furrow soils, when extracted via lysimeter in the field (with lower vacuum pressure than in the lab), the porewater C substrates are dominated by compounds with relatively higher nominal oxidation states, such as carbohydrates, but when put under more negative pressure (-0.29 MPa), the substrate group extracted corresponds more closely with the substrate class extracted in the berm. The largest pore filled diameter associated with vacuum pressures in the lysimeter and pressure plate extractions are 12 µm and 1 µm, respectively (Bailey et al. 2017).

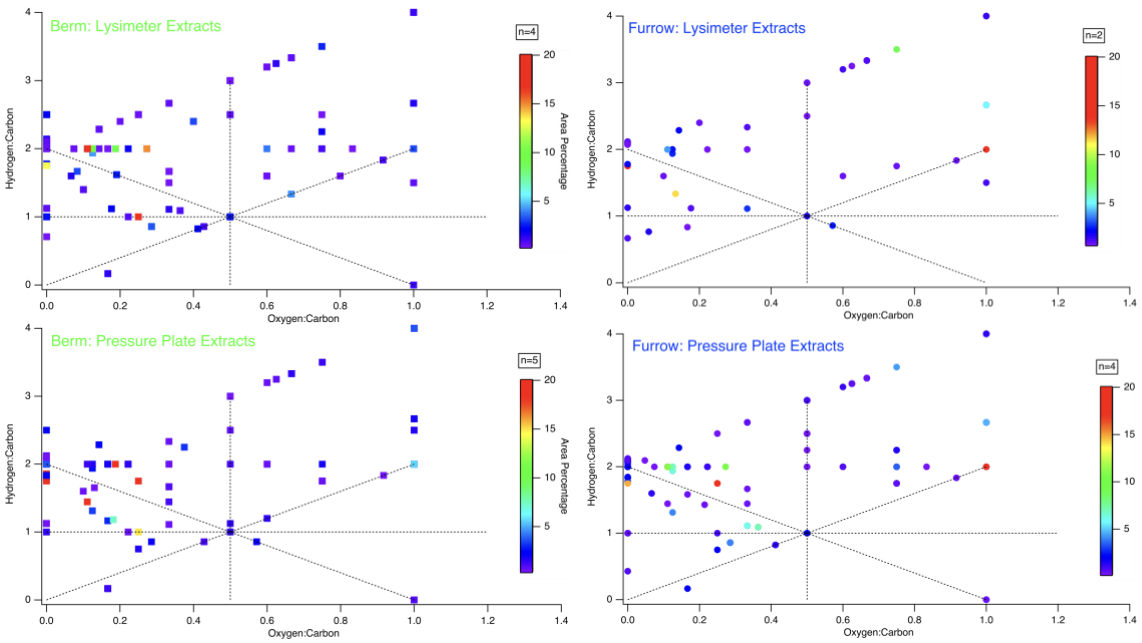

Figure 2.9. Van Krevelen plots of characterized substrate in porewater analyzed via GC/EI-MS. Nominal oxidation state of carbon (NOSC) increases as O:C increases. (Top left) Pore water extracted from berm after precipitation via lysimeter. (Top right) Pore water extracted from furrow during irrigation via lysimeter. (Bottom left) Pore water extracted from saturated intact berm soil core via pressure plate extraction. (Bottom right) Pore water extracted from saturated intact furrow soil core via pressure plate extraction.

2.3.10 Microbial community composition

Differences in induced soil moisture dynamics and the apparent response of soil C between berm and furrow soils differentiates soil conditions on a sub-field scale. We

hypothesized that the microbial community composition in berm and furrow soils would reflect these differences. Comparison of 16S rRNA and ITS data between berm and furrow soils shows distinct differences in relative abundance of bacterial and fungal communities, reflecting differences in soil environments (Figure 2.10).

Distinct bacterial communities reside in the berm and furrow soils, where in particular furrow and berm communities from the shallow soils (0-10 cm) form relatively tight clusters that are highly distinct (filled circles in Figure 2.10). Furrow soil had a greater relative abundance of anaerobic bacteria and fermenters (Figure 2.11A-C) while the berm exhibited a greater relative abundance of aerobic bacteria (Figure 2.11D-F).

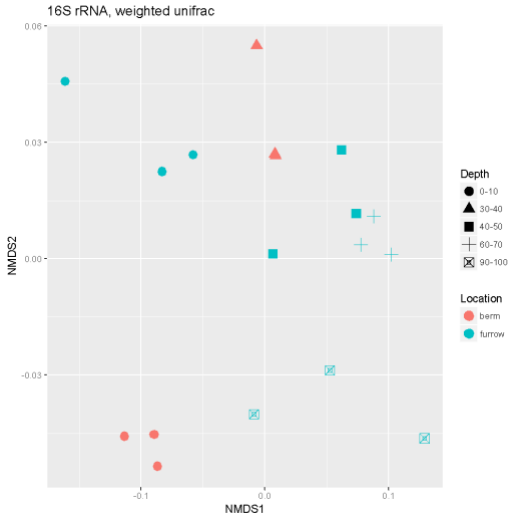

Figure 2.10. Bacterial community composition of the berm and furrow at different depths.

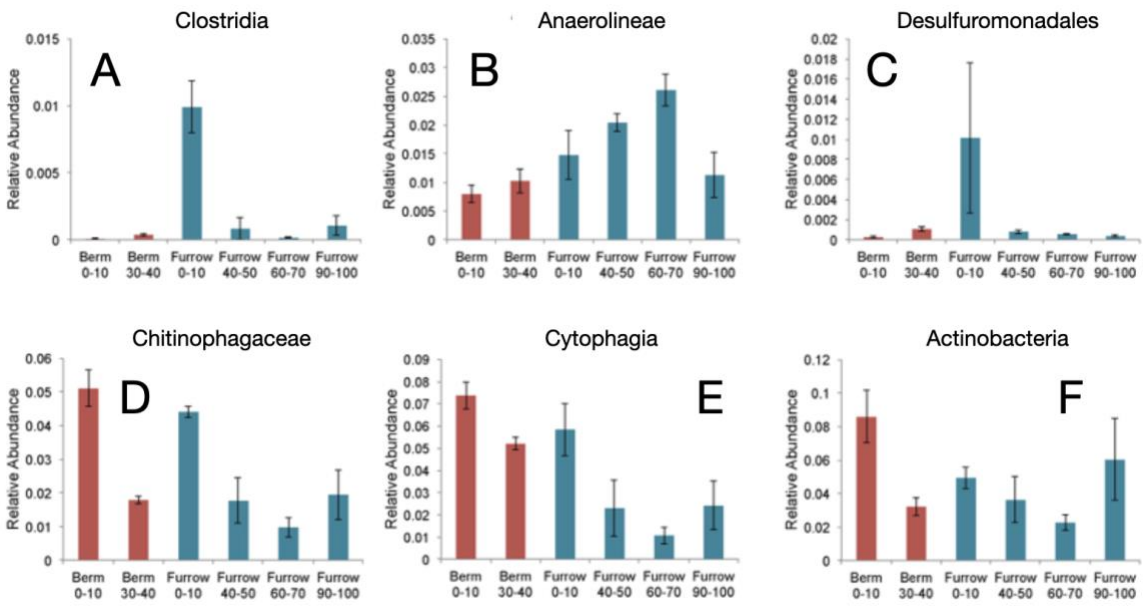

Figure 2.11. Bacterial lineages by relative abundance of (A) Clostridia, (B) Anaerolineae, (C) Desulfuromonadaies, (D) Chitinophagaceae, (E) Cytophagia, (F) Actinobacteria.

The fungal communities between the berm and furrow overall show no clear differences in richness. However, observed differences in richness were apparent between the furrow surface soils (0-10 cm) and the subsoils (greater than 10 cm depth) (Figure 2.12). There was a significantly higher relative abundance of Basidiomycota in the berm than the furrow, (Table 2.2); Glomeromycota were also more abundant in the furrow soils than in the berm soil (Figure 2.13).

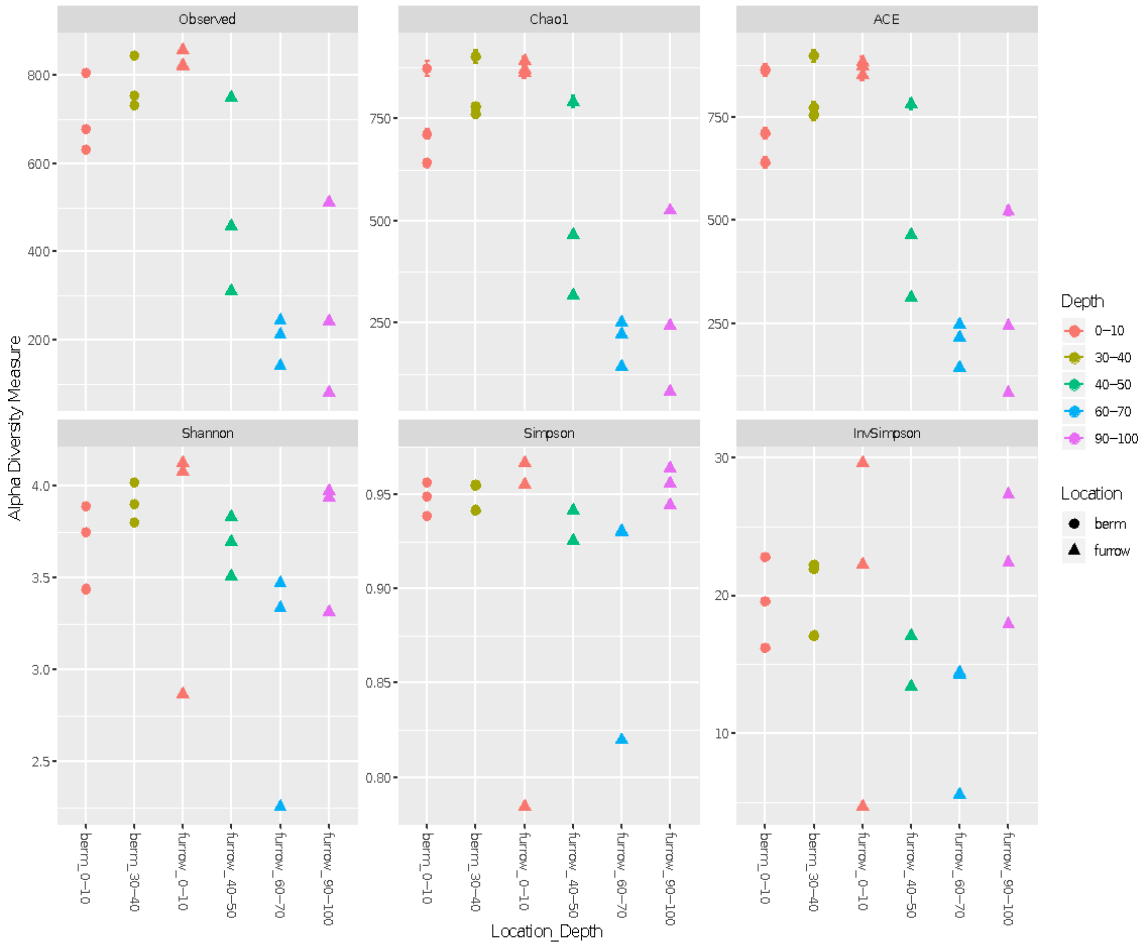

Figure 2.12. Fungal richness within berm and furrow subsoils and surface soils.

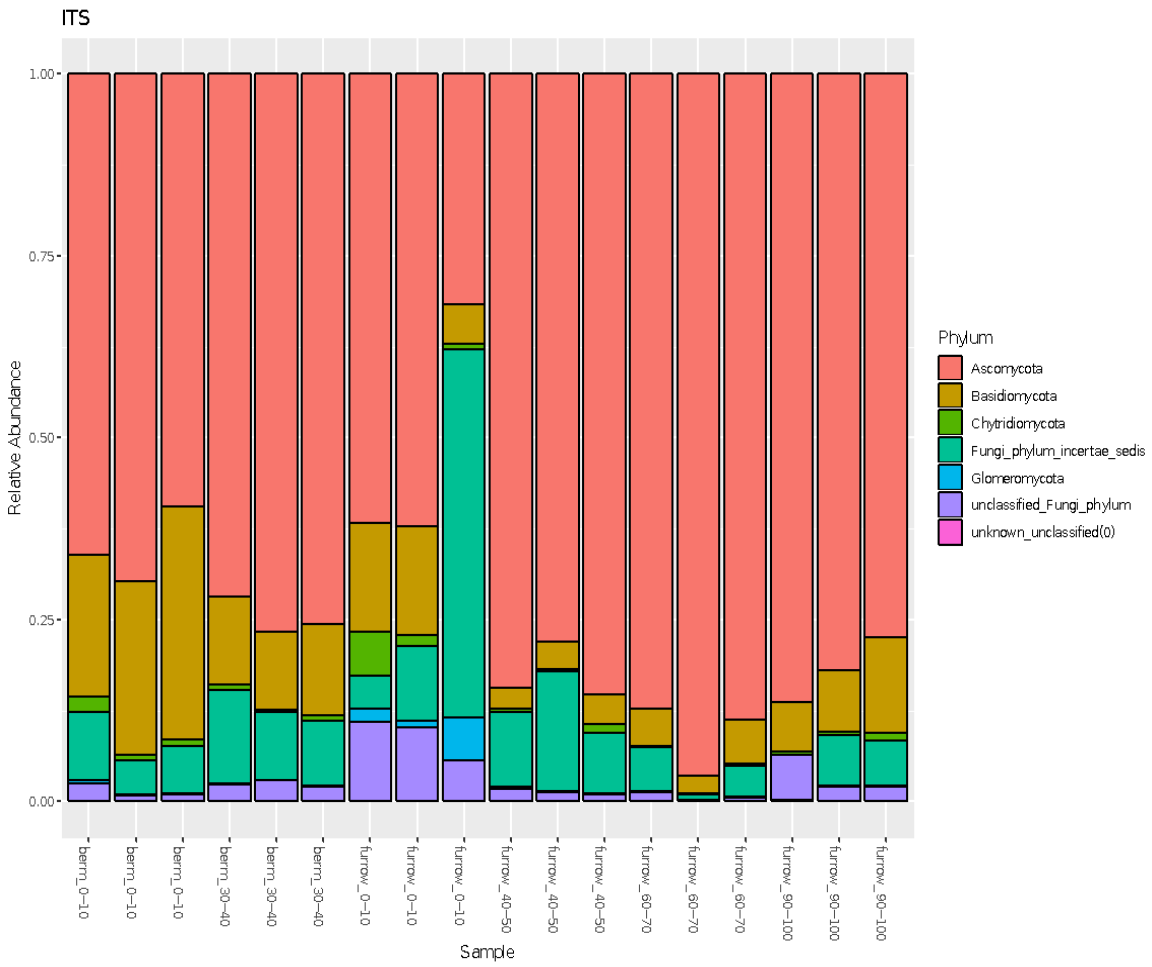

Figure 2.13. ITS community structure, relative abundance between fungal phyla found in furrow and berm soils.

Table 2.2: Differential abundance stats (DESeq2) between surface soils of furrow and berm. Significant p-values ($p<0.05$) are denoted with *.

Phylum	p_{adj} Value
Basidiomycota	0.000013*
Unclassified_Fungi_phylum	0.005078*
Ascomycota	0.005078*
Fungi_phylum_incertae_sedis	0.493145
Glomeromycota	NA
Chytridiomycota	0.604777
Unknown_unclassified(0)	0.851941

2.4 Discussion

2.4.1 Proposed mechanisms for observed CO_2 flux patterns

Because of the bidirectional interaction between climate and agriculture, mitigating climate change can increase crop yield and quality (Lal 2004), while optimizing irrigation management practices can minimize greenhouse gas emissions while maximizing soil C storage (Fernández et al. 2006). In California, nearly 10 million acres of agricultural land are irrigated with over 34 million acre-ft of water annually (California Department of Water Resources 2020). Of those irrigated lands, approximately 3.5 million acres are gravity or furrow irrigated which leads to regular wet-dry cycling of irrigated soils (R. Johnson and Cody 2015). Johnson et al. (2007) compiled the many opportunities in agricultural soil management to decrease greenhouse gas emissions but fails to associate any benefits or drawbacks to emissions based on irrigation method, which is an important land

management decision. A review of field-based studies, however, showed that in many cases, furrow or gravity driven irrigation corresponded to lower CO_2 emissions when compared to lower volume irrigation or as saturated soils were intermittently drained (Sapkota et al. 2020).

The characteristic 'Birch Effect' (Birch 1958) which describes how CO_2 flux changes after a wetting event, models microbial activity as a function of wet-dry cycles. The conditions immediately after irrigation in the furrow show that the soil is saturated which was observed visually by ponded water above the soil and the soil moisture readings. As the soil begins to dry, the optimum conditions for microbial activity develop. This daily initial increase in CO_2 flux as the soil drains within the furrow is likely due to the quick oxidation of carbon that is readily available in soil solution. In the winter measurements, the repeated wetting events (rain or irrigation) repeat the "dampening effect' where saturation yields zero flux. This is likely due to suppression of aerobic respiration as O_2 diffusion into the soil matrix is limited from saturation of soil pores along with surface ponding (Xiang et al. 2008). In the dry season, however, the decrease in flux after the initial 3-5 days maximum peak in the furrow is likely due to the depletion or inaccessibility (i.e. pore connectivity decreases) of carbon substrates that fuel microbial activity (Fierer and Schimel 2002). The furrow soil is only receiving water inputs in the form of irrigation during the dry season and will only continue to dry down and the CO_2 flux will drop until pre-wetting respiration rates are resumed.

The magnitude of the Birch effect is likely controlled by a combination of physical, chemical, biological factors, but are ultimately catalyzed by a wetting event. In the berm

soil, where water delivery is less frequent but expected in the winter rainy season, the base respiration rate was higher than that of the furrow, which is likely due to root respiration. The response of berm soil to precipitation demonstrates that microbial respiration is water-limited within the berm soil environment. When a rain event occurred during this period, the berm soil did not exhibit a "dampened" effect as in the furrow but did show an immediate increase in the flux. It is likely that the amount of water delivered to the berm increased pore connectivity to quickly oxidize the available C but not enough to limit oxygen diffusion. When the soils were drier for longer periods of time, however, the magnitude of the birch effect was far greater. Jenerette and Chatterjee (2012) found that water addition triggers response, but that pulse magnitude is primarily controlled by substrate availability. Through the addition of water in the form of an artificial wet up event in the berm after a prolonged dry period (summer months), we found that that large pulses in CO_2 flux generally occurred when watering events occur outside of the typical wet seasons where substrate is accumulated over the dry period and then made accessible as water connects microbes to substrate, as observed in Jenerette and Chatterjee. Not only does pore connectivity influence the carbon dynamics, the water stress history of the soil also influences the magnitude of carbon release. Previous studies that examined the effect of extended drought on soil C dynamics have reported similar CO_2 pulses, where researchers have suggested a build-up of soluble C in the subsoil during the dry period which is ultimately made accessible to microbes of from the disruption of aggregates through slaking mechanisms (Lopez-Sangil et al. 2018; Fierer and Schimel 2002). A previous study by Homyak et. al found that water extractable organic carbon (WEOC),

even when plant inputs are excluded, increase as soils dry, concluding that physical processes that occur as soils dry are greater contributions to C accumulation than exo-enzymatic decomposition by microbes (2018).

2.4.2 Proposed mechanism for C stabilization

Soil organic C that enters soil systems as large complex polymers must first be cleaved into smaller monomers before microbes can metabolize them (Fenchel, Blackburn, and King 2012). Exoenzymes produced and excreted by microbes can aid in this rate-limiting step for C mineralization; however, mineral-associations can prevent enzymatic degradation of organic C compounds, leading to an accumulation of SOC (Kleber, Sollins, and Sutton 2007). Carbon species, which can range in energetic favorability for microbial metabolism, can be easily accessed as particulate organic matter or can be more protected via co-precipitating with mineral oxides or through OM coating mineral surfaces (Sollins et al. 2006; Kleber, Sollins, and Sutton 2007). The carbon chemistry of these soils shows the larger abundance of aromatic C compounds in the furrow soils compared to the berm in both the intermediate and heavy density fractions, which are C associated with co-precipitates and mineral coatings, respectively. This suggests that in the furrow, the active substrate that is utilized for metabolic processes is less aromatic C because what remains in the solid phase is the aromatic C. In the furrow, what remains in the solid phase is more thermodynamically stable C. Through the density fractionations, we also found that a larger abundance of aromatic C was associated with the mineral coatings in the furrow while in the berm, the larger aromatic C abundance was in co-precipitated mineral and organic

matter. This suggests that the primary mode of SOC stabilization in the furrow is through the formation of mineral organic associations while the berm soil is more through co-precipitations with mineral oxides.

Iron minerals are important in controlling soil C dynamics through binding and precipitating C particularly within redox fluctuating environments (Thompson et al. 2018). We hypothesized that the redox fluctuating environment within the furrow driven by periods of inundation would lead to reductive dissolution of Fe(III) oxides during flooded periods and the release of $Fe^{2+}_{(aq)}$. Upon drying, oxidation of soluble Fe^{2+} to Fe(III) oxides could occlude soluble and particulate C through co-precipitation of Fe oxides and C. The proportion of poorly crystalline and crystalline Fe(III) oxides in berm and furrow show that Fe(III) oxide co-precipitation is likely not a significant source of C stabilization due to the low proportion of Fe(III) oxides that compose the solid phase overall and the very minor fraction that is composed of poorly-crystalline Fe(III) oxides.

In water limited environments, exchangeable Ca^{2+} is a likely binding mechanism for SOM as it is relatively abundant and can form cation bridges between clay particles and organic matter (Rasmussen et al. 2018). The higher percentage of exchangeable Ca in the furrow, paired with the increased C contribution in the heavy fraction of the furrow, relative to the berm, indicates that Ca is the more likely stabilizing mechanism responsible for the increased C content and aromaticity associated with mineral coatings that resulted in decreased respiration. The constant wet-dry cycle exhibited in the furrow increased the proportion of microaggregates, which are responsible for the larger C and N pool that are relatively more inaccessible to microbes.

2.4.3 Proposed selectivity of microbial community

The C cycle is largely mediated by microbial processes and the relative activity of the microbial community was first assessed through the isotopic C and N differences measured in the bulk, density fractionated, and water stable aggregated fractions. Our findings suggest that C within the berm soils is more microbially-degraded while the less negative $\delta^{13}C$ of the furrow soil indicates presence of less processed C (Figure 6B). The pore water analysis taken from furrow soils show a higher abundance of carbohydrates while the berm soil pore water contained a higher relative abundance of lignin-like C. The soluble material for microbes to act on in the berm soils are oxidatively depolymerized and then respired, while the more reducing conditions of the furrow allow for low molecular weight C to remain soluble in the larger pore-throat diameters as well as being tightly held in the smallest diameter measured. Even as pressures increased in the pressure plate extractions, the soluble material in the berm pore water was of lower nominal oxidation state, which is energetically more stable against being respired by surrounding microbial communities.

The physical and chemical limitations in terrestrial ecosystems make bacterial metabolisms particularly dependent on the presence of liquid water, where activity is limited to aqueous films (Fenchel, Blackburn, and King 2012). In times of water stress, bacteria can produce spores or cysts as anti-desiccation measures to prevent cell lysis. Fungi, on the other hand, can be active in gas-filled pore space and can decompose complex polymers even when bacteria are inactive due to water limitations. In addition to the need for liquid water for most microbial activity, the redox status of that solution also limits

metabolisms at play. Microbial communities have been observed to shift as redox status fluctuates, showing distinct molecular profiles of physiologies of the microbial communities better suited to each soil condition (Pett-Ridge and Firestone 2005). Plasticity, or the ability of microbes to withstand and proceed with normal physiological processes in all redox settings is generally not the case in soil. The major metabolic pathways active in redox fluctuating soils are more often tolerant aerobes or anaerobes, who are competitive with the presence (aerobes) or absence (anaerobes) of O_2 and are inactive during periods where they are incompatible. Facultative organisms on the other hand are most competitive when redox conditions are not static. In agricultural soils, where redox status is driven by irrigation, drying and rewetting and the extent of each can lead to divergent microbial communities in parts of the field that have contrasting soil moisture input.

Furrow soil had a greater relative abundance of anaerobic bacteria and fermenters reflecting the extended and frequent periods of flooding during irrigation events. Clostridia are obligate anaerobic spore formers that are likely selected for in the furrow environment due to their ability to withstand the large variation in soil moisture (L. Ds. Smith 1975). The anaerolineae subphylum of Chloroflexi bacteria are gram-negative bacteria with fermentative metabolism that grow under strict anaerobic conditions and are more abundant in the furrow and increase with depth (up to 70 cm) where soil moisture is maintained at a relatively high value throughout the year (Figure 2.11B). There is enrichment of δ-Proteobacteria Desulfuromonadales in the top 10 cm of the furrow soil

that may be using the simple organic acids produced by the fermenters present in the furrow soil (Figure 2.11C).

In contrast, the berm exhibits a greater relative abundance of aerobic bacteria that are known to degrade more complex substrates. Increased abundance of Chitinophagaceae have been correlated with increases in enzymes able to break down cellulose (C. R. Smith et al. 2016) and are abundant in both berm and furrow surface soils but are most abundant in the berm surface soil (Figure 2.11A, 2.11B, 2.11C). A similar trend is observed in the relative abundance of bacteria belonging to class Cytophagia in the surface soils, which are aerobic bacteria that are proficient digesters of insoluble cellulose (McBride et al. 2014). These findings are consistent with the expected microbial community in the more reducing conditions of the furrow and more aerated status of the berm. These finding supports the hypothesis that long-term differences in soil moisture regimes and management may lead to distinct microbial communities that drive contrasting respiration/CO_2 flux patterns and solid phase C chemistry.

2.5 Conclusions

Using a combination of cutting-edge analytical tools and a systems-level approach, we unraveled the network of physical, microbiological, and chemical controls on C dynamics within furrow irrigated and semi-arid agricultural lands. This research has demonstrated that due to the difference in magnitude and frequency of water input, furrow and berm soils have opposing CO_2 flux dynamics leading to a highly heterogeneous landscape. When furrow soils are flooded, slowed oxygen diffusion limits aerobic

respiration, suppressing CO_2 flux; the magnitude of CO_2 flux increases upon drying. Using synchrotron X-ray methods, we demonstrated that carbon associated with minerals from furrow soils is characterized by higher aromaticity compared to berm soil carbon which is likely stabilized by calcium-ion bridging. The composition of microbial communities within furrow soils corroborates the chemical characteristics, being dominated by fermenters and anaerobic bacteria that thrive on simple organic acids. In contrast, when rainfall wets berm soils after a prolonged dry period, increased pore network connectivity and microbial death contribute to a large immediate pulse of soil CO_2. The relatively drier, more seasonally influenced berm soil shows a larger fraction of C co-precipitated with redox active minerals, which is not as strongly bound as C associated with mineral surfaces. The microbial communities within the berm soils are relatively more diverse than those in the furrow with a wider range of metabolisms represented, leading to less selectivity in the carbon substrates used for respiration. Pore-water analysis shows that the majority of that substate pool is composed of complex hydrocarbons, lignin, and lipids with low C nominal oxidation state (NOSC), whereas pore water substrates within redox fluctuating furrow soils are dominated by compounds with higher nominal oxidation states. Organic substrates with higher NOSC are more energetically favorable for microbes to metabolize, but we do not observe higher rates of CO_2 flux from these redox fluctuating zones. These findings together suggest that there is a stabilizing mechanism for carbon in furrow irrigated soils and is likely to apply to other gravity irrigated soils that similarly undergo drastic redox fluctuations.

2.6 References

Bailey, V. L., A. P. Smith, M. Tfaily, S. J. Fansler, and B. Bond-Lamberty. 2017. "Differences in Soluble Organic Carbon Chemistry in Pore Waters Sampled from Different Pore Size Domains." Soil Biology and Biochemistry 107 (April): 133–43. https://doi.org/10.1016/j.soilbio.2016.11.025.

Bhattacharyya, Amrita, Ashley N. Campbell, Malak M. Tfaily, Yang Lin, Ravi K. Kukkadapu, Whendee L. Silver, Peter S. Nico, and Jennifer Pett-Ridge. 2018. "Redox Fluctuations Control the Coupled Cycling of Iron and Carbon in Tropical Forest Soils." Environmental Science & Technology 52 (24): 14129–39. https://doi.org/10.1021/acs.est.8b03408.

Birch, H. F. 1958. "The Effect of Soil Drying on Humus Decomposition and Nitrogen Availability." Plant and Soil 10 (1): 9–31. https://doi.org/10.1007/BF01343734.

Boye, Kristin, Vincent Noël, Malak M. Tfaily, Sharon E. Bone, Kenneth H. Williams, John R. Bargar, and Scott Fendorf. 2017. "Thermodynamically Controlled Preservation of Organic Carbon in Floodplains." Nature Geoscience 10 (6): 415–19. https://doi.org/10.1038/ngeo2940.

Brown, Sandra, and Ariel E. Lugo. 1982. "The Storage and Production of Organic Matter in Tropical Forests and Their Role in the Global Carbon Cycle." Biotropica 14 (3): 161–87. https://doi.org/10.2307/2388024.

Cable, Jessica M., and Travis E. Huxman. 2004. "Precipitation Pulse Size Effects on Sonoran Desert Soil Microbial Crusts." Oecologia 141 (2): 317–24. https://doi.org/10.1007/s00442-003-1461-7.

Caporaso, J. Gregory, Kyle Bittinger, Frederic D. Bushman, Todd Z. DeSantis, Gary L. Andersen, and Rob Knight. 2010. "PyNAST: A Flexible Tool for Aligning Sequences to a Template Alignment." Bioinformatics 26 (2): 266–67. https://doi.org/10.1093/bioinformatics/btp636.

Chen, Jin Y., Huanhuan Jiang, Stacy Jy Chen, Cody Cullen, C. M. Sabbir Ahmed, and Ying-Hsuan Lin. 2019. "Characterization of Electrophilicity and Oxidative Potential of Atmospheric Carbonyls." Environmental Science: Processes & Impacts 21 (5): 856–66. https://doi.org/10.1039/C9EM00033J.

Davidson, Eric A., and Ivan A. Janssens. 2006. "Temperature Sensitivity of Soil Carbon Decomposition and Feedbacks to Climate Change." Nature 440 (7081): 165–73. https://doi.org/10.1038/nature04514.

DeAngelis, Kristen M., Whendee L. Silver, Andrew W. Thompson, and Mary K. Firestone. 2010. “Microbial Communities Acclimate to Recurring Changes in Soil Redox Potential Status: Fluctuating Redox Microbial Communities.” Environmental Microbiology 12 (12): 3137–49. https://doi.org/10.1111/j.1462-2920.2010.02286.x.

DWR. 2020. “Agricultural Water Use Efficiency.” California Department of Water Resources. 2020. http://water.ca.gov/Programs/Water-Use-And-Efficiency/Agricultural-Water-Use-Efficiency.

Edgar, Robert C. 2010. “Search and Clustering Orders of Magnitude Faster than BLAST.” Bioinformatics 26 (19): 2460–61. https://doi.org/10.1093/bioinformatics/btq461.

———. 2013. “UPARSE: Highly Accurate OTU Sequences from Microbial Amplicon Reads.” Nature Methods 10 (10): 996–98. https://doi.org/10.1038/nmeth.2604.

Edgar, Robert C., Brian J. Haas, Jose C. Clemente, Christopher Quince, and Rob Knight. 2011. “UCHIME Improves Sensitivity and Speed of Chimera Detection.” Bioinformatics 27 (16): 2194–2200. https://doi.org/10.1093/bioinformatics/btr381.

Fang, C, and J. B Moncrieff. 2001. “The Dependence of Soil CO2 Efflux on Temperature.” Soil Biology and Biochemistry 33 (2): 155–65. https://doi.org/10.1016/S0038-0717(00)00125-5.

Fenchel, Tom, Henry Blackburn, and Gary M. King. 2012. Bacterial Biogeochemistry: The Ecophysiology of Mineral Cycling. Academic Press.

Fierer, Noah, and Joshua P. Schimel. 2002. “Effects of Drying–Rewetting Frequency on Soil Carbon and Nitrogen Transformations.” Soil Biology and Biochemistry 34 (6): 777–87. https://doi.org/10.1016/S0038-0717(02)00007-X.

Gao, Bing, Tao Huang, Xiaotang Ju, Baojing Gu, Wei Huang, Lilai Xu, Robert M. Rees, David S. Powlson, Pete Smith, and Shenghui Cui. 2018. “Chinese Cropping Systems Are a Net Source of Greenhouse Gases despite Soil Carbon Sequestration.” Global Change Biology 24 (12): 5590–5606. https://doi.org/10.1111/gcb.14425.

Gillespie, Adam W., Courtney L. Phillips, James J. Dynes, David Chevrier, Thomas Z. Regier, and Derek Peak. 2015. “Chapter One - Advances in Using Soft X-Ray Spectroscopy for Measurement of Soil Biogeochemical Processes.” In Advances in Agronomy, edited by Donald L. Sparks, 133:1–32. Academic Press. https://doi.org/10.1016/bs.agron.2015.05.003.

Guo, Xiaobin, Craig F. Drury, Xueming Yang, and W. Daniel Reynolds. 2014. “Water-Soluble Carbon and the Carbon Dioxide Pulse Are Regulated by the Extent of Soil Drying and Rewetting.” Soil Science Society of America Journal 78 (4): 1267–78. https://doi.org/10.2136/sssaj2014.02.0059.

Homyak, Peter M., Joseph C. Blankinship, Eric W. Slessarev, Sean M. Schaeffer, Stefano Manzoni, and Joshua P. Schimel. 2018. “Effects of Altered Dry Season Length and Plant Inputs on Soluble Soil Carbon.” Ecology 99 (10): 2348–62. https://doi.org/10.1002/ecy.2473.

Jastrow, J. D. 1996. “Soil Aggregate Formation and the Accrual of Particulate and Mineral-Associated Organic Matter.” Soil Biology and Biochemistry 28 (4): 665–76.
Jenerette, G. Darrel, and Amitava Chatterjee. 2012. “Soil Metabolic Pulses: Water, Substrate, and Biological Regulation.” Ecology 93 (5): 959–66. https://doi.org/10.1890/11-1527.1.

Johnson, Jane M. -F., Alan J. Franzluebbers, Sharon Lachnicht Weyers, and Donald C. Reicosky. 2007. “Agricultural Opportunities to Mitigate Greenhouse Gas Emissions.” Environmental Pollution 150 (1): 107–24. https://doi.org/10.1016/j.envpol.2007.06.030.

Johnson, Renée, and Betsy A Cody. 2015. “California Agricultural Production and Irrigated Water Use,” June, 28.

Kaiser, K., and G. Guggenberger. 2003. “Mineral Surfaces and Soil Organic Matter.” European Journal of Soil Science 54 (2): 219–36. https://doi.org/10.1046/j.1365-2389.2003.00544.x.

Kakumanu, Madhavi L., Li Ma, and Mark A. Williams. 2019. “Drought-Induced Soil Microbial Amino Acid and Polysaccharide Change and Their Implications for C-N Cycles in a Climate Change World.” Scientific Reports 9 (1): 10968. https://doi.org/10.1038/s41598-019-46984-1.

Kallenbach, Cynthia M., Dennis E. Rolston, and William R. Horwath. 2010. “Cover Cropping Affects Soil N2O and CO2 Emissions Differently Depending on Type of Irrigation.” Agriculture, Ecosystems & Environment 137 (3): 251–60. https://doi.org/10.1016/j.agee.2010.02.010.

Kleber, M., P. Sollins, and R. Sutton. 2007. “A Conceptual Model of Organo-Mineral Interactions in Soils: Self-Assembly of Organic Molecular Fragments into Zonal Structures on Mineral Surfaces.” Biogeochemistry 85 (1): 9–24. https://doi.org/10.1007/s10533-007-9103-5.

LaRowe, Douglas E., and Philippe Van Cappellen. 2011. “Degradation of Natural Organic Matter: A Thermodynamic Analysis.” Geochimica et Cosmochimica Acta 75 (8): 2030–42. https://doi.org/10.1016/j.gca.2011.01.020.
Lehmann, Johannes, Biqing Liang, Dawit Solomon, Mirna Lerotic, Flavio Luizão, James Kinyangi, Thorsten Schäfer, Sue Wirick, and Chris Jacobsen. 2005. “Near-Edge X-Ray Absorption Fine Structure (NEXAFS) Spectroscopy for Mapping Nano-Scale Distribution

of Organic Carbon Forms in Soil: Application to Black Carbon Particles." Global Biogeochemical Cycles 19 (1). https://doi.org/10.1029/2004GB002435.

Lopez-Sangil, Luis, Iain Hartley, Pere Rovira, Pere Casals, and Emma J. Sayer. 2018. "Drying and Rewetting Conditions Differentially Affect the Mineralization of Fresh Plant Litter and Extant Soil Organic Matter." June 7, 2018. https://doi.org/10.1016/j.soilbio.2018.06.001.

Love, Michael I., Wolfgang Huber, and Simon Anders. 2014. "Moderated Estimation of Fold Change and Dispersion for RNA-Seq Data with DESeq2." Genome Biology 15 (12): 550. https://doi.org/10.1186/s13059-014-0550-8.

Lundquist, E. J, L. E Jackson, and K. M Scow. 1999. "Wet–Dry Cycles Affect Dissolved Organic Carbon in Two California Agricultural Soils." Soil Biology and Biochemistry 31 (7): 1031–38. https://doi.org/10.1016/S0038-0717(99)00017-6.

Mehra, O. P., and M. L. Jackson. 2013. "IRON OXIDE REMOVAL FROM SOILS AND CLAYS BY A DITHIONITE–CITRATE SYSTEM BUFFERED WITH SODIUM BICARBONATE." In Clays and Clay Minerals, edited by EARL Ingerson, 317–27. Pergamon. https://doi.org/10.1016/B978-0-08-009235-5.50026-7.

Moni, C., D. Derrien, P.-J. Hatton, B. Zeller, and M. Kleber. 2012. "Density Fractions versus Size Separates: Does Physical Fractionation Isolate Functional Soil Compartments?" Biogeosciences 9 (12): 5181–97. https://doi.org/10.5194/bg-9-5181-2012.

Navarro-García, Federico, Miguel Ángel Casermeiro, and Joshua P. Schimel. 2012. "When Structure Means Conservation: Effect of Aggregate Structure in Controlling Microbial Responses to Rewetting Events." Soil Biology and Biochemistry 44 (1): 1–8. https://doi.org/10.1016/j.soilbio.2011.09.019.

Pérez Castro, Sherlynette, Elsa E. Cleland, Robert Wagner, Risha Al Sawad, and David A. Lipson. 2019. "Soil Microbial Responses to Drought and Exotic Plants Shift Carbon Metabolism." The ISME Journal 13 (7): 1776–87. https://doi.org/10.1038/s41396-019-0389-9.

Pett-Ridge, J., and M. K. Firestone. 2005. "Redox Fluctuation Structures Microbial Communities in a Wet Tropical Soil." Appl. Environ. Microbiol. 71 (11): 6998–7007. https://doi.org/10.1128/AEM.71.11.6998-7007.2005.

Poulton, Simon W., and Donald E. Canfield. 2005. "Development of a Sequential Extraction Procedure for Iron: Implications for Iron Partitioning in Continentally Derived Particulates." Chemical Geology 214 (3): 209–21. https://doi.org/10.1016/j.chemgeo.2004.09.003.

Price, Morgan N., Paramvir S. Dehal, and Adam P. Arkin. 2010. “FastTree 2 – Approximately Maximum-Likelihood Trees for Large Alignments.” PLOS ONE 5 (3): e9490. https://doi.org/10.1371/journal.pone.0009490.

Rasmussen, Craig, Katherine Heckman, William R. Wieder, Marco Keiluweit, Corey R. Lawrence, Asmeret Asefaw Berhe, Joseph C. Blankinship, et al. 2018. “Beyond Clay: Towards an Improved Set of Variables for Predicting Soil Organic Matter Content.” Biogeochemistry 137 (3): 297–306. https://doi.org/10.1007/s10533-018-0424-3.

Ravel, B., and M. Newville. 2005. “ATHENA, ARTEMIS, HEPHAESTUS: Data Analysis for X-Ray Absorption Spectroscopy Using IFEFFIT.” Journal of Synchrotron Radiation 12 (4): 537–41. https://doi.org/10.1107/S0909049505012719.

Sapkota, Anish, Amir Haghverdi, Claudia C. E. Avila, and Samantha C. Ying. 2020. “Irrigation and Greenhouse Gas Emissions: A Review of Field-Based Studies.” Soil Systems 4 (2): 20. https://doi.org/10.3390/soilsystems4020020.

Schimel, Joshua P. 2018. “Life in Dry Soils: Effects of Drought on Soil Microbial Communities and Processes.” Annual Review of Ecology, Evolution, and Systematics 49 (1): 409–32. https://doi.org/10.1146/annurev-ecolsys-110617-062614.

Schloss, Patrick D., Sarah L. Westcott, Thomas Ryabin, Justine R. Hall, Martin Hartmann, Emily B. Hollister, Ryan A. Lesniewski, et al. 2009. “Introducing Mothur: Open-Source, Platform-Independent, Community-Supported Software for Describing and Comparing Microbial Communities.” Applied and Environmental Microbiology 75 (23): 7537–41. https://doi.org/10.1128/AEM.01541-09.

Six, J., K. Paustian, E. T. Elliott, and C. Combrink. 2000. “Soil Structure and Organic Matter I. Distribution of Aggregate-Size Classes and Aggregate-Associated Carbon.” Soil Science Society of America Journal 64 (2): 681–89.

Smith, Chris R., Peter L. Blair, Charlie Boyd, Brianne Cody, Alexander Hazel, Ashley Hedrick, Hitesh Kathuria, et al. 2016. “Microbial Community Responses to Soil Tillage and Crop Rotation in a Corn/Soybean Agroecosystem.” Ecology and Evolution 6 (22): 8075–84. https://doi.org/10.1002/ece3.2553.

Smith, Louis Ds. 1975. “Common Mesophilic Anaerobes, Including Clostridium Botulinum and Clostridium Tetani, in 21 Soil Specimens.” Applied Microbiology 29 (5): 590–94.

Sollins, Phillip, Christopher Swanston, Markus Kleber, Timothy Filley, Marc Kramer, Susan Crow, Bruce A. Caldwell, Kate Lajtha, and Richard Bowden. 2006. “Organic C and N Stabilization in a Forest Soil: Evidence from Sequential Density Fractionation.” Soil Biology and Biochemistry, Ecosystems in Flux: Molecular and stable isotope Assessments

of Soil Organic Matter Storage and Dynamics, 38 (11): 3313–24. https://doi.org/10.1016/j.soilbio.2006.04.014.

Solomon, Dawit, Johannes Lehmann, James Kinyangi, Biqing Liang, and Thorsten Schäfer. 2005. "Carbon K-Edge NEXAFS and FTIR-ATR Spectroscopic Investigation of Organic Carbon Speciation in Soils." Soil Science Society of America Journal 69 (1): 107. https://doi.org/10.2136/sssaj2005.0107dup.

Thompson, Aaron, Diego Barcellos, Christine O'Connell, Whendee L. Silver, and Christof Meile. 2018. "Hot Spots and Hot Moments of Soil Moisture Explain Fluctuations in Iron and Carbon Cycling in a Humid Tropical Forest Soil." November 1, 2018. https://www.mdpi.com/2571-8789/2/4/59.

Torn, Margaret S., Susan E. Trumbore, Oliver A. Chadwick, Peter M. Vitousek, and David M. Hendricks. 1997. "Mineral Control of Soil Organic Carbon Storage and Turnover." Nature 389 (6647): 170–73. https://doi.org/10.1038/38260.

Wang, Qiong, George M. Garrity, James M. Tiedje, and James R. Cole. 2007. "Naïve Bayesian Classifier for Rapid Assignment of RRNA Sequences into the New Bacterial Taxonomy." Applied and Environmental Microbiology 73 (16): 5261–67. https://doi.org/10.1128/AEM.00062-07.

Xiang, Shu-Rong, Allen Doyle, Patricia A. Holden, and Joshua P. Schimel. 2008. "Drying and Rewetting Effects on C and N Mineralization and Microbial Activity in Surface and Subsurface California Grassland Soils." Soil Biology and Biochemistry 40 (9): 2281–89. https://doi.org/10.1016/j.soilbio.2008.05.004.

Zhao, Qian, Sarrah Dunham-Cheatham, Dinesh Adhikari, Chunmei Chen, Aman Patel, Simon R. Poulson, Daniel Obrist, et al. 2020. "Oxidation of Soil Organic Carbon during an Anoxic-Oxic Transition." Geoderma 377 (November): 114584. https://doi.org/10.1016/j.geoderma.2020.114584.

Chapter 3: Seasonality Effects on Soil Carbon Pools of Furrow Irrigated Soils

3.0 Abstract

Maintaining and sequestering soil carbon provides an array of societal and environmental benefits including improved agricultural yields and soil health while also contributing to climate change mitigation. It is estimated that agricultural soils have the greatest potential for sequestering C, but this potential has been difficult to accurately predict due to spatiotemporal heterogeneity in soil biogeochemistry caused by seasonality and variations in management practices. Past studies have shown that non-irrigated soils exhibit seasonal variations in total soil carbon; however, contributions to these temporal variations by specific C pools—which are more indicative of C emission potential—is lacking, especially in irrigated crop systems. Furrow irrigated fields provide an opportunity to compare seasonal trends in biogeochemical effects of contrasting soil moisture regimes, where furrow soils are regularly flooded and dried on a biweekly basis while berm soils remain dry with only water delivered through rainfall. Here, we report seasonal variation in soil C at a furrow-irrigated orchard under a Mediterranean climate by characterizing temporal trends in total C and N, labile C, C:N, $\delta^{13}C$, and $\delta^{15}N$ over the course of a year. We further quantified the short-lived C pool during the wet and dry season in berm and furrow soils. On average, total soil C is consistently greater in the berm than in the furrow likely from litter accumulation, nitrogen limitations, and inhibited access to carbon substrates by soil microbes; however, no seasonal trends in total C was observed. In contrast, the labile C pool did show seasonal trends in the berm but not in the furrow. The only observed seasonally-associated change in the furrow soils for the parameters

measured was a dramatic C:N decrease over the wet season likely caused by the sustained anoxic conditions that limit organic decomposition. By evaluating the short-lived C pool, we attributed seasonal trends exhibited in the berm as being caused by a pulse of mass microbial death at the onset of the wet season followed by an increase in weed growth as soils dried. The findings from this study can help parameterize belowground processes within ecological models to more accurately estimate C sequestration in Mediterranean furrow irrigated orchard ecosystems.

3.1 Introduction

Soils account for the largest terrestrial resource for sequestering carbon (C), where estimations range from 0.4 Pg of C yr^{-1} in natural landscapes (Lal 2005) to 0.9 - 1.85 Pg C yr^{-1} in managed ecosystems (Zomer et al. 2017). Inputs and outputs of C can vary considerably in agricultural soils making it difficult to capture how such managed soils will fare as climate changes (Thornton 2012). Many best management practices have evolved to increase the carbon sequestering capacity of soils, which have a variety of productive benefits, including increased infiltration, reduced erosion, and increased nutrient uptake, all of which can improve crop yields (Lal 2005; Quinton et al. 2010; Reicosky 2003; Lal 2004). However, large swaths of managed soils have shifted from being carbon sinks to sources (Vermeulen, Campbell, and Ingram 2012; Paustian et al. 2000). With the expanding need for arable land, agricultural soils are currently estimated to have the largest potential for increasing topsoil C stocks (Chen et al. 2019).

Estimating C budgets in managed soils has typically been done by identifying C outputs, such as heterotrophic respiration, leaching, and erosion; and C inputs, such as fertilizer application, root exudates, and litter accumulation. The soil C accounting can vary widely depending on the climatic conditions, crop type, and specific management decisions, such as the incorporation of cover crops, residue management, and tillage intensity. When assessing the potential to achieve the "4 per mille" (Minasny et al. 2017) initiative to increase soil organic C (SOC) stocks and decrease greenhouse gas (GHG) emissions globally, a comprehensive analysis of Mediterranean agricultural soils found that adding organic amendments led to a significantly larger increase (1.5 times) in SOC storage rates if the addition was made to woody crops when compared to arable crops (Francaviglia et al. 2019) revealing the importance of understanding the variability in C pools in these types of crop systems.

A previous study of a Mediterranean dryland farm system found that seasonal variability was observed in biogeochemical parameters (total organic C, water soluble C, labile C, microbially biomass C), more significantly in the amount of bioavailable C, than was observed in total organic C content between spring and autumn sampling events (Panettieri et al. 2015). Seasonal variations in C dynamics are to be expected in soils that receive no additional water in a Mediterranean climate, but it is unclear if these changes occur at the onset of the wet season or are depleted/accumulated slowly when temporal resolution of sampling is limited to the start and end of a growing season. Additionally, frequent drying/re-wetting in regularly irrigated crop systems has been shown to increase dissolved organic C but does not correspond to additional C loss via respiration. This is

particularly notable for soils that are not conventionally tilled, identifying the need to capture the range in spatiotemporal variation in soils that are tilled and irrigated within similar regions (Lundquist, Jackson, and Scow 1999; Schaefer et al. 2020).

A multi-year study of C in rainfed crops under various tillage practices revealed that soil organic C can follow seasonal trends which were highly dependent on soil management (Wuest 2014). This study highlighted the importance of temporal variability that could bias C sequestration estimations of managed soils, particularly if ecosystem-imposed controls are not accounted for (seasonal precipitation and temperature). However, the contributions to total C by various C pools was not estimated but hypothesized to be the driving influence for observed seasonal variation. Additionally, spatial heterogeneity in soil organic C has been widely documented (Post et al. 2001) but spatial heterogeneity imposed by irrigation (wet-dry and dry zones) further complicates C assessments in managed ecosystems.

In this study, we aim to characterize the fluctuations in soil C pools in the topsoil of orchards in a semi-arid Mediterranean climate zone by comparing regions of contrasting soil moisture fluctuations over the course of a year. Our questions in this study included 1) how does the frequency and magnitude of change in volumetric water content contributed by infrequent rainfall versus frequent irrigation events lead to contrasting concentrations in various types of soil C pools; 2) what are the potential mechanisms leading to greater or lesser variability in these contrasting soil moisture zones; 3) what, if any, seasonal trends can be observed in the soil C and N concentrations over the course of a year.

3.2 Materials and Methods

3.2.1 Field description and sampling

Soils were sampled over the course of one year from a Washington Navel orange orchard utilizing furrow irrigation for over a hundred years in Riverside's historic citrus region in Riverside County, California (33.9086 N, 117.4295 W). There are approximately 400 trees within 4 acres of the property and has a total of 15 furrows on the SW region and 8 furrows on the NE region of the orchard (drone images included in SI), each with a water source at the top of the graded field with unlined furrows that are reconstructed approximately five times throughout the year using disk ridger and maintained manually with a shovel when needed. The region is a hot semi-arid Mediterranean climate, and the field site soil is characterized as an Alfisol with a loamy sand surface texture (surface pH 7.0, 1 dS m^{-1} EC). The mean annual air temperature is 17°C and the annual precipitation is 305 mm, which is typically deposited in the winter months. The dry season, which typically extends from June- October, often reaches air temperature of 35°C and above. The orchard is certified organic, and the only managed inputs are fish fertilizer and horse manure, which are typically only applied to segments of the field at one time.

Soils at the orchard can be described as two main categories: 1) the dry zone at the base of the trees which receives water only through rainfall events (hereafter referred to as "berm") and 2) the wet-dry fluctuating zones where water is gravity deposited within the furrows and allowed to dry between irrigation events (hereafter referred to as "furrow"). Triplicate soil moisture sensors (Decagon 5TM, Decagon Devices, Pullman, WA, USA)) were placed within different furrows and berm soils at a depth of 10 cm below surface and

measured at 5-minute intervals for 365 continuous days (EM50 Datalogger, Decagon Devices, Pullman, WA, USA). Daily precipitation data from a nearby California irrigation management information system (CIMIS) station (California Department of Water Resources; UC Riverside Station 044) was used to record rain events (mm day $^{-1}$) in the region.

Five surface soils (0 - 10 cm depth) were collected from both the berm and furrow (10 samples per sampling date) on 17 different days between February 2019 and February 2020 (2/8/2019 2/27, 3/8, 4/2, 4/19, 5/6, 5/22, 6/21, 7/12, 7/22, 8/13, 8/23, 9/4, 9/19 10/12, 1/14, 2/7/2020 and each time soil was sampled from different furrow and the berm soils were collected within 1 – 2 meters of the furrow sampling point. Samples were transported to the laboratory within 2 hrs and immediately air-dried at room temperature for 5 - 14 days; ground with mortar and pestle; and homogenized to <2 mm for solid phase characterization and chemical extractions and assays.

3.2.2 Solid Phase Analysis

A subset of the soils was further ground and homogenized to a finer particle size (<0.15 mm) and analyzed for total C, total N, C/N, $\delta^{13}C$, and $\delta^{15}N$ (Costech ECS4010 Elemental Analyzer coupled through Thermo Scientific Conflo IV to Thermo Scientific Delta V Advantage Isotope Ratio Mass Spectrometer). First, 25 mg of soil were precisely weighed in 5 x 9 mm tin capsules for C and N analysis; USGS 64 & 66 (glycine), acetanilide, and an internal soil standard reference material were used for calibration and

peach leaves (NIST1547) were utilized as a quality check. Isotopic values were reported in δ notation (‰), where δ is calculated as

$$\delta = \frac{[R_{sample} - R_{standard}]}{R_{standard}} \times 1000\ ‰ \quad (3.1)$$

where R is the ratio of the heavy isotope to light isotope and the reference material for $\delta^{13}C$ is Vienna Pee Dee Belemnite (VPDB) and atmospheric N_2 for $\delta^{15}N$. C/N ratios were normalized from mass by calculating [(% C by weight of sample/12)]/[(% N by weight of sample/14)]. Bulk elemental concentrations were measured using energy-dispersive X-ray fluorescence (ED-XRF) spectroscopy (Spectro XEPOS). Carbonate concentrations were measured using an automated CO_2 coulometric method (Coulometrics, model 5030) using a pure carbonate standard reference material, an internal lab standard of know carbonate concentration, and a blank for background CO_2 concentrations.

3.2.3 Chemical extractions

Permanganate oxidizable carbon

Active C pool in soil samples was estimated by measuring POXC fraction as described by Culman et al. (2012). Approximately 2.5 g (± 0.05 g) of air-dried soil was mixed with 18 mL of ultrapure water and 2 mL 0.2 M $KMnO_4$ prepared with 1.4 M $CaCl_2$ and pH adjusted to 7.2 with 0.1 N NaOH. Samples were shaken on an oscillating shaker (120 rpm) for 2 min and allowed to settle for 10 min. Approximately 0.5 mL of the supernatant was then immediately diluted with 49.5 mL of ultrapure water and analyzed on a spectrophotometer at 550 nm (using DDI water as blank) and compared to a standard curve of known $KMnO_4$ concentrations (0.05, 0.01, 0.015, and 0.02 M $KMnO_4$) that were

diluted in the same way as the treated soil extracts. POXC was then calculated as described by Weil et al. (2003):

$$POXC\ (mg\ kg^{-1}) = [0.02\ mol\ L^{-1} - (a + b \times Abs)] \times (9000\ mg\ C\ mol^{-1}) \times (0.02\ L\ solution/Wt.) \quad (3.2)$$

where *a* is the intercept of the standard curve; *b* is the slope of the standard curve; *Abs* is the measured absorbance of the unknown; 9000 = mg of C oxidized by 1 mole of MnO_4 ($Mn^{7+} \rightarrow Mn^{4+}$); and *Wt* is the weight of the air-dried soil sample in kg. Standards were made fresh each day of the analysis and the stock 0.2 M $KMnO_4$ solution was remade every 3 months. A homogenized internal lab soil standard that has been previously and repeatedly measured for POXC of similar mass and particle size was also analyzed each time the unknown samples were measured to ensure permanganate solution was still viable and contaminant free. A solution blank (ultrapure water) was also included every 10 samples to check for solution reduction or C contamination in the reaction process. Recently, there has been some new evidence to suggest that this method could result in an inaccurate estimation of the labile C pool, specifically if the method of homogenization (mass and sieve size used) differs between field sites (Pulleman et al. 2021). However, as this method was used in this study to estimate the active C pool within the same field site, similar mass (2.5 g) and identical particle homogenization (< 0.25 mm) was done in preparing the soils for analysis, as has been recommended to ensure repeatability (Wade et al. 2020).

Water extractable organic carbon

Water extractable organic C was measured in samples with the maximum (wet season) and minimum (dry season) active C pool concentrations as indicated by POXC in

both soils to elucidate the maximum and minimum bioavailable C. The wet season is represented by samples taken on 4/2, 4/19, and 5/6 and the dry season is represented by soils taken on 7/22, 8/13, and 8/23. 32 mL of deionized water was added to 8 g of homogenized soil from the berm or furrow, shaken on an oscillating shaker (120 rpm) for 4 hrs, and then centrifuged for 30 min (2,000 x g) then decanted and filtered with 0.2 µm syringe filter. The filtered extracts were then analyzed for total organic C (TOC-V CSN, Shimadzu Scientific Instruments, Columbia, Maryland, USA). Carbonate concentrations were measured in berm and furrow soils using an automated coulometric method, and were found to be low in both soils (< 0.02 %) (Table S1); therefore, total C is assumed to closely approximate total organic C.

3.2.4. Microbial fumigation

Microbial biomass C was measured using chloroform fumigation extraction as described by Fierer and Schimel (2002). Two treatments were applied to each sample: 1) 8 g of homogenized soil was reacted with 40 mL of 0.5 M K_2SO_4; 2) 8 g of homogenized soil reacted with 0.5 mL of ethanol-free chloroform followed by 40 mL of 0.5 M K_2SO_4. The slurries were then capped and placed on an orbital shaker (150 rev min^{-1}) for 4 hrs. Both sets of samples were then bubbled for 20 min with a manifold tubing system with lab air to allow for degassing of chloroform and to ensure the same treatment was applied for all samples. Tubes containing the K_2SO_4-only treated soil and the glass bottles containing the chloroformed soils were then allowed to sit for 10 min. Approximately 20-30 mL of the soil extracts were then gravity filtered with filter paper (Whatman No.1) and then

analyzed for total organic C (TOC-V CSN, Shimadzu Scientific Instruments, Columbia, Maryland, USA). The difference between C concentration in the chloroform fumigated sample and the K_2SO_4-only extracted sample represents the "flush" of C held in microbial biomass without correcting for extraction efficiency.

3.2.5 Statistical analyses and data transformations

The annual survey data were tested for normality using a Shapiro-Wilk test. Those that did exhibit normal distribution (POXC, $\delta^{15}N$, and elemental concentrations Na, Ca, and Fe) where then compared (berm vs furrow) using a t-test. Those measured values that did not meet the criteria for parametric statistical analyses (total C, total N, $\delta^{13}C$, C/N, and elemental concentrations Mg, Al, Si, P, and S) were then compared using a Wilcoxon Signed-rank test. Means are reported with ± standard error of the mean. To capture any seasonal variation within the data, averages of each sampling date were standardized against the annual mean for both berm and furrow samples. [(Mean [measured parameter] of that sampling date – annual mean)/(annual standard deviation of the measured parameter).

3.3 Results

3.3.1 Total C

The year-long averaged total C between the berm and furrow was significantly different ($p < 0.05$) with concentrations being higher in the berm soils (mean of 2.16 % C) than in furrow soil (mean of 1.56 % C (Table 3.1). The total C over the course of the year

followed similar trends in both soils, where total C concentration within furrow soils was consistently lower than in berm soils with the exception of one date (9/19) (Figure 3.1), where the berm and furrow soils are not significantly different. Total C was the highest in the peak of the dry season in the berm (July 2019), while the furrow had the most total C observed towards the latter part of the summer (Sept 2019).

3.3.2 Carbon to Nitrogen Ratio

The annual average carbon to nitrogen ratio in the berm was 11.7 and the furrow was 12.0 (Table 3.1). The greatest difference ($p < 0.01$) between the berm and furrow C:N was at the start of the sampling campaign prior to an intense rain event in Feb 2019, with the furrow exhibiting a greater C:N of 15.8 and a C:N of 11.9 in berm soils (Figure 3.1B). However, after the heavy rain event that accounted for 24% of the annual precipitation, the C:N ratio of the berm increased to 16.1 and the furrow decreased slightly to 15.3 but are not statistically significantly different. After subsequent rain events, C:N in both the berm and furrow soil decreased to similar values for the remainder of the year.

3.3.3 $\delta^{13}C$ and $\delta^{15}N$ Stable Isotopes

The $\delta^{13}C$ of the berm and furrow soil C were significantly different ($p < 0.05$) where the furrow soil annual average $\delta^{13}C$ was -24.8 ‰ and the berm average $\delta^{13}C$ was -26.2 ‰ (Table 3.1). The $\delta^{13}C$ of furrow soil C tended to increase after precipitation but fluctuated throughout the summer months (Figure 3.1). $\delta^{13}C$ of berm soil C was less variable (annual standard deviation of 0.66 ‰) compared to furrow (annual standard deviation 1.00 ‰) and changes in response to precipitation did not show any consistent trend. The $\delta^{15}N$ of the

berm and furrow soil were significantly different ($p < 0.05$) with an annual average of 10.2 ‰ in furrow soil and an average 9.6 ‰ in berm soil. The $\delta^{15}N$ of furrow soil showed the greatest deviation from the annual mean in September 2019 during the driest and hottest period while the berm soil had the greatest deviation in $\delta^{15}N$ in Feb 2019 during the wettest period. The $\delta^{15}N$ of the berm was highest in Feb 2019 and decreased to the lowest measured average by Feb 2020 (Figure 3.1). With the exception of the first sampling date prior to the first intense rain event, the berm soils consistently exhibited lower $\delta^{15}N$ than the furrow soil (Figure 3.1).

Table 3.1: The annual average of total C, POXC, total N, $\delta^{13}C$, $\delta^{15}N$, and C:N (± SEM) from furrow and berm soils. Max deviations indicate the largest standard deviation from the annual mean greater than (positive) or less than (negative) the annual average. The time of year when the max positive and negative deviations occur is provided in Figure S4.

Annual		Furrow			Berm		
	Unit	Mean (± SEM)	Max Positive Dev	Max Negative Dev	Mean (± SEM)	Max Positive Dev	Max Negative Dev
Total C[a]	% wt	1.56 ± 0.06	1.27	-1.23	2.16 ± 0.09	0.99	-1.07
POXC[a]	mg kg^{-1}	556.6 ± 21.2	0.72	-0.82	688.7 ± 22.1	1.09	-0.72
Total N	% wt	0.15 ± 0.01	1.36	-1.12	0.22 ± 0.01	0.98	-0.80
$\delta^{13}C$[a]	‰	-24.8± 0.11	1.45	-0.94	-26.2 ± 0.07	0.95	-1.59
$\delta^{15}N$[a]	‰	10.2 ± 0.08	1.27	-0.97	9.6 ± 0.08	1.35	-1.35
C:N	Ratio	12.0 ± 0.19	2.19	-0.79	11.7 ± 0.18	2.73	-1.11

[a] Annual comparisons are significantly different between furrow and berm at $p < 0.05$.

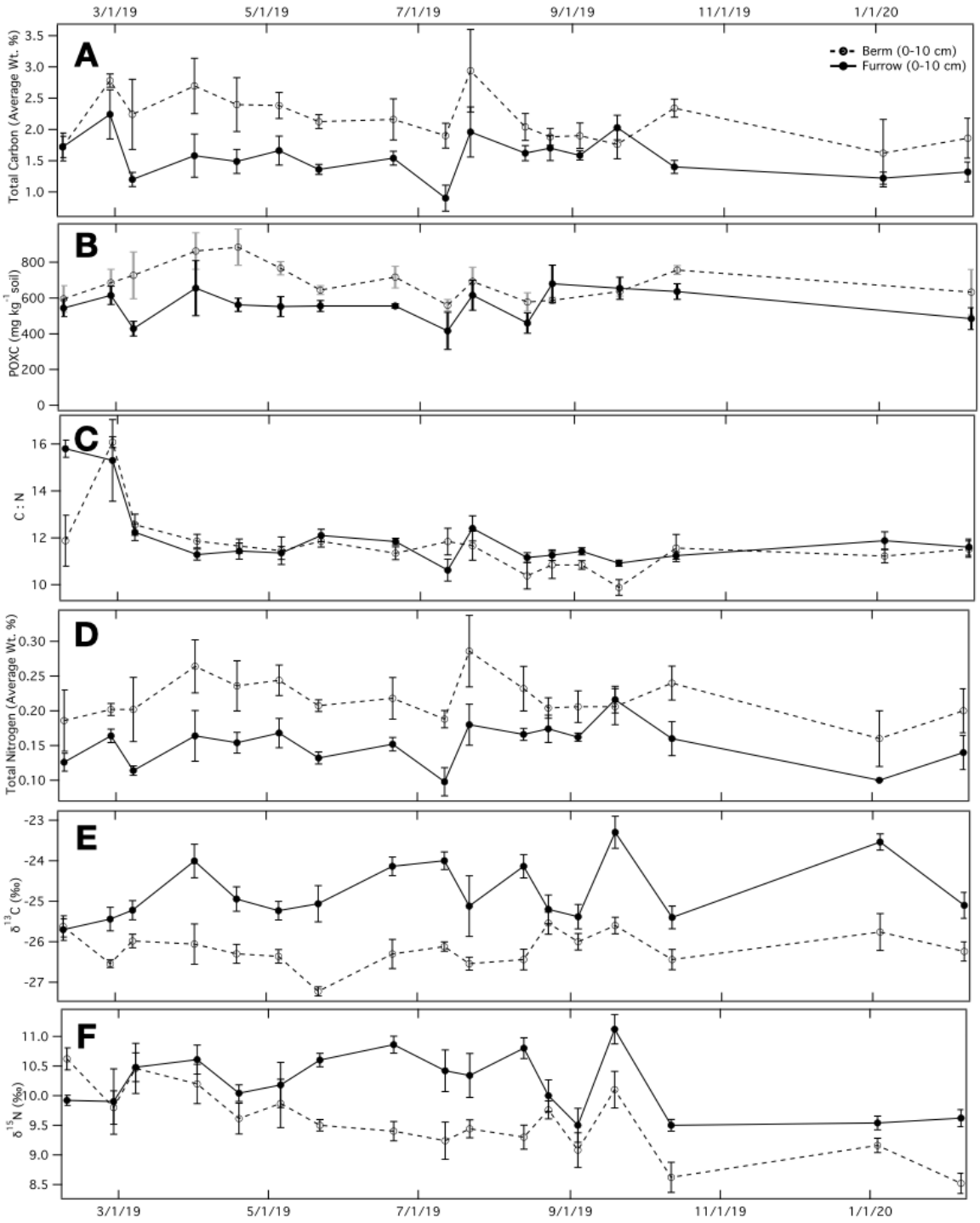

Figure 3.2: The average (± SEM; n = 5) (A) total carbon, (B) permanganate oxidizable carbon, (C) C:N, (D) total N, (E) $\delta^{13}C$, and (F) $\delta^{15}N$ of the berm and furrow soil over the course of a year.

3.3.4 Permanganate Oxidizable Carbon (POXC)

The annual average of the estimated labile carbon pool determined by POXC fraction of the berm and furrow soils were significantly different ($p < 0.05$). The mean POXC for berm soils was 688.7 mg kg^{-1} and the furrow was 556.6 mg kg^{-1}. In general, POXC content in berm soils remained higher than in furrow soils during the wet winter season but were comparable between during the dry summer season. The repeated wet-dry conditions from irrigation in the furrow soils, even after the rainy season, maintained a relatively stable labile C pool until the start of the summer dry season. In contrast, POXC in berm soils continued a steady decrease after the first major rain event in winter, followed by more variability during the dry summer months, though concentrations remained relatively low compared to winter season values. The seasonal trends can be observed by standardizing the labile C pool to the annual average and are provided in Figure A2.3, which show a steady increase in POXC throughout the wet season. The maximum deviation of POXC content from the annual mean was greater in the berm than the furrow, which occurred during the wet winter season; correspondingly, a greater negative deviation from the mean was observed in the berm than furrow during the dry summer months. In contrast, the annual variance in furrow soil POXC was significantly less ($p<0.05$; 9%) than the berm. These results demonstrate that overall seasonal fluctuations in POXC was greater in the berm than the furrow and is also much more spatially variable (Figure A2.4).

3.3.5 Soil and Air Temperature and Moisture

The average soil moisture (VWC) at a depth of 10 cm in the furrow was 0.2 cm^3cm^{-3} with an average increase of 0.10 cm^3cm^{-3} after a 48-hr irrigation event. The average berm

VWC was 0.1 cm^3cm^{-3} with the lowest VWC of 0.02 cm^3 cm^{-3} occurring at the end of the summer, and the highest VWC occurring during the wet season as expected (Figure 3.2A). The soil temperature at 10 cm in the berm varied much more widely than in the furrow soil with an annual average of 18.4°C. In contrast, the furrow soil temperature fluctuated far less, with a slightly higher annual average of 18.8 °C at a depth of 10 cm (Figure 3.2B). The precipitation in the region was mostly limited to the first month and second to last month of this study, with small rain events occurring in May 2019 and most intense rain events occurring in Feb 2019 (Figure 3.2). The average air temperature was the highest in August 2019, which corresponds to when soil temperatures at a depth of 10 cm fluctuated the most within the furrow and berm soils, though temperature fluctuations were greater in the berm soils (Figure 3.2).

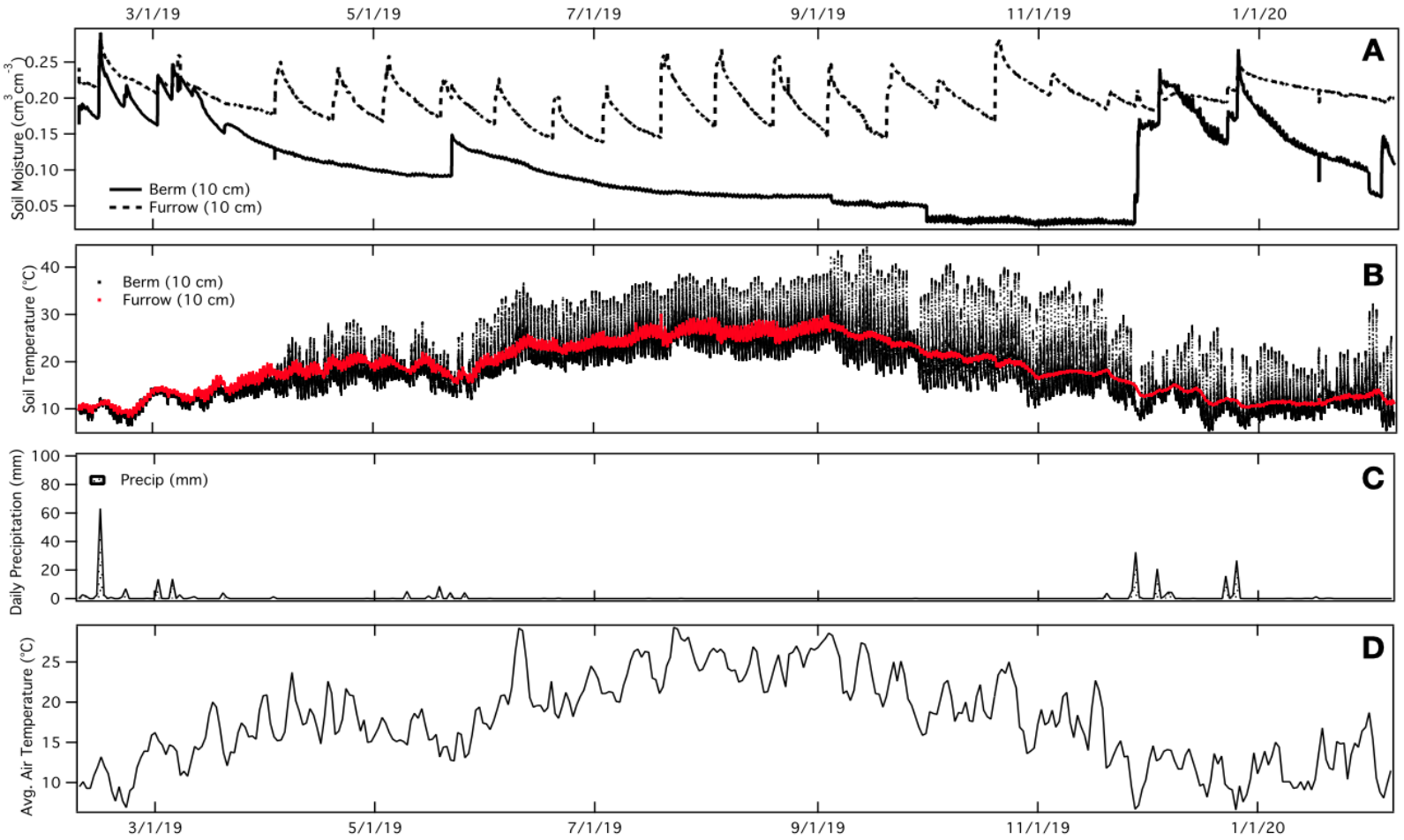

Figure 3: The field conditions of the berm and furrow over the course of the year. A) Average soil moisture (n = 3) of the berm and furrow at a depth of 10 cm. B) Average soil temperature (n = 3) of the berm and furrow at a depth of 10 cm. C) Daily measured precipitation (CIMIS) D) Average daily air temperature in the region (CIMIS).

3.3.6 Water Extractable Organic Carbon

The labile C pool estimated via the POXC fraction is very sensitive to management change, which is why it was utilized for the annual survey trends to capture quick changes in soil chemistry. We utilized the points that were highest (wet season) and lowest (dry season) in the labile C pool to measure the maximum and minimum bioavailable C pool, which is estimated by measuring the water extractable organic C (WEOC) concentration. The average WEOC of berm soils during the wet season was 339.9 µg C g^{-1} soil; berm soil WEOC increased as volumetric water content decreased over the course of a month during the wet season, reaching a maximum concentration of 482.1 µg C g^{-1} soil (Figure 3.3). Berm soil WEOC concentrations then dropped to 202.9 µg C g^{-1} soil during the dry season with very little variation among the three dry-season timepoints. Similarly, WEOC of furrow soils was also higher in the wet season (average concentration of 318.9 µg C g^{-1} soil), which was ~109% greater than the dry season WEOC of the furrow. Berm soils had ~73% higher WEOC concentrations than furrow soils during the dry season.

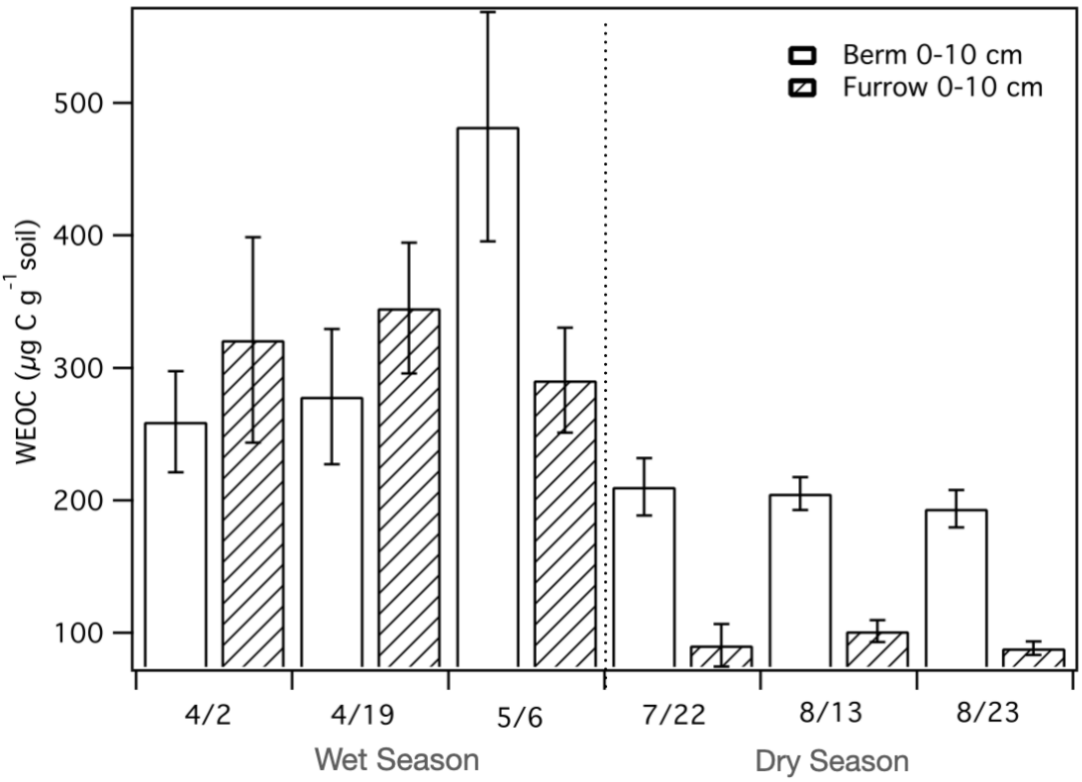

Figure 3.4: The average water extractable organic carbon from berm and furrow soils (± SEM; n = 5). Time points were chosen when the labile carbon pool was the highest (wet season, 4/2, 4/19, and 5/6) and when they were the lowest (dry season, 7/22, 8/13, 8/23) in both soils.

3.3.7 Microbial Biomass C

The microbial biomass flush was the highest in the berm soil at first timepoint of the wet season while MBC in furrow soil is relatively stable across the wet season (Figure 3.4). The mean microbial flush from berm and furrow soils in the wet season was 135.6 µg C g^{-1} soil and 89.1 µg C g^{-1} soil, respectively, but was these means were not statistically significantly different. In both soils, the microbial biomass flush decreased in the dry season (43.6 µg C g^{-1} soil in berm soil; 29.6 µg C g^{-1} soil in furrow soil). The only timepoint where the microbial biomass flush was larger in the furrow was at the peak of the dry season, where the rate of dry down after irrigation is the fastest due to high air and soil

temperatures. The decrease in the microbial biomass flush between the wet and dry season was significantly different in the berm soils ($p<0.01$), but not in the furrow soils.

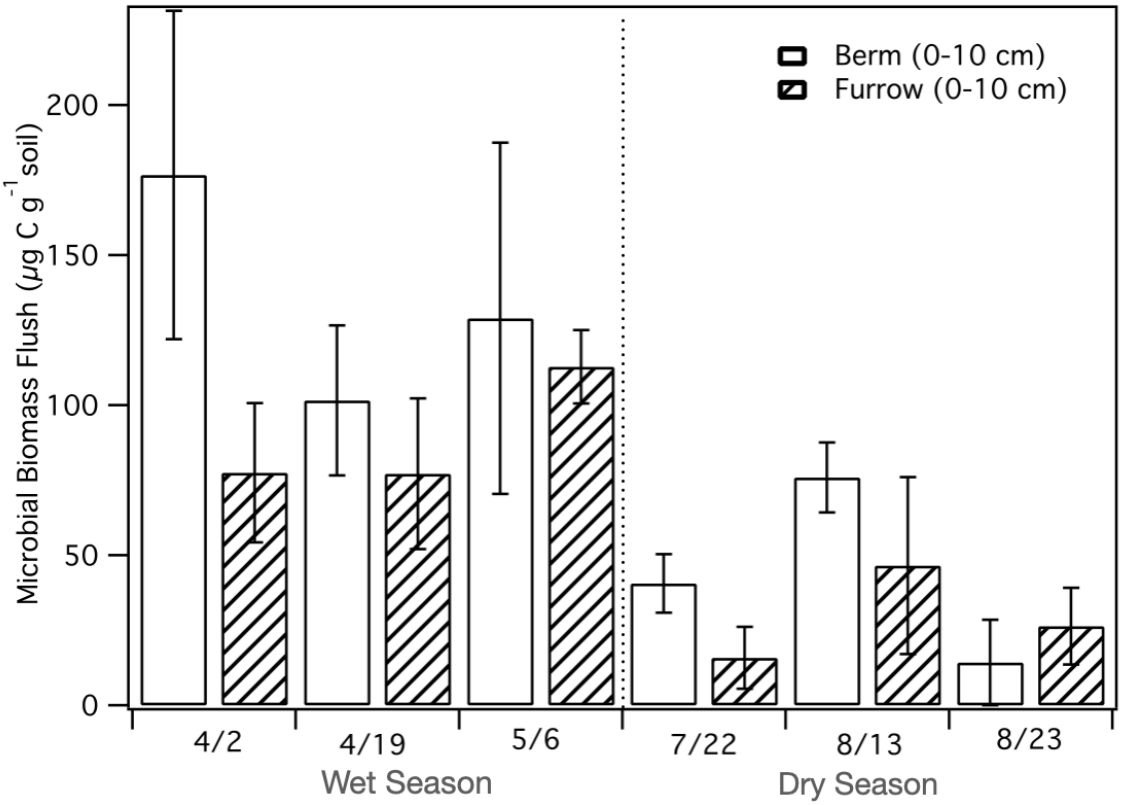

Figure 3.4: The average microbial flush from berm and furrow soils (± SEM; n = 5). Time points were chosen when the labile carbon pool was the highest (wet season, 4/2, 4/19, and 5/6) and when they were the lowest (dry season, 7/22, 8/13, 8/23) in both soils.

3.4 Discussion

3.4.1 Solid phase C and N

There are no obvious trends observed throughout the annual total soil C concentrations to suggest seasonal changes in either the berm or furrow, even when standardized to the annual mean. While the berm only receives water during the wet season, in contrast to furrow soils which are repeatedly undergoing rapid moisture fluctuations, the

onset of precipitation does not correspond necessarily lead to a consistent increase or decrease in the berm soil C pool. Soil organic C has been shown to gradually increase in agricultural soils in long-term studies under conservation tillage practices, likely due to increased aggregation (Awale, Emeson, and Machado 2017), where crop residues and soil organic matter can be physically occluded from microbial degradation. A previous study investigating row crops under varying tillage treatments showed seasonal trends in total organic C, with the most prominent seasonal trends observed under no-till management, though seasonal patterns in soil C concentrations did also emerge from conventionally tilled soil (Wuest 2014). In this orchard, tillage was only done on the furrow soil to maintain water flow for gravity irrigation from upstream sources, while berm soils remain intact year-round. This is likely the reason the overall total organic C was significantly higher in the berm, in addition to being the region that has the most leaf litter input and accumulation. However, row crops generally have more shallow roots that contribute to priming effects, where root exudates destabilize mineral-associated C leading to an increase in the accessible organic C pool. In contrast, both berm and furrow surface soils do not have high concentration of shallow roots from crops, as orange trees are deeply rooted. Weeds can be found in both the berm and furrow soils but are regularly removed from the furrow and only present after the wet season and in the berm during and after rain events. Overall, weed growth is not substantial enough to result in large changes in the overall C content of either soil throughout the course of this study.

The most significant change in soil C:N was observed after the intense rain event at the start of the study period, which suggests that decomposition of organic matter is

driven by seasonal wetting events when the limiting factor is nitrogen availability. Prior to the rain event, the C:N of the berm soil was ~12 followed by an immediate increase after rainfall, likely because the increased soil moisture led to slaking which redistributed labile C and N-bearing compounds in the surface soils temporarily. The nitrogen released during this process potentially fueled biomass decomposition and was then exhausted leaving the system nitrogen limiting once again, resulting in minimal change in C:N after subsequent rain events. In contrast, additional water inputs as rain to the furrow soils decreased the C:N significantly at the start of the wet season and remained low for the rest of the year, comparable to the berm soil values. Rainwater is likely maintaining anoxic conditions within the furrow soils for longer periods than with irrigation only, which can eventually slow decomposition rates and lead to an accumulation of reduced nitrogen as ammonium. Our data shows that furrow soil C:N does not rebound to pre-rain conditions; these results demonstrate that large rain events on semi-arid soils that are subject to frequent wet-dry cycles likely have lasting impact on rate of decomposition.

The $\delta^{13}C$ of furrow soils were generally higher (less negative) throughout the year when compared to the berm soils, where the greatest shift in $\delta^{13}C$ is caused by the intense rain event. Higher $\delta^{13}C$ are often attributed to more microbially processed C (Baisden et al. 2002; Moni et al. 2012). Because water is readily available in the furrow soils, microbes and C substrates can be easily mobilized through water-filled pores which can lead to greater organic carbon degradation compared to in berm soils where microbes are more often isolated from organic substrates due consistently lower VWC. However, the microbially processed C within the furrow soils can then potentially become physically

occluded in mineral-associated complexes that remain abundant in the furrow or saturated conditions can lead to thermodynamic limitations that prevents further metabolic degradation of highly reduced C substrates (Keiluweit et al. 2016). The relatively lower $\delta^{13}C$ in the berm soils indicates that the C in these soils is more complex, likely contributed by fresh leaf litter that accumulates on the berm. The increase in $\delta^{15}N$ at the start of the sampling campaign and throughout the wet season in the furrow is likely caused by sustained microbial biomass input or another microbial N-processing mechanism, however previous work has shown that $\delta^{15}N$ increases as N outputs increase (Houlton, Sigman, and Hedin 2006; Lyu et al. 2019). However, it remains unclear why both $\delta^{13}C$ and $\delta^{15}N$ increase significantly in both berm and furrow soils on 9/19.

3.4.2 Chemical C pools

It has been observed that active and labile C (chemical pools) are more sensitive to management shifts, including various forms of tillage and organic matter inputs (Bongiorno et al. 2019; Culman et al. 2012; Awale, Emeson, and Machado 2017) than total organic C content alone. Active C pool increased during the wet season in berm soils, which is also when concentrations were most variable. Furrow soils, however, undergo frequent wet-dry cycles throughout the year where the labile C pool is not as influenced by seasonal rains. The more consistent labile C pool within furrow soils could be due to selection of metabolisms that can withstand frequent and large changes in soil moisture and because management and C inputs to furrows remain unchanged throughout the year.

To determine why the active C pool within berm soils increased during the wet season, WEOC and microbial biomass C were measured during the months when maximum and minimum active C concentrations were recorded. The gradual increase in WEOC in berm soils during the wet season is likely due to the growth of annual weeds that grow for a short period of time after the early winter and spring rains followed by death and degradation by summer. Weed growth in the furrows is observed but is routinely removed to maintain flow of irrigation water in furrows. The higher concentration of microbial biomass carbon observed in the berm at the start of the wet season was likely caused by a pulse of microbial death from the sudden increase in VWC in the typically dry soils. Because both WEOC and microbial biomass C are lower in the dry season, it can be concluded that the changes the active C pool is most likely contributed by root growth that occurs in the wet season, suggesting that any changes to the soil C dynamics throughout the year is largely mediated by this active and labile C pool.

3.5 Conclusions

This study aimed to characterize the typical range and annual trends in total C and labile C pools of furrow-irrigated soils within a semi-arid climate region. By examining such trends within a furrow-irrigated landscape, we are able to capture the contributions of infrequent, seasonal rainfall versus frequent wet-dry cycled soils to alterations in seasonal soil carbon and nitrogen dynamics. We found that on average, berm soils which only receive water through seasonal rain events contained greater total soil C than furrow soils which undergo continuous drying-rewetting cycles throughout the year. The C content was

greater due to a combination of substrate accumulation from leaf litter, being N limited, and very little water to increase pore networks to allow for microbial degradation of organic matter. We also found that while the furrow undergoes frequent and repetitive soil moisture fluctuations that often results in ponding, sustained anoxic conditions, especially after an intense rain event was significant enough dramatically limit decomposition. However, given the trends identified in this study, the active C pools between the wet and dry season was most significantly different in the berm which is likely first increased at the onset of precipitation due to microbial death but increases as soils begin to dry from weed growth. It is hypothesized that seasonal variation in soil C is due to the short-lived C pool (Wuest 2014), but most agricultural soil C studies have been limited to very few time points, such as only collecting samples at the start and end of a growing season or at the same time of the year for consecutive years (West et al. 2004; West and Marland 2002). Because of the lack of temporally resolved measurements, it is difficult to parameterize models for either inverse or predictive modeling in managed soils. Additionally, many models that incorporate ecosystem level processes to predict GHG emissions, such as the ecosys (Thomas, Bond, and Hiscock 2013) have widely parameterized aboveground and belowground processes in energy crops, where tree crop parameterization is lacking. The findings from this study highlight the importance of pairing not just overall C content to seasonal water availability, but the labile C pools that are more indicative of C emissions.

3.5 References

Awale, Rakesh, Micco A. Emeson, and Stephen Machado. 2017. “Soil Organic Carbon Pools as Early Indicators for Soil Organic Matter Stock Changes under Different Tillage Practices in Inland Pacific Northwest.” *Frontiers in Ecology and Evolution* 5. https://doi.org/10.3389/fevo.2017.00096.

Baisden, W. T., R. Amundson, A. C. Cook, and D. L. Brenner. 2002. “Turnover and Storage of C and N in Five Density Fractions from California Annual Grassland Surface Soils.” *Global Biogeochemical Cycles* 16 (4): 64-1-64–16. https://doi.org/10.1029/2001GB001822.

Bongiorno, Giulia, Else K. Bünemann, Chidinma U. Oguejiofor, Jennifer Meier, Gerrit Gort, Rob Comans, Paul Mäder, Lijbert Brussaard, and Ron de Goede. 2019. “Sensitivity of Labile Carbon Fractions to Tillage and Organic Matter Management and Their Potential as Comprehensive Soil Quality Indicators across Pedoclimatic Conditions in Europe.” *Ecological Indicators* 99 (April): 38–50. https://doi.org/10.1016/j.ecolind.2018.12.008.

Chen, Songchao, Dominique Arrouays, Denis A. Angers, Manuel P. Martin, and Christian Walter. 2019. “Soil Carbon Stocks under Different Land Uses and the Applicability of the Soil Carbon Saturation Concept.” *Soil and Tillage Research*, Soil Carbon and Climate Change: the 4 per Mille Initiative, 188 (May): 53–58. https://doi.org/10.1016/j.still.2018.11.001.

Culman, Steven W., Sieglinde S. Snapp, Mark A. Freeman, Meagan E. Schipanski, Josh Beniston, Rattan Lal, Laurie E. Drinkwater, et al. 2012. “Permanganate Oxidizable Carbon Reflects a Processed Soil Fraction That Is Sensitive to Management.” *Soil Science Society of America Journal* 76 (2): 494–504. https://doi.org/10.2136/sssaj2011.0286.

Fierer, Noah, and Joshua P. Schimel. 2002. “Effects of Drying–Rewetting Frequency on Soil Carbon and Nitrogen Transformations.” *Soil Biology and Biochemistry* 34 (6): 777–87. https://doi.org/10.1016/S0038-0717(02)00007-X.

Francaviglia, Rosa, Claudia Di Bene, Roberta Farina, Luca Salvati, and José Luis Vicente-Vicente. 2019. “Assessing ‘4 per 1000’ Soil Organic Carbon Storage Rates under Mediterranean Climate: A Comprehensive Data Analysis.” *Mitigation and Adaptation Strategies for Global Change* 24 (5): 795–818. https://doi.org/10.1007/s11027-018-9832-x.

Houlton, Benjamin Z., Daniel M. Sigman, and Lars O. Hedin. 2006. “Isotopic Evidence for Large Gaseous Nitrogen Losses from Tropical Rainforests.” *Proceedings of the National Academy of Sciences* 103 (23): 8745–50. https://doi.org/10.1073/pnas.0510185103.

Keiluweit, Marco, Peter S. Nico, Markus Kleber, and Scott Fendorf. 2016. “Are Oxygen Limitations under Recognized Regulators of Organic Carbon Turnover in Upland Soils?” *Biogeochemistry* 127 (2): 157–71. https://doi.org/10.1007/s10533-015-0180-6.

Lal, R. 2004. “Soil Carbon Sequestration Impacts on Global Climate Change and Food Security.” *Science* 304 (5677): 1623–27. https://doi.org/10.1126/science.1097396.

———. 2005. “Forest Soils and Carbon Sequestration.” *Forest Ecology and Management*, Forest Soils Research: Theory, Reality and its Role in TechnologY, 220 (1): 242–58. https://doi.org/10.1016/j.foreco.2005.08.015.

Lundquist, E. J, L. E Jackson, and K. M Scow. 1999. “Wet–Dry Cycles Affect Dissolved Organic Carbon in Two California Agricultural Soils.” *Soil Biology and Biochemistry* 31 (7): 1031–38. https://doi.org/10.1016/S0038-0717(99)00017-6.

Lyu, Maokui, Xiaojie Li, Jinsheng Xie, Peter M. Homyak, Liisa Ukonmaanaho, Zhijie Yang, Xiaofei Liu, Chaoyue Ruan, and Yusheng Yang. 2019. “Root–Microbial Interaction Accelerates Soil Nitrogen Depletion but Not Soil Carbon after Increasing Litter Inputs to a Coniferous Forest.” *Plant and Soil* 444 (1): 153–64. https://doi.org/10.1007/s11104-019-04265-w.

Minasny, Budiman, Brendan P. Malone, Alex B. McBratney, Denis A. Angers, Dominique Arrouays, Adam Chambers, Vincent Chaplot, et al. 2017. “Soil Carbon 4 per Mille.” *Geoderma* 292 (April): 59–86. https://doi.org/10.1016/j.geoderma.2017.01.002.

Moni, C., D. Derrien, P.-J. Hatton, B. Zeller, and M. Kleber. 2012. “Density Fractions versus Size Separates: Does Physical Fractionation Isolate Functional Soil Compartments?” *Biogeosciences* 9 (12): 5181–97. https://doi.org/10.5194/bg-9-5181-2012.

Panettieri, M., A. E. Berns, H. Knicker, J. M. Murillo, and E. Madejón. 2015. “Evaluation of Seasonal Variability of Soil Biogeochemical Properties in Aggregate-Size Fractioned Soil under Different Tillages.” *Soil and Tillage Research* 151 (August): 39–49. https://doi.org/10.1016/j.still.2015.02.008.

Paustian, K., J. Six, E.T. Elliott, and H. W. Hunt. 2000. “Management Options for Reducing CO2 Emissions from Agricultural Soils.” *Biogeochemistry* 48 (1): 147–63. https://doi.org/10.1023/A:1006271331703.

Post, W. M., R. C. Izaurralde, L. K. Mann, and N. Bliss. 2001. “Monitoring and Verifying Changes of Organic Carbon in Soil.” In *Storing Carbon in Agricultural Soils: A Multi-Purpose Environmental Strategy*, edited by Norman J. Rosenberg and

Roberto C. Izaurralde, 73–99. Dordrecht: Springer Netherlands. https://doi.org/10.1007/978-94-017-3089-1_4.

Pulleman, Mirjam, Skye Wills, Rachel Creamer, Richard Dick, Rich Ferguson, Diane Hooper, Candiss Williams, and Andrew J. Margenot. 2021. "Soil Mass and Grind Size Used for Sample Homogenization Strongly Affect Permanganate-Oxidizable Carbon (POXC) Values, with Implications for Its Use as a National Soil Health Indicator." *Geoderma* 383 (February): 114742. https://doi.org/10.1016/j.geoderma.2020.114742.

Quinton, John N., Gerard Govers, Kristof Van Oost, and Richard D. Bardgett. 2010. "The Impact of Agricultural Soil Erosion on Biogeochemical Cycling." *Nature Geoscience* 3 (5): 311–14. https://doi.org/10.1038/ngeo838.

Reicosky, D. C. 2003. "Conservation Agriculture: Global Environmental Benefits of Soil Carbon Management." In *Conservation Agriculture: Environment, Farmers Experiences, Innovations, Socio-Economy, Policy*, edited by Luis García-Torres, José Benites, Armando Martínez-Vilela, and Antonio Holgado-Cabrera, 3–12. Dordrecht: Springer Netherlands. https://doi.org/10.1007/978-94-017-1143-2_1.

Schaefer, Michael, Nathaniel Bogie, Daniel Rath, Alison Marklein, Abdi Garniwan, Thomas Haensel, Ying Lin, et al. 2020. "Effect of Cover Crop on Carbon Distribution in Size and Density Separated Soil Aggregates." *Soil Systems* 4 (January): 6. https://doi.org/10.3390/soilsystems4010006.

Thomas, Amy R. C., Alan J. Bond, and Kevin M. Hiscock. 2013. "A Multi-Criteria Based Review of Models That Predict Environmental Impacts of Land Use-Change for Perennial Energy Crops on Water, Carbon and Nitrogen Cycling." *GCB Bioenergy* 5 (3): 227–42. https://doi.org/10.1111/j.1757-1707.2012.01198.x.

Thornton, Philip K. 2012. "Recalibrating Food Production in the Developing World: Global Warming Will Change More Than Just the Climate," October. https://cgspace.cgiar.org/handle/10568/24696.

Vermeulen, Sonja J., Bruce M. Campbell, and John S.I. Ingram. 2012. "Climate Change and Food Systems." *Annual Review of Environment and Resources* 37 (1): 195–222. https://doi.org/10.1146/annurev-environ-020411-130608.

Weil, Ray R., Kandikar R. Islam, Melissa A. Stine, Joel B. Gruver, and Susan E. Samson-Liebig. 2003. "Estimating Active Carbon for Soil Quality Assessment: A Simplified Method for Laboratory and Field Use." *American Journal of Alternative Agriculture* 18 (1): 3–17. https://doi.org/10.1079/AJAA200228.

West, Tristram O, and Gregg Marland. 2002. “A Synthesis of Carbon Sequestration, Carbon Emissions, and Net Carbon Flux in Agriculture: Comparing Tillage Practices in the United States.” *Agriculture, Ecosystems & Environment* 91 (1): 217–32. https://doi.org/10.1016/S0167-8809(01)00233-X.

West, Tristram O., Gregg Marland, Anthony W. King, Wilfred M. Post, Atul K. Jain, and Kenneth Andrasko. 2004. “Carbon Management Response Curves: Estimates of Temporal Soil Carbon Dynamics.” *Environmental Management* 33 (4). https://doi.org/10.1007/s00267-003-9108-3.

Wuest, Stewart. 2014. “Seasonal Variation in Soil Organic Carbon.” *Soil Science Society of America Journal* 78 (4): 1442–47. https://doi.org/10.2136/sssaj2013.10.0447.

Zomer, Robert J., Deborah A. Bossio, Rolf Sommer, and Louis V. Verchot. 2017. “Global Sequestration Potential of Increased Organic Carbon in Cropland Soils.” *Scientific Reports* 7 (1): 15554. https://doi.org/10.1038/s41598-017-15794-8.

Chapter 4: Gas Flux and Substrate Changes Brought on by Shifting Irrigation Strategy in a Legacy Furrow Irrigated Soil

4.0 Abstract

Switching from high to low-volume irrigation methods is a common practice to reduce water waste and adapt to worsening drought conditions, but such a change can lead to biogeochemical ramifications such as shifts in C flux and pore water biogeochemical composition that have not been thoroughly examined. The volume and frequency of water delivered to a soil will alter microbial access to carbon substrates and thermodynamic favorability of using specific compounds, and therefore, alter the amount of soil carbon (C) that is either sequestered or lost. To investigate how a shift to low-volume irrigation may change C dynamics in semi-arid soils, we conducted *ex situ* low-volume irrigation experiments using intact soil cores taken from an orange orchard in a semi-arid region that has been furrow-irrigated for over a century. We collected cores near the base of trees (berm soils) with volumetric water content (VWC) of ~0.05 cm^3cm^{-3} in the dry season, and from furrow soils where VWC ranges between 0.2 - 0.3 cm^3cm^{-3}. Cores were dried to comparable soil moisture followed by wet up during 48-hour irrigation events simulating microsprinkler practice in the region to VWC of ~0.15 cm^3cm^{-3}. CO_2 flux was monitored throughout the irrigation simulation and labile C pool and C substrate composition were determined at the start and end of the simulations to identify shifts in C biogeochemistry. Our results show that CO_2 flux dynamics was nearly identical between the two soils but differed in other parameters. The labile C pool in berm soils increased 75% after VWC was increased whereas labile C concentrations remained unchanged in furrow soils, likely due

to the total C input being greater in berm soils which are destabilized at the onset of irrigation. Berm soil pore water also showed relatively lower abundance of thermodynamically favorable substrates for microbial respiration. In contrast, the composition of substrates in furrow soil pore water shifted to being dominated by compounds with relatively lower nominal oxidation state C (NOSC), indicating that the switch in irrigation solubilized previously preserved lipids. Our results demonstrate how soil C flux and pore water dynamics is altered as low-volume irrigation is applied revealing the multi-dimensional biogeochemical impact of shifting irrigation management.

4.1 Introduction

There is a well-established feedback between climate and agriculture, where management of soils can be used a strategy to mitigate the effects of climate change—specifically through increasing soil carbon (C) stocks. Soil water content controls many chemical, physical, and biological processes in soil matrices, which is altered significantly by shifts in irrigation. Growers' decision to implement specific irrigation strategies is largely dependent upon economic costs and water availability (Schwankl et al., 1999), which has become an increasing cause for concern due to intensifying drought conditions on a global scale (Dai, 2013). Optimizing how drought and C are managed on agricultural lands in semi-arid landscapes has large socio-economic implications. In California, more than a quarter of the state's land-area is farmland; nearly 10 million acres are irrigated with over 34 million acre-ft of water annually (California Department of Water Resources 2020). Recurring and extended droughts in recent decades have negatively impacted

agricultural production as associated revenues (Howitt et al., 2015). Water resource strategies have and will be addressed in the form of shifting management and policy (California Natural Resources Agency, 2021) as more frequent and intense droughts are expected to occur (Marvel et al., 2019).

In the Colorado River and South Coast watersheds of California where agricultural lands are predominantly irrigated with surface water, a shift towards more precise, water-saving irrigation methods (i.e. drip and micro-sprinkler irrigation) has been observed (Johnson and Cody 2015). Switching irrigation method has been implemented in many crop systems, but most significantly in orchard systems (tree crops) that were previously surface irrigated largely via furrow irrigation. Orchards dominate in the state as having the most acreage of any crop system irrigated by micro-sprinkler, which increased by 78% between 1991 and 2010 (Tindula et al., 2013). Field crops are still predominantly surface irrigated, while irrigation of vegetable crops have largely shifted from surface irrigation to sprinkler or drip irrigation. Orchard systems, overall, are more likely than other crop systems to be switched from furrow irrigation to micro-sprinkler irrigation.

Accordingly, this study investigates changes to soil C flux and pore water chemistry with simulated change in irrigation proactive by reducing volumetric water content in a legacy furrow-irrigated orchard soil in a semi-arid region in California. Furrow-irrigated fields in this area and other Mediterranean regions are composed of soils that have two contrasting soil moisture regimes: berms are predominantly dry throughout the year aside from receiving water from seasonal rainfall during colder winter months, while furrows are repeatedly flooded then dried at high temporal resolution usually ranging from every other

week to once a month. When such a landscape is switched to low volume irrigation methods such as microsprinkler systems that distribute water more homogeneously throughout the landscape, the soil moisture in in the berm will become more consistently wetter while furrow soils will become drier. These changes in soil moisture regime across the landscape will likely alter microbial access to carbon substrates and therefore results in changes in carbon flux dynamics and chemical composition.

Therefore, our questions for this study included the following: (1) how do CO_2 flux dynamics shift when switching to low volume irrigation? (2) How is the aqueous phase C chemistry changed when soil moisture is maintained at a lower volumetric water content (VWC) in furrow soils that have historically undergone repeat drying-rewetting cycles versus berm soils with increased VWC in soils that are typically dry? To answer these questions, we conducted simulated irrigation shifts by taking intact soil cores from a semi-arid, historically furrow irrigated orange orchard in Riverside, CA, USA and simulated *ex situ* irrigation events. We hypothesize that increased water delivery to berm soils will result in an immediate pulse of C lost as CO_2, as this soil typically accumulates substrate that can quickly be metabolized by aerobic microbes as demonstrated by our previous study (Chapter 2). In contrast, we hypothesize that relatively higher abundance of high energetically favorable substrate and the increasingly aerobic conditions in furrow soils would result in greater CO_2 flux, but would remain lower than the berm soils. Overall, we expect that a switch to micro-sprinkler would result in greater CO_2 emissions from originally berm soils, while CO_2 flux from furrow soils will increase slowly as more aerobic conditions favor the release of previously protected C.

4.2 Materials and Methods

4.2.1 Field description

Soil cores were collected from a commercial Washington navel orange orchard in the greenbelt region of Riverside, CA, USA (33.9086 N, 117.4295 W). The soil at the grove is characterized as an Alfisol with loamy sand surface texture with a layer of sandy loam at a depth of about 70 cm (surface pH 7.0, 1 dS m^{-1} EC). The climate in the region is hot semi-arid (BSh) with a mean annual air temperature of 17°C and annual precipitation of 305 mm occurring predominantly in the winter months. The orchard has been furrow-irrigated for over a century; irrigation water is applied semi-monthly for 48 hours with the exception of heavy winter rain events when irrigation is not needed, which occurs once or twice in an average year, and where two consecutive irrigation cycles (1 month) are skipped. Irrigation water is drawn from the Gage Canal that delivers water to the region from the Santa Ana River. The furrows are reconstructed with a disk ridger approximately five times per year and manually maintained with a shovel when needed. Soil moisture was monitored in surface soils (0-10 cm) using soil moisture and temperature sensors and a datalogger (Decagon 5TM and EM50, Decagon Devices, Pullman, WA, USA). To understand how wet-up from differs under microsprinkler irrigation, surface soil moisture was also monitored at a neighboring micro-sprinkler irrigated Washington navel orange orchard (33.8932 N, 117.4277 W) 1.7 km from the furrow-irrigated site, which receives water from the same irrigation canal twice monthly for 48 hours. In this orchard, VWC typically reaches a maximum of 0.15 cm^3 cm^{-3} at the base of the trees and in the regions

that were formerly furrowed that were converted to micro-sprinkler irrigation in 2001. Soils at both sites are of the same classification and are in close enough proximity to receive comparable rainfall frequency and intensity.

4.2.2 Intact core sampling

Ten total intact soil cores were collected in July 2019 across the furrow-irrigated orchard from the furrows (n = 5) and the berms (n = 5). An additional set of ten cores were collected in November 2019 again with five cores each from the furrow and berm. One furrow (July 2019) core was excluded from ex-situ analysis due to an ant colony infestation. Intact soil cores were collected using a 10 cm diameter PVC collar with a height 15 cm. The PVC collar was pressed into the soil with a wood block and rubber mallet to ensure even burial to a depth of 10 cm. A shovel was used to dig around the intact core for retrieval. Each core was then capped on both ends with a sewer and drain cap and secured for direct transport to the lab.

4.2.3 *Ex situ* simulated irrigation

Two experiments were performed with different initial conditions: in Experiment 1, cores were dried down to comparable soil moistures (~0.035 $cm^3\ cm^{-3}$) prior to *ex situ* irrigation, where the average VWC at the time of collection was 0.14 $cm^3\ cm^{-3}$ in the furrow cores and 0.09 $cm^3\ cm^{-3}$ in the berm cores; in Experiment 2, fresh soil cores were used without drying, where the average VWC of furrow soils was 0.26 $cm^3\ cm^{-3}$ and 0.05 $cm^3\ cm^{-3}$ in berm soils at the time of collection. The second experiment allowed us to determine the role of pore connectivity as VWC changes, with one condition that closely matched the

VWC in a micro-sprinkler irrigated orchard (0.15 $cm^3\ cm^{-3}$) and one with higher VWC hypothesized to provide additional pore connectivity but is still reduced irrigation (0.25 $cm^3\ cm^{-3}$) compared to VWC reached in furrow soils (> 0.3 $cm^3\ cm^{-3}$).

A schematic of the intact core parts, dimensions, and experimental equipment are provided in Figure A3.1. Once the intact soil cores were extract from the field, they were immediately transported to the lab and soil moisture sensors (Decagon 5TM, Decagon Devices, Pullman, WA, USA) were installed to pre-cut slits in the PVC of two of the soil cores, one for each treatment (berm and furrow) at an approximate depth of 5 cm. The sensors were then connected to a data logger (EM50 Datalogger, Decagon Devices, Pullman, WA, USA) and soil moisture and temperature were measured continuously at 5 min intervals. For Experiment 1, top caps were removed and the cores were allowed to dry for 21 days. Once cores were dried to comparable water contents, bottom caps were replaced with a drain cap fitted with drain holes and a stainless-steel fine mesh (0.125 mm) to drain excess water during the simulated irrigation events to prevent clogging of the gas tubing. Top caps were fitted with Tygon tubing for applying irrigation water (ultrapure water;18.2 $M\Omega\ cm^{-1}$) and tubing for CO_2 flux measurements. The precise addition of water was calculated by measuring the volume of the soil in the core, the VWC prior to water addition, and then calculating the volume of water needed to acquire a maximum VWC of 0.15 $cm^3 cm^{-3}$ or 0.25 $cm^3\ cm^{-3}$ over a 48-hour period. Once the flow rate was calculated, a peristaltic pump (Ismatec IPC) and 0.76 mm diameter tubing was used to deliver water to each soil core and monitored with soil moisture sensors.

For Experiment 2, the same number of soil cores were taken from the field site in the same manner described above. However, the soils were not allowed to dry and were instead immediately fitted with the water delivery system and gas analyzer caps. Due to the furrow soil cores being saturated from an irrigation event occurring at the time of collection, Experiment 2 only reports findings for the 5 cores collected from berm soils. For the 5 berm intact soil cores, three were brought to a maximum VWC of 0.15 $cm^3\ cm^{-3}$, and the other two were brought to a maximum VWC of 0.25 $cm^3\ cm^{-3}$.

4.2.4 CO_2 flux measurements

Carbon dioxide flux from intact cores was monitored using a LI-COR 8100 IR analyzer with a LI-COR 8150 multiplexer (LI-COR, Lincoln, NE, USA) to collect readings from multiple cores simultaneously. An additional pump was used to release any CO_2 to prevent build-up in the headspace of the core between measurements. Carbon dioxide concentrations were measured over 3 min with pre- and post-purge lengths of 30 s and a dead band time of 15 s per measurement. Flux was calculated using Soil Flux Pro software (v4.0; LI-COR, Lincoln, NE, USA). For Experiment 1, measurements were taken continuously over 13 days with two irrigation events that lasted approximately 48 hours each on days 0 to 3, and 8 to 11 on lab air-dried soil. For Experiment 2, CO_2 flux was measured for 12 days with only one 48-hour irrigation event (on days 0 to 2) on fresh soil cores.

4.2.5 Active carbon pool

The active C pool in each soil was estimated by measuring the permanganate oxidizable C (POXC) fraction as described by Culman et al. (2012). All POXC measurements were made on soils from the same field site, with comparable mass (2.5 g ± 0.05 g), and identical particle homogenization (< 0.25 mm) to ensure repeatability (Wade et al., 2020) and minimize known errors introduced by differences in sampling techniques (Pulleman et al., 2021). Soil for POXC determination was collected when the first intact soil cores were collected (7/05/19; 0 - 10 cm depth, n = 10) in the same location. POXC was then measured in triplicate per soil core (0 - 10 cm depth from surface of intact soil core) after the simulated irrigation experiments were terminated. Approximately 2.5 g (± 0.05 g) of air-dried and sieved soil was mixed with 18 mL of ultrapure water and 2 mL 0.2 M $KMnO_4$ (prepared with 1.4 M $CaCl_2$ and pH adjusted to 7.2 with 0.1 N NaOH). Samples were shaken on an oscillating shaker (120 rpm) for 2 min and allowed to settle for 10 min. Approximately 0.5 mL of the supernatant was then immediately diluted with 49.5 mL ultrapure water and analyzed on a spectrophotometer at 550 nm (using ultrapure water as blank) and compared to a standard curve of known $KMnO_4$ concentrations (0.05, 0.01, 0.015, and 0.02 M $KMnO_4$) that were diluted in the same way as the treated soil extracts. POXC was then calculated as described by Weil et al. (2003): POXC (mg kg^{-1}) = [0.02 mol L^{-1} – (a + b x Abs)] x (9000 mg C mol^{-1}) x (0.02 L solution/Wt.), where *a* is the intercept of the standard curve; *b* is the slope of the standard curve; *Abs* is the measured absorbance of the unknown; 9000 = mg of C oxidized by 1 mole of MnO_4 ($Mn^{7+} \rightarrow Mn^{4+}$); and *Wt.* is the weight of the air-dried soil sample in kg. Standards and the 0.2 M $KMnO_4$ solution

were made fresh the day of the analysis. An internal lab soil standard that has been previously and repeatedly measured for POXC of similar mass and particle size was also included during sample analysis to ensure that stock solutions were not contaminated during preparation. A solution blank (ultrapure water) was also used to check for solution reduction or C contamination.

4.2.6 Carbon substrate quality

To gauge substrate changes before and after the new irrigation method, water extractable organic C (WEOC**)** was qualitatively assessed to identify the types of C present that could potentially become available to microbial communities using GC/EI-MS. For WEOC, 32 mL of ultrapure water was mixed with approximately 8 g of <2 mm sieved soils taken from before (from the field, 0-10 cm, n=5 from berm and furrow) and after (from the intact cores, 0-10 cm, n = 3 from each core) the simulated irrigation experiment from both berm and furrow soils and shaken on an oscillating shaker (120 rpm) for 4 hours, and then centrifuged for 30 min (2,000 x g). The decanted WEOC water samples were frozen immediately after collection and freeze-dried in 5 mL aliquots to concentrate porewater C compounds. Samples were then reacted with N,O-Bis(trimethylsilyl)trifluoroacetamide (BSTFA) + TMCS, 99:1 (Sylon BFT) to promote silylation to target hydroxyl groups. Derivatized samples were run on a GC/MS (Agilent 6890N GC coupled with 5975 MSD, Agilent) for aqueous carbon species characterization. Species were identified by comparing the retention time of the species in the samples to spectral data from the NIST library (Chen et al. 2019). Once identified, the parent compounds were estimated by accounting for the

derivatization that reacted -OH functional groups with -Si(CH3)3 [Parent compound: C= C_{GC} – 3X, H= H_{GC} – 9X + X , where subscript GC is the number of C or H present in the derivatized compound and X is the number of $Si(CH_3)_3$ identified in the GC/EI-MS.

4.3 Results

4.3.1 Surface soil moisture of furrow and microsprinkler irrigated orchard soils

Within the furrows, the soil moisture at a depth of 10 cm typically ranged between 0.2 - 0.3 $cm^3\ cm^{-3}$ and with a minimum of 0.15 $cm^3\ cm^{-3}$ reached during the dry summer months for 1 to 3 days before a semi-monthly irrigation event (Figure A3.2). In contrast, berm soil typically remained at a soil moisture content of ~0.05 $cm^3\ cm^{-3}$, which increased to 0.18 $cm^3\ cm^{-3}$ after a moderate rain event (3 mm) and up to 0.30 $cm^3\ cm^{-3}$ after a heavy rain (40 mm). A nearby micro-sprinkler irrigated orchard that was converted from furrow irrigation in 2001 uses the same water source where soils are irrigated for 48 hours twice monthly. There, typical irrigation events increase the surface (0 – 10 cm) soil VWC beneath the tree line and previously furrowed soils to ~0.15 $cm^3\ cm^{-3}$ (Figure 4.1). A comparison of surface soil VWC at the two sites shows that previously furrowed soils receive consistently less water under microsprinkler irrigation than furrow irrigation while soils along the berm receive more.

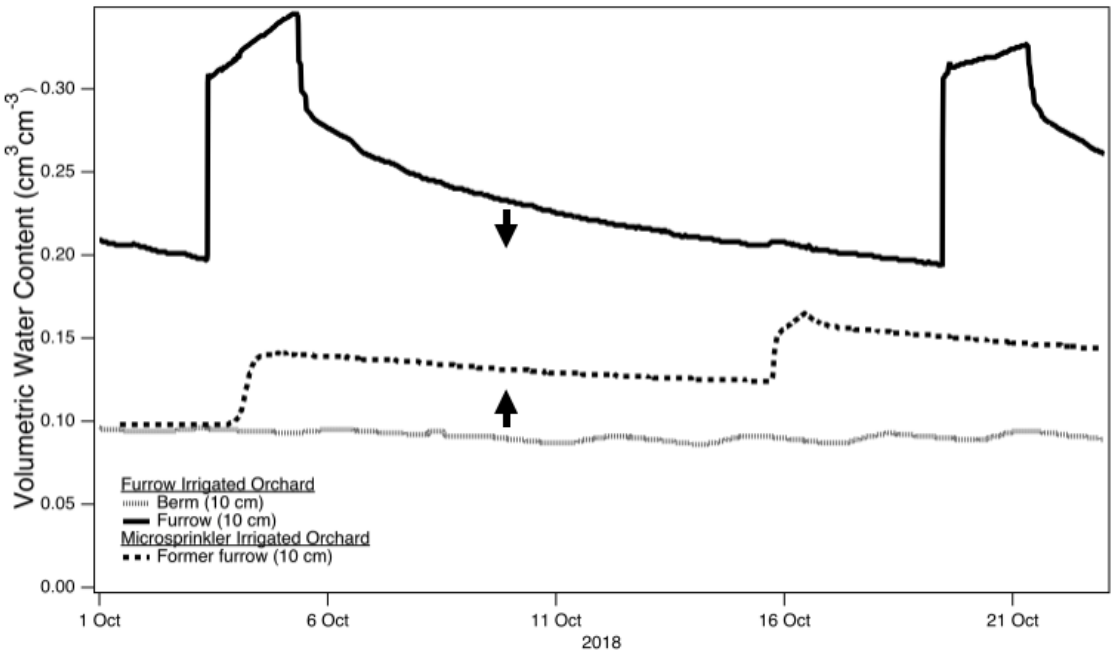

Figure 4.5: A comparison of soil moisture dynamics as indicated by volumetric water content of furrow-irrigated versus microsprinkler irrigated orchard soils at 10 cm below soil surface. The microsprinkler irrigated orchard was previously furrow-irrigated prior to 2001. It should be noted that at the microsprinkler irrigated orchard, both the previously furrowed soils and soils under the base of trees have comparable soil moisture dynamics and are both represented by the dashed line. The up-arrow indicates that berm soil moisture content will generally increase if the field is switched from furrow-irrigation to microsprinkler irrigation, while the down arrow shows that furrow soil moisture content will generally decrease.

4.3.2 CO_2 flux under simulated microsprinkler irrigation

The simulated irrigation imposed on the intact cores created more homogenous soil moisture than typical conditions under furrow irrigation at the field site. The CO_2 flux increased as soon as water was applied to both berm and furrow soils in the first intact core simulation where both soils were first dried to VWC of 0.03 cm^3 $^c m^{-3}$ followed increases to ~0.11 cm^3 cm^{-3} after irrigation (Figure 4.2). For the furrow soil cores, an initial peak flux of 0.12 ± 0.05 µmol m^{-2} s^{-1} was reached after 21 hours of watering when the VWC reached 0.04 cm^3 cm^{-3}. The flux then decreased after 46 hours of watering, where a secondary peak flux occurred reaching a maximum of 0.11 ± 0.06 µmol m^{-2} s^{-1} at hour 48 when the

volumetric water content reached a maximum of ~0.11 $cm^3\ cm^{-3}$. The overall trend of CO_2 flux in berm soil cores relative to timing of water was similar to the dynamics seen in furrow soil cores, but with slightly suppressed peak values: CO_2 flux initially peaked at 0.09 ± 0.02 µmol $m^{-2}\ s^{-1}$ at hour 21 with a secondary peak of 0.10 ± 0.02 µmol $m^{-2}\ s^{-1}$ when VWC reached 0.11 $cm^3\ cm^{-3}$ prior to the end of the first simulated irrigation event.

The first irrigation event did not wet soils to the expected VWC of 0.15 $cm^3\ cm^{-3}$ to simulate micro-sprinkler field conditions; therefore, the flow rate of the peristaltic pumps was adjusted for the second irrigation event, but only minorly to prevent the overall water content from exceeding 0.15 $cm^3\ cm^{-3}$. After the first wetting (irrigation) period ended, both soils gradually decreased to similar minimum CO_2 flux (0.02 µmol $m^{-2}\ s^{-1)}$. When the soils are rewetted a second time CO_2 flux immediately increased again, but the peak flux was lower than the first irrigation event (0.08 ± 0.02 µmol $m^{-2}\ s^{-1}$ in furrow cores and 0.07 ± 0.01 µmol $m^{-2}\ s^{-1}$ in berm cores). Similar to the effect of the first irrigation event, the second watering also led to two peaks in CO_2 flux while water was applied; however, the secondary peak occurring 3 days after watering was greater for the furrow cores (0.15 ± 0.04 µmol $m^{-2}\ s^{-1}$) than berm cores (0.12 ± 0.02 µmol $m^{-2}\ s^{-1}$). When comparing the CO_2 flux between replicate cores, flux from berm cores varied less than furrow cores, with the least variation observed between cores immediately before the second watering event when soil moisture was the lowest.

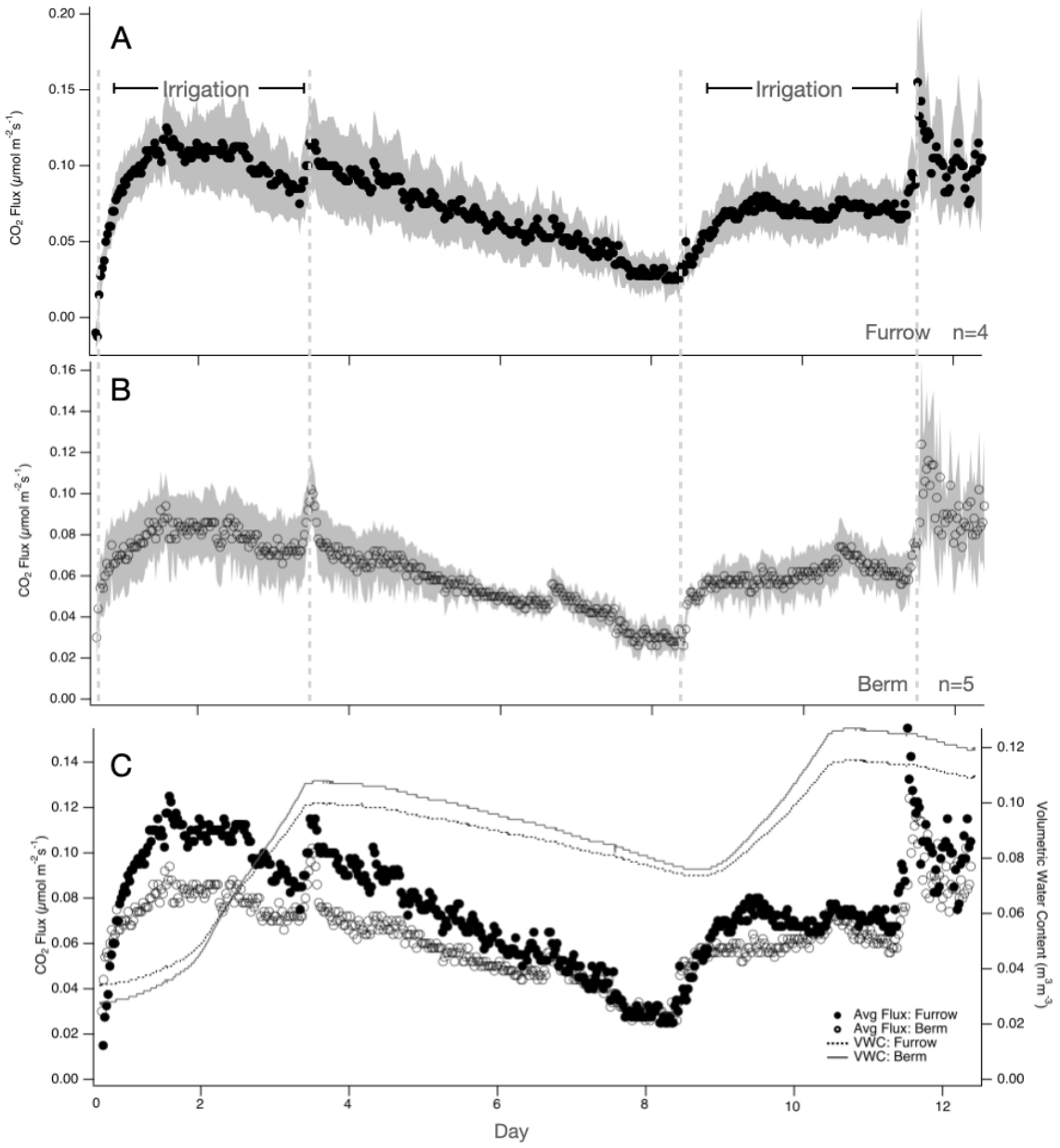

Figure 4.6: Average (± SEM) CO_2 flux and soil moisture of intact soil cores after ex situ low-volume irrigation. Furrow and berm soil cores were first dried to 0.03 cm^3 cm^{-3} prior to day 0 and were then irrigated to a target VWC of ~0.15 cm^3 cm^{-3} over 48 hours. The vertical dashed lines delineate the period during which water was added. Average CO_2 flux (± SEM) from irrigated furrow soil cores (n= 4) (A), average CO_2 flux (± SEM) from the berm soil cores (n= 5) (B) are shown. Average CO_2 flux (without SEM) of both furrow and berm cores with the average soil moisture from both treatments is provided in (C) for ease of comparison between treatments.

4.3.3 CO_2 flux dynamics in berm soils with elevated VWC

Experiment 1 results demonstrated that average CO_2 flux from berm soil cores was lower than furrow soil cores when microsprinkler equivalent VWC was imposed. This finding is contrary to our initial hypothesis that CO_2 flux from berm soil cores would be enhanced by the irrigation simulation which raises the average VWC compared to field conditions. We then hypothesized that as VWC continued to increase in berm soils, that CO_2 flux increase correspondingly by further connecting internal pores between microbes and their substrates.

Accordingly, berm soil cores were irrigated to both the VWC content observed in microsprinkler irrigated fields (0.15 $cm^3\ cm^{-3}$) and a higher VWC (0.25 $cm^3\ cm^{-3}$) to provide greater pore connectivity in Experiment 2. Additionally, irrigation simulations were conducted on moist cores immediately after collection without dry down to observe C dynamics after adjusted irrigation with native conditions. When intact berm cores taken from the field site were irrigated without first drying to the same moisture content, the CO_2 flux dynamics exhibited different trends between replicate cores, likely due to variability in initial soil moisture conditions; therefore, only two total cores (one for irrigated to VWC of 0.15 $cm^3\ cm^{-3}$ and one to VWC of 0.25 $cm^3\ cm^{-3}$) and their respective soil moisture trends are shown in Figure 4.3. The berm soil core irrigated to a target VWC of 0.15 $cm^3\ cm^{-3}$ (which slightly exceeded the target and reached a soil moisture peak of 0.18 $cm^3\ cm^{-3}$), reached a maximum CO_2 flux of 2.0 $\mu mol\ m^{-2}\ s^{-1}$. When a higher irrigation rate was applied to the duplicate berm soil core targeting a final VWC of 0.25 $cm^3\ cm^{-3}$ (final VWC of 0.26

cm^3 cm^{-3} reached) the CO_2 flux peaked twice, once during the irrigation period at a maximum of 4.91 µmol m^{-2} s^{-1} and at 5.50 µmol m^{-2} s^{-1} after irrigation had ended.

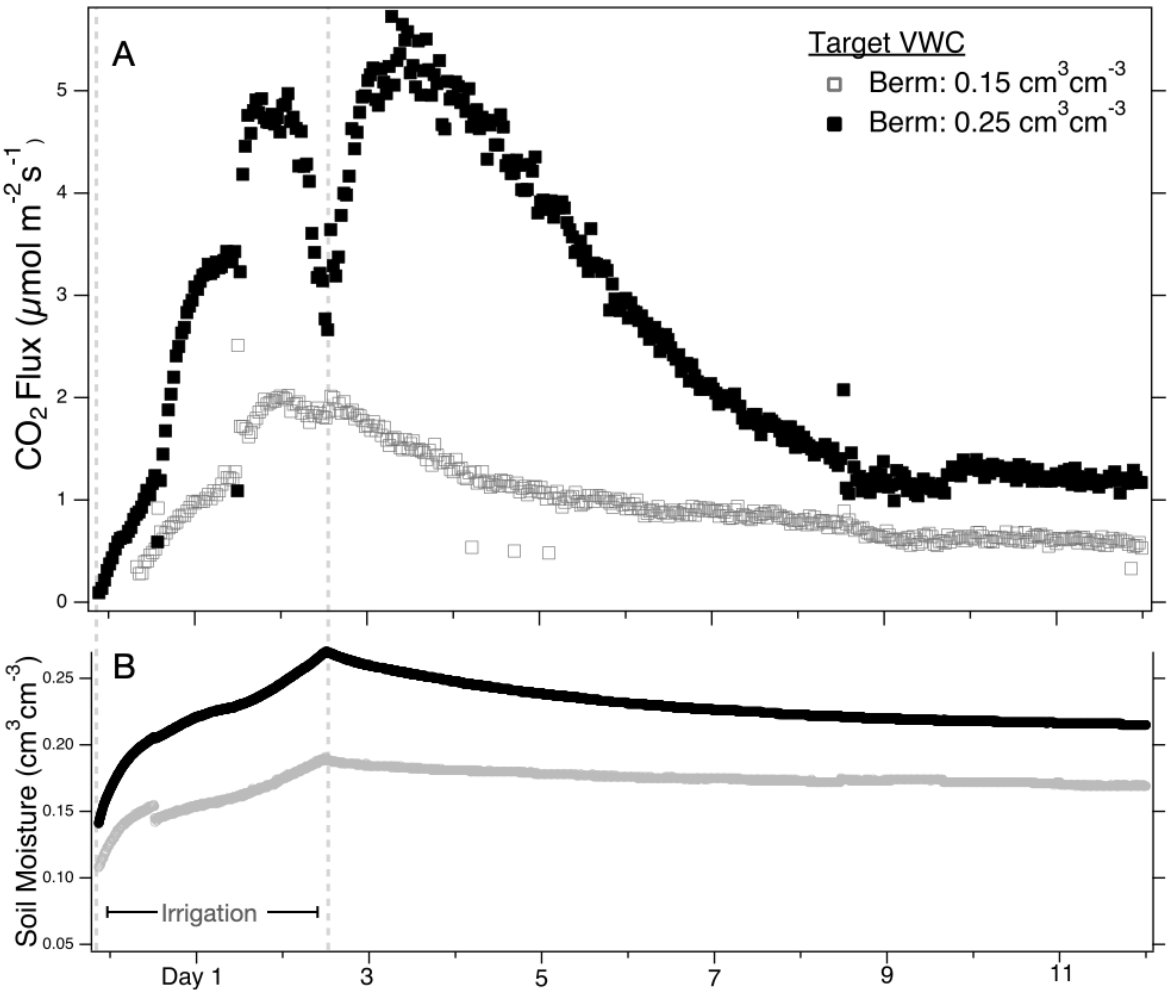

Figure 4.7: The CO_2 flux measured in berm soils in the second set of intact soil experiments (taken in November). The vertical dashed lines delineate the period during which water was added. A) The CO_2 flux measured from intact soil cores from the berm and subjected to target VWC maximums of approximately 0.15 cm^3cm^{-3} and 0.25 cm^3cm^{-3}. B) The wet-up experienced in berm cores where water was added to reach a target maximum VWC of 0.15 $cm^{3c}m^{-3}$ and 0.25 cm^3cm^{-3}.

4.3.4 Labile C pool:

The labile C pool in fresh soils collected from berm and furrow during intact soil core collection was on average 582 ± 26 mg POXC g^{-1} soil in berm soils (n = 10) and 569

± 67 mg POXC g^{-1} soil on average in furrow soils (n = 10) (Figure 4.4), with no significant difference between the two soils. After the soils were subjected to low-volume irrigation, the labile C pool in berm soil cores (average of 1,019 ± 42 mg POXC g^{-1} soil) was significantly higher than furrow soil cores ($p < 0.01$). The berm soil core labile C concentration after low-volume irrigation was also significantly higher than berm soils from the field ($p < 0.01$). The furrow soils taken from the field had a slightly increased average labile C pool of about 612 ± 49 mg POXC g^{-1} soil after simulated irrigation as compared to furrow soils from the field, but the change in concentration was not statistically significant ($p > 0.05$).

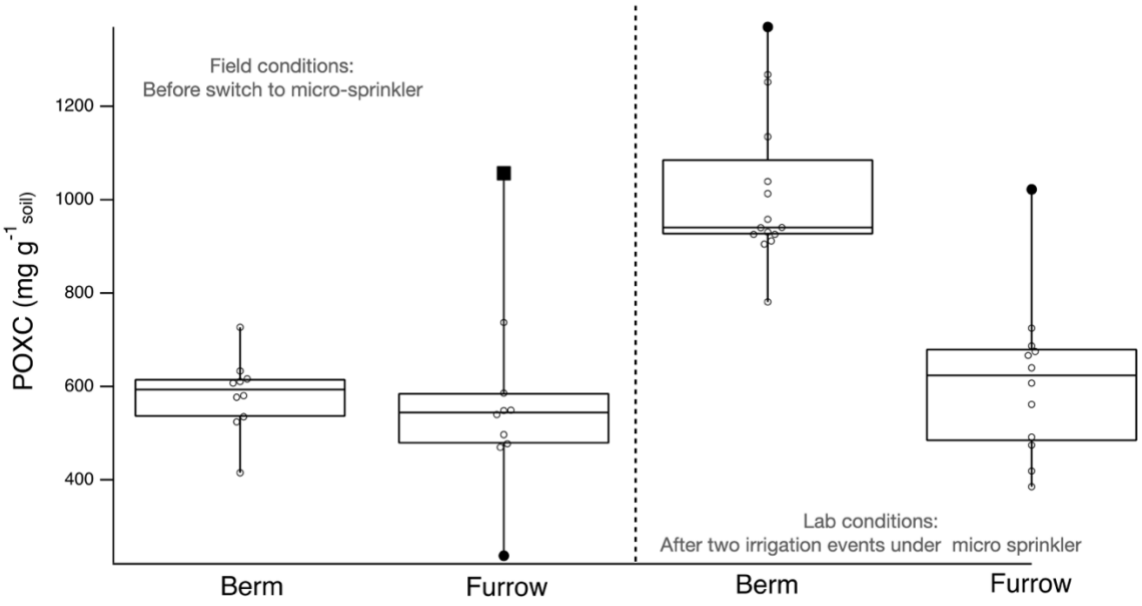

Figure 4.8: Labile C concentrations in soils before and after imposing low-volume irrigation simulating microsprinkler irrigation on originally furrow-irrigated berm and furrow soils. (Left) Berm and furrow soils were collected from the field at the time of the intact core sampling and POXC analysis was performed on air-dried and homogenized samples (n=10). (Right) Post ex-situ experiment conditions: triplicate subsamples were taken from each core (berm n=5, furrow n=4) after they had been subjected to the two irrigation events (simulation #1, target VWC of 0.15 $cm^3\ cm^{-3}$) and POXC analysis was completed on homogenized air-dried soils.

4.3.5 Substrate Quality

To examine changes in speciation of C substrates likely accessed by microbes before and after microsprinkler irrigation simulation, water extractable C from cores were derivatized and characterized using EI/GC-MS. Our results show that the majority of water extractable hydroxyl-containing C compounds in furrow soils prior to irrigation simulations did not classify into typical soil C compound categories (e.g., carbohydrates, lipids, lignins), and instead contain C of relatively higher nominal oxidation state (NOSC) than compounds that compose the rest of the species in the water extractable fraction (Figure 4.5). The second most abundant class of C compounds in furrow soil water extracts prior to the *ex situ* experiment were lipids and some contribution of carbohydrates. After microsprinkler simulation was imposed on furrow soil cores, the most dominant substrate shifted to lipids, with the second most abundant species being carbohydrates. In contrast, water extractable C pool in berm soils was dominated by lipids with the second most abundant class of compounds composed of high nominal oxidation state with H:C ratios more closely resembling hydrogenated amino sugars (Sleighter and Hatcher, 2007). After microsprinkler irrigation was imposed on berm soil cores, lipids became the second most abundant compound class while the most abundant class was composed of high NOSC compounds. Water extracts from berm soils after microsprinkler irrigation simulations was the only treatment where proteins were abundant enough to be detected.

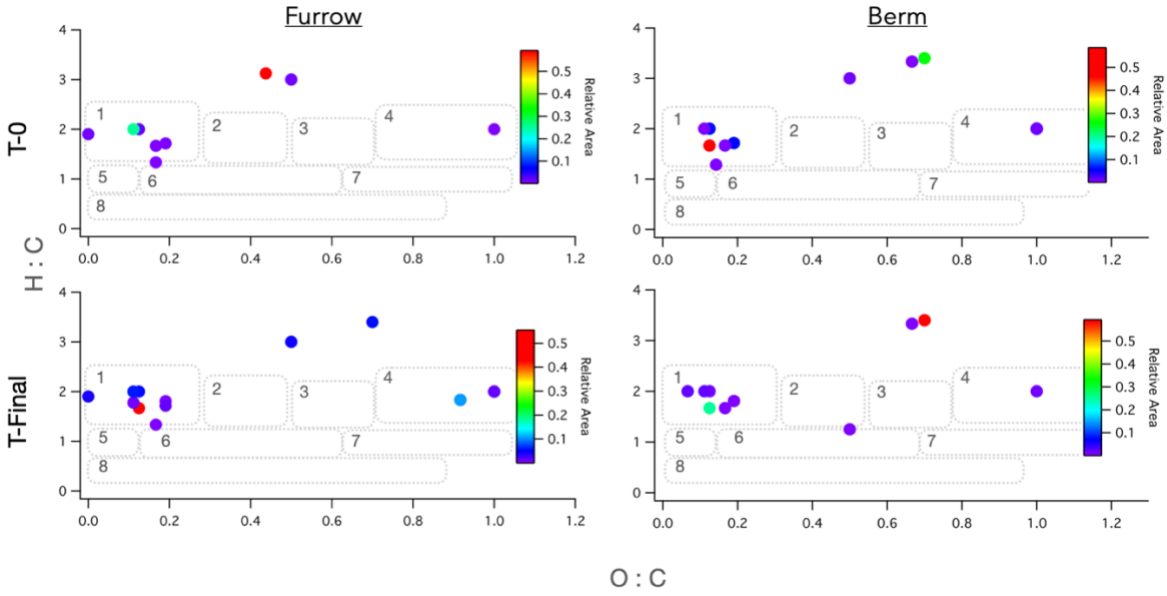

Figure 4.5: The van Krevelen diagram of the water extractable C compounds identified via GC/MS from before (T-0: field samples) (n = 3) and after (T-Final: intact cores) the irrigation switch (n = 3). Only compounds that were present in each of the replicates were included and the average percent abundance of that compound is denoted by the color scale. Compounds identified are plotted with typical C compound classes 1) Lipids, 2) Proteins 3) Amino sugars 4) Carbohydrates 5) Uncondensed hydrocarbons 6) Lignin 7) Tannins 8) Condensed hydrocarbons. Compounds with higher O:C and H:C are of higher nominal oxidation state of C.

4.4 Discussion

4.4.1 Soil CO_2 flux dynamics after shift from furrow to sprinkler irrigation

We expected that imposing microsprinkler irrigation on berm soils would increase soil VWC leading to corresponding increase in CO_2 flux. We hypothesized that a higher VWC would provide greater pore connectivity between microbes and C substrates for respiration as compared to under drier field conditions. Berm soils typically receive more litter and plant inputs leading to subsequent accumulation of readily respirable C substrates because limited water decreases overall rate of biogeochemical processes including microbial respiration (Jenerette and Chatterjee, 2012), along with inhibited C and microbial transport through soil matrices (Zachara et al., 2016). Correspondingly, we expected that

previously furrowed soils that became relatively drier with microsprinkler irrigation (decrease in 0.10 cm^3 cm^{-3}) would have suppressed CO_2 flux compared to berm soils due to less carbon inputs overall and also greater selectivity in C compounds metabolized by microbes due to extreme wetting and drying conditions in furrows. Instead, results from the first simulated irrigation experiment where berm soil VWC was raised from dried (0.035 cm^3 cm^{-3}) to microsprinkler irrigated conditions (0.13 cm^3 cm^{-3}) berm soils exhibited a lower maximum CO_2 flux after irrigation events than flux from furrow soils. In a previous study, berm soils with VWC of 0.02 cm^3 cm^{-3} after an extended dry season were wet-up *in situ* with distilled water to a final VWC of 0.15 cm^3 cm^{-3}; the resultant CO_2 flux from berm soils increased by 11 times compared to flux prior to the wet-up treatment (Figure A3.3). The reason for the significantly higher increase in berm soil CO_2 flux in the field is likely because of the time over which water was applied: in the field experiment, a large volume of water was added within seconds to raise the VWC to 0.15 cm^3cm^{-3}; whereas water was added slowly over a 48-hour period in the *ex situ* intact core experiments. The slower rate of water addition in micro-sprinkler irrigated soil may prevent slaking processes that can occur when there are sudden and large increases in soil VWC. Therefore, lower flux in ex situ cores maybe due to C in soil aggregates remaining protected from microbial degradation or could have allowed for preferential flow paths that prevented a sudden release of C as CO_2.

4.4.2 CO_2 flux is water limited in berm soils

Due to the berm soil exhibiting lower C flux with VWC simulated microsprinkler levels compared to flux from furrow soils (which was contrary to our original hypothesis), we further hypothesized that the VWC simulating microsprinkler irrigation could still lead to limited pore connectivity within the soil matrix, which prevented microbial communities from reaching C substrates for respiration. To test our revised hypothesis, the core experiment was repeated using un-dried berm soil cores with two VWC imposed including one treatment with 66% greater VWC compared to microsprinkler-irrigated field conditions. The berm soils cores for this second experiment were collected in November 2019, which corresponds to when berm soils have undergone a much longer dry period compared to cores extracted for the first experiment, which were collected in mid-summer (July 2019). Carbon substrate accumulation in the berm soils is not consistent temporally and is greatest before seasonal rains commence. This likely explains why the individual cores of each replicate set exhibited differing CO_2 flux dynamics. Instead, the higher volume simulation (0.25 cm^3 cm^{-3}) likely facilitated soil pore connectivity between microbes and their C substrates to the extent that C mineralization continued for an extended time post-irrigation. These findings overall show that both low volume and slow rate of water application can limit C flux.

4.4.3 Porewater C substrates accessed by microbial communities under low-volume irrigation

Aside from physical separation of microbes from their C substrates contributing to limited C flux from microbial respiration, certain classes of organic substrates are

chemically more energetically favorable than others for aerobic and anerobic respiration (Jin and Bethke, 2005). By assessing the size of the active C pool pre-and post-microsprinkler simulation, our results show there is a significant increase in the size of active C pool in berm soils after one microsprinkler simulated irrigation, but then CO_2 flux response is decreased after two irrigation events. By comparing water extractable fraction of dissolved carbon from the berm and furrow soils prior to simulated irrigation, the C substrate composition in furrow soils shows a greater abundance of compounds with high NOSC. This suggests that the relatively higher CO_2 flux exhibited in the furrow is not due to the higher amount of labile C but may instead be due to higher abundance of thermodynamically favorable C substrates available in pore water. After applying microsprinkler irrigation, the dominant substrate class in furrow soil core pore water is lipids, which have a relatively low NOSC and are expected to be preserved under anerobic conditions in soils (Keiluweit et al., 2016). The furrow soils, which are frequently inundated, are likely to harbor ample anaerobic microsites where these low NOSC C substrates can be preserved. It should be noted that because the soil was homogenized to extract and characterize water-soluble C compounds and were also first derivatized, the species identified represents all possible hydroxyl-containing compounds potentially accessed by microbes without considering the role of soil structural heterogeneity. Additionally, because both samples prior to irrigation simulation (T-0) and core samples post-simulation (T-final) were homogenized, and yet C speciation shows that the composition of dominant compounds shifted to different classes for both berm and furrow

soils, it demonstrates that the change in C composition is due to the low volume irrigation treatment rather than just due to physical protection.

4.4.4 Assumptions, limitations, and future directions

There are a variety of assumptions made in this study that constrain the extent to which our findings can be applied to soils that undergo biogeochemical changes after a shift to low volume irrigation application. First, we assumed that the intact soil cores extracted from the field maintain comparable values for master variables controlling C flux and pore water chemistry to be representative of field soil characteristics. Previous studies have shown paired *in situ* and *ex situ* soil respiration experiments may not be comparable (Davidson et al., 1998). Studies that compare gas flux from multiple soils often homogenize samples to remove the contribution of variation in soil aggregation, presence of roots, and plant residue to variations in gas flux (Baveye et al., 2018; McGowen et al., 2018; Thomson et al., 2010). In this study, we elected to use intact soil cores to more accurately capture the role of soil structure on C dynamics as soil moisture changes (Hangs et al., 2016; Meyer et al., 2019). However, C substrate compositional analysis was performed on water extractable C, as opposed to porewater samples due to the low VWC of the microsprinkler simulation. Previous work characterizing compositional diversity of soluble C species as a function of pore diameters showed that more complex C compounds (i.e., aromatic and condensed) are associated with finer pore throats (~20 μm diameter), while larger pore domains (~200 μm) are dominated by lipids, proteins, and carbohydrates (Bailey et al., 2017). By homogenizing the soils, the analysis may overestimate the

presence of more complex C compounds, that are typically harbored within fine pores while underestimating the relative abundance of other compounds that are accessible to microbial communities.

4.4.5 Management considerations when switching irrigation methods

It is estimated that furrow irrigated soils on average utilize approximately 65% of the total volume of water that is applied to meet crop needs, while micro-sprinkler irrigated soils have an average application efficiency of 85%, with efficiency estimates of up to 95% if appropriate measures are taken to minimize water loss (Howell, 2003). Although limited water resources may be alleviated by switching to lower volume irrigation methods, there are a variety of economic and operational reasons why a grower may decide against making the switch to precision irrigation. The first drawback of implementing micro-sprinkler irrigation is the upfront capital costs and maintenance needed to successfully irrigate large plots of land (Evans, 2010). Micro-sprinkler systems also require filtration of the inflow irrigation water to prevent salt and sediment build up in distribution systems and irrigation lines. Additionally, micro-sprinkler and other precision irrigation systems require acquisition and maintenance of a pumping system which can be particularly difficult to maintain in arid regions where salt accumulation is prevalent. In contrast, furrow irrigation only requires a graded field to allow water to flow down a trench which requires no pumping. Further, furrow and other gravity irrigation methods use large volumes of water that can dissolve and “flush” salts as a low maintenance solution to sodicity and salinity issues. The salt content of available irrigation water sources and the installation,

maintenance, and pumping costs must also be carefully considered with precision irrigation systems. Nevertheless, this study demonstrates that more studies are needed to thoroughly understand the cost-benefit of adopting low-volume irrigation systems with increased C flux (loss) as a "cost" consideration. Furthermore, our study demonstrates that C substrates accessible to microbial communities can shift dramatically with change in irrigation, which can either enhance or inhibit microbial respiration; further investigation is needed to examine how consistent the shift in C chemistry seen in this study are in other agricultural systems, climates, and soil types.

4.5 Conclusions

Orchard crop systems are frequently switched from gravity-driven irrigation, such as furrow irrigation, to micro-sprinkler irrigation due to the water saving benefits. The biogeochemical landscape of a furrow-irrigated field would be reshaped by this change, where the low volume of water applied could reduce surface losses but has the potential to catalyze dramatic shifts in the C sequestering capacity of soils. By conducting a set of *ex situ* precision irrigation simulations on soils taken from a furrow-irrigated orchard, we found that CO_2 flux is most different between soils of contrasting rewetting history after one irrigation event. A large release of C in soils that are only seasonally wet up was not observed, likely due to low pore connectivity. However, the C substrate quality of pore water from seasonally dry soils do shift to more energetically favorable substrates after low volume irrigation methods are adopted, suggesting that the gaseous release of C could be greater over time.

4.6 References

Bailey, V.L., Smith, A.P., Tfaily, M., Fansler, S.J., and Bond-Lamberty, B. (2017). Differences in soluble organic carbon chemistry in pore waters sampled from different pore size domains. Soil Biol. Biochem. *107*, 133–143.

Baveye, P.C., Otten, W., Kravchenko, A., Balseiro-Romero, M., Beckers, É., Chalhoub, M., Darnault, C., Eickhorst, T., Garnier, P., Hapca, S., et al. (2018). Emergent Properties of Microbial Activity in Heterogeneous Soil Microenvironments: Different Research Approaches Are Slowly Converging, Yet Major Challenges Remain. Front. Microbiol. *9*.

California Department of Water Resources (2020). Agricultural Water Use Efficiency.

California Natural Resources Agency (2021). Report to the Legislature on the 2012-2016 Drought.

Culman, S.W., Snapp, S.S., Freeman, M.A., Schipanski, M.E., Beniston, J., Lal, R., Drinkwater, L.E., Franzluebbers, A.J., Glover, J.D., Grandy, A.S., et al. (2012). Permanganate Oxidizable Carbon Reflects a Processed Soil Fraction that is Sensitive to Management. Soil Sci. Soc. Am. J. *76*, 494–504.

Dai, A. (2013). Increasing drought under global warming in observations and models. Nat. Clim. Change *3*, 52–58.

Davidson, E.A., Belk, E., and Boone, R.D. (1998). Soil water content and temperature as independent or confounded factors controlling soil respiration in a temperate mixed hardwood forest. Glob. Change Biol. *4*, 217–227.

Evans, R.G. (2010). Irrigation Technologies Comparisons (US Department of Agriculture).

Hangs, R.D., Ahmed, H.P., and Schoenau, J.J. (2016). Influence of Willow Biochar Amendment on Soil Nitrogen Availability and Greenhouse Gas Production in Two Fertilized Temperate Prairie Soils. BioEnergy Res. *9*, 157–171.

Howell, T. (2003). Irrigation Efficiency. Encycl. Water Sci.

Howitt, R., MacEwan, D., Medellín-Azuara, J., Lund, J., and Sumner, D. (2015). Economic Analysis of the 2015 Drought For California Agriculture. 31.

Jenerette, G.D., and Chatterjee, A. (2012). Soil metabolic pulses: water, substrate, and biological regulation. Ecology *93*, 959–966.

Jin, Q., and Bethke, C.M. (2005). Predicting the rate of microbial respiration in geochemical environments. Geochim. Cosmochim. Acta *69*, 1133–1143.

Keiluweit, M., Nico, P.S., Kleber, M., and Fendorf, S. (2016). Are oxygen limitations under recognized regulators of organic carbon turnover in upland soils? Biogeochemistry *127*, 157–171.

Marvel, K., Cook, B.I., Bonfils, C.J.W., Durack, P.J., Smerdon, J.E., and Williams, A.P. (2019). Twentieth-century hydroclimate changes consistent with human influence. Nature *569*, 59–65.

McGowen, E.B., Sharma, S., Deng, S., Zhang, H., and Warren, J.G. (2018). An Automated Laboratory Method for Measuring CO2 Emissions from Soils. Agric. Environ. Lett. *3*, 180008.

Meyer, N., Welp, G., and Amelung, W. (2019). Effect of sieving and sample storage on soil respiration and its temperature sensitivity (Q10) in mineral soils from Germany. Biol. Fertil. Soils *55*, 825–832.

Pulleman, M., Wills, S., Creamer, R., Dick, R., Ferguson, R., Hooper, D., Williams, C., and Margenot, A.J. (2021). Soil mass and grind size used for sample homogenization strongly affect permanganate-oxidizable carbon (POXC) values, with implications for its use as a national soil health indicator. Geoderma *383*, 114742.

Schwankl, L., Prichard, T., Hanson, B., and Wellman, I. (1999). Costs of pressurized orchard irrigation vary with system design. Calif. Agric. *53*, 14–20.

Sleighter, R.L., and Hatcher, P.G. (2007). The application of electrospray ionization coupled to ultrahigh resolution mass spectrometry for the molecular characterization of natural organic matter. J. Mass Spectrom. *42*, 559–574.

Thomson, B.C., Ostle, N.J., McNamara, N.P., Whiteley, A.S., and Griffiths, R.I. (2010). Effects of sieving, drying and rewetting upon soil bacterial community structure and respiration rates. J. Microbiol. Methods *83*, 69–73.

Tindula, G.N., Orang, M.N., and Snyder, R.L. (2013). Survey of Irrigation Methods in California in 2010. J. Irrig. Drain. Eng. *139*, 233–238.

Wade, J., Maltais-Landry, G., Lucas, D.E., Bongiorno, G., Bowles, T.M., Calderón, F.J., Culman, S.W., Daughtridge, R., Ernakovich, J.G., Fonte, S.J., et al. (2020). Assessing the sensitivity and repeatability of permanganate oxidizable carbon as a soil health metric: An interlab comparison across soils. Geoderma *366*, 114235.

Zachara, J., Brantley, S., Chorover, J., Ewing, R., Kerisit, S., Liu, C., Perfect, E., Rother, G., and Stack, A.G. (2016). Internal Domains of Natural Porous Media Revealed: Critical Locations for Transport, Storage, and Chemical Reaction. Environ. Sci. Technol. *50*, 2811–2829.

Chapter 5: Conclusions

5.0 Overview

The previous three chapters provided an in-depth investigation to understand how soil moisture regimes imposed by irrigation and alterations in irrigation method can change soil C dynamics and by first taking a systems level approach, followed by investigating the spatiotemporal variation of soil C pools, and then by using these approaches to decipher how soil C inputs and outputs can change with a shift to low-volume irrigation to adapt to limited and uncertain water resources. The following are conclusions and recommendations based on the findings reported in the Chapters.

5.1 Systems approach to understanding soil C dynamics

Landscape level CO_2 flux monitoring alone does not capture the heterogeneity of furrow irrigated soils, which can only provide limited mechanistic understanding of C transformations in agricultural soils with heterogeneous soil moisture conditions. In the previous Chapters, we were able to further untangle the factors that contribute the magnitude of C release. First, we found that repeated water fluctuations in furrow soils create conditions that vastly limit C release, largely due to low oxygen availability which limits microbial respiration. Due to the redox fluctuations imposed upon the furrow soils, more complex C compounds were associated with minerals than relatively more aerated soils of the berm, establishing a more stable sequestering mechanism. In berm soils, however, C loss as CO_2 flux from soil was much more limited by pore connectivity, where microbial communities capable of using the accumulated C substrates were less selective,

leading to the degradation of both complex and simple organic compounds whenever water is available. While these studies focused on C dynamics, it is important to also consider that other biogeochemical cycles are simultaneously occurring in these soils which are also influenced by the varied soil moisture. Therefore, while furrow soils are capable of sequestering C due to lower redox conditions from inundation during irrigation events, these fluctuations may also create other GHG emissive sources, where nitrogen can be released to the atmosphere.

5.2 Importance of spatiotemporal variation in soil C

Mediterranean climates are defined by mild, wet winters and hot, dry summers when soil moisture can be extremely low, but when irrigation water is available, Mediterranean ecosystems can be very productive agricultural areas. Although the soil moisture regimes imposed by irrigation control soil C dynamics, it is important to consider the seasonal changes that occur in these regions can have distinct effects on various C pools. The berm soils, where C inputs are highest in a furrow-irrigated landscape, accumulate C substrate throughout the year; however, our findings show that labile C pools are increased at the onset of seasonal rains due to microbial death and then sustained by weed growth in the wet season. Seasonal effects in the short-lived C pool had a greater influence in the berm; however, furrow soils were also subject to seasonality, especially if seasonal rain events were large enough to maintain anoxic conditions, which decreases decomposition rates and potential. While this study was focused on one field site, the study

provides greater detail of the expected variation in C pools in a heterogenous landscape that is currently necessary for ecological modeling, especially in tree crop systems.

5.3 Switching irrigation method has the potential for altered C dynamics

The last study provided a first glance at the potential changes that can occur if furrow irrigated soils in this region are switched to microsprinkler irrigation. We found that the uniform application of water resulted in comparable flux between regions of distinct rewetting history (i.e. berm versus furrow soils). However, due to the greater C inputs accumulated under the tree line (berm), the species of C compounds that are being respired are more labile and energetically favorable. But because water is slowly applied in microsprinkler irrigation, CO_2 flux was not as dramatically increased at the onset of the new irrigation strategy as expected. This suggests that berm soils that typically exhibit a large magnitude pulse release of labile C seasonally, could have lower C losses over the course of a year under microsprinkler irrigation. However, the relatively more oxic conditions of previously furrowed soil that are shifted to microsprinkler irrigated could begin to release C that was previously stabilized. Our results demonstrate that soil C flux and pore water dynamics is altered as low-volume irrigation is applied revealing the multi-dimensional biogeochemical impact of shifting irrigation management that needs to be explored further.

Appendix 1: Appendix to A multi-phase approach to characterizing carbon dynamics as a function of soil moisture within a semi-arid furrow irrigated orchard

A1.1 Determining K_{sat} using Darcy's Law

Soil from the berm and furrow (0 - 10 cm) were placed in columns [cross sectional area A, (cm^2), height of soil ΔX (cm^2)] sealed on the bottom side with cheesecloth and saturated by capillary rise in triplicate. Water was then added to a specific height (ΔH) and maintained for the remainder of the measurement. Outflow water was collected [volume of water V, (cm^3)] for 30 min [t (hr)] to calculate K_{sat} (cm/hr).

$$Q = V \times A \times t = K_{sat} \times \frac{\Delta H}{\Delta X} \quad \text{(A1.1)}$$

A1.2 Long term soil moisture and temperature

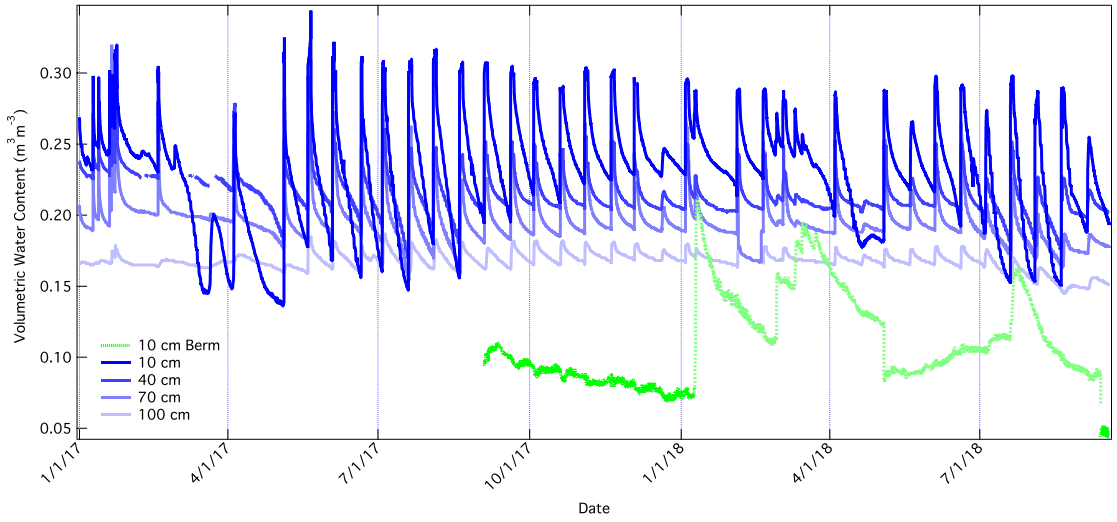

Figure A1.2. Volumetric water content and soil temperature at 10, 40, 70, and 100 cm within furrow and berm soils from Jan 2017 to Jan 2019.

A1.3 Total C and $\delta^{13}C$: Annual Average

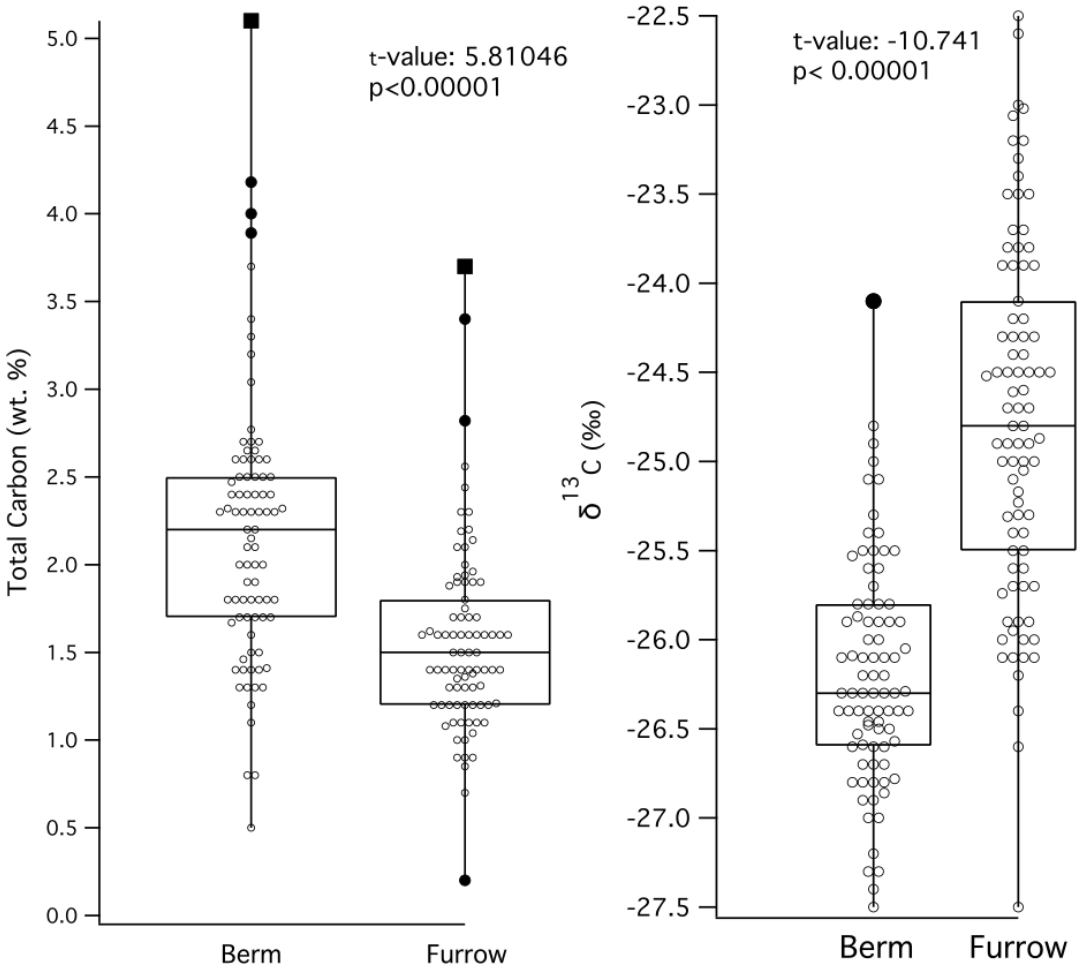

Figure A1.3. Total C (left) and $\delta^{13}C$ (right) content of berm and furrow soils. Surface soil samples (0 – 10 cm) were taken twice a month for 12 months for a total of 85 samples. Open circle symbols represent individual sample measurements. Closed circles denote outliers, and closed squares denote far outliers.

A1.4 Total N and $\delta^{15}N$: Annual Average

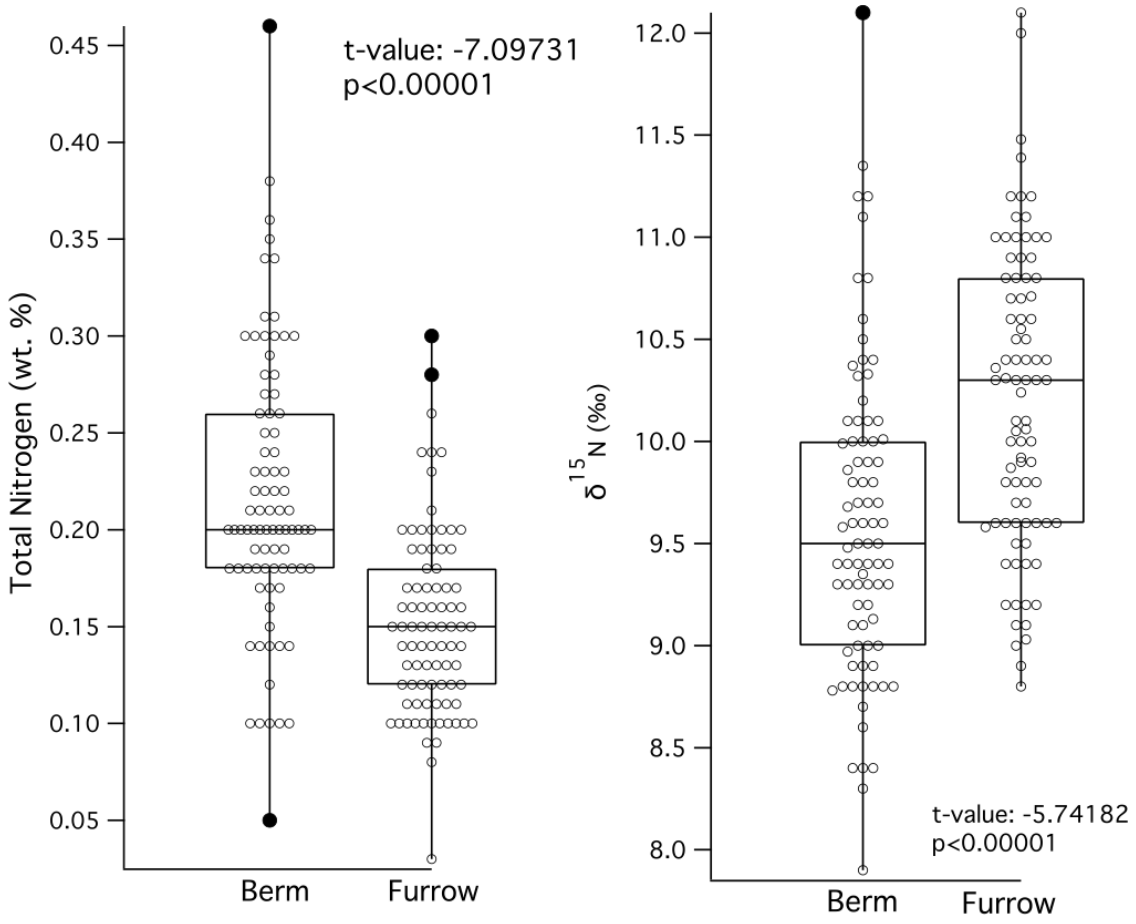

Figure A1.4 Total N (left) and $\delta^{15}N$ (right) content of berm and furrow soils. Surface soil samples (0 – 10 cm) were taken twice a month for 12 months for a total of 85 samples in each location. Open circle symbols represent individual sample measurements while closed circles denote outliers.

A1.5 Bulk and heavy density metal concentration

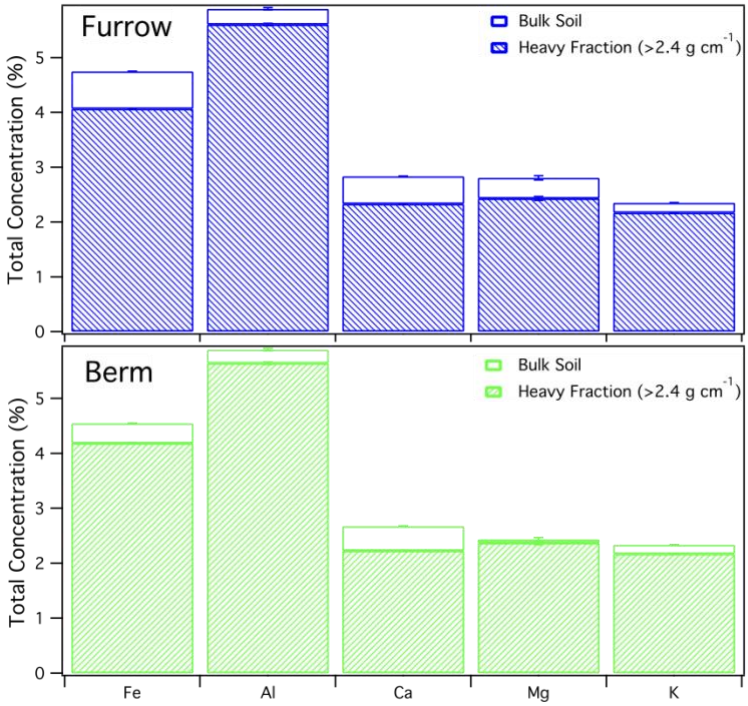

Figure A1.5. Total elemental composition determined by ED-XRF of furrow (top) and berm (bottom) soils (0 – 10 cm) in bulk soils and in the heavy fraction (> 2.4 g cm-1) after density fractionation. Triplicate samples were analyzed from bulk and heavy fractions; average values are presented along with standard error displayed with error bars.

A1.6 Water stable aggregate fraction isotopes

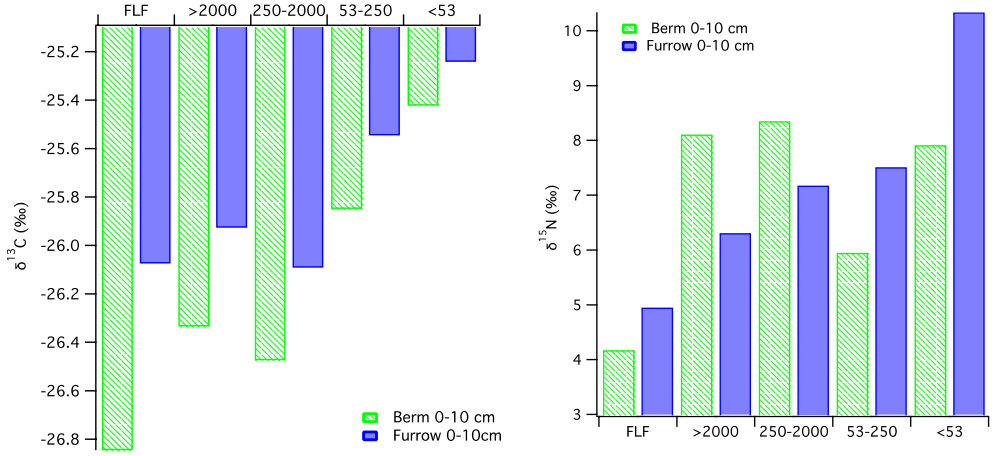

Figure A1.6. The measured values for $\delta^{13}C$ (left) and $\delta^{15}N$ (right) of the water stable aggregate fractions of the berm and furrow (0-10 cm) soils.

A1.7 Method for determining particle size analysis

Particle size analysis (PSA) was conducted via a laser diffraction type granulometer with polarization intensity differential scattering. [where samples were taken from/etc.] Organic matter was first removed in preparation for analysis by exposing approximately 0.5 cm^3 of soil, measured using a truncated plastic syringe, to 20 mL of hydrogen peroxide (30%) and left to soak for 24 hours. After the initial soaking period, the samples with H_2O_2 were heated to a temperature of < 70° C in the fume hood until the solution remaining was < 5 mL. Large, visible organics were removed, and water was added to suspend any remaining organics, if present, then heated once more until < 5 mL of solution remained. After organics were removed, we deflocculated the samples by adding 0.1 g of sodium hexametaphosphate to a clean 20 mL scintillation vial with the evaporated samples, spraying the beaker with DI water to ensure transfer off all soil into the final scintillation vial, leaving a small headspace, and placing them on a shaker for 24 hours. Once prepared, the samples were analyzed by pouring each sample solution into the reservoir of a Beckman-Coulter LS 13-320 (Beckman Coulter Inc., Fullerton, CA, USA). The output PSA data statistics was calculated using GRADISTAT and were then binned following the USDA textural classification system for % sand (0.05 – 2.0 mm), silt (0.002-0.05 mm), and clay (< 0.002 mm).

Appendix 2: Appendix to seasonality effects on soil carbon pools in wet-dry and dry zones of furrow irrigated soils

A2.1 Annual average elemental composition of furrow and berm (0-10 cm)

Table A2.1: Average annual elemental composition of soils from berm (0 - 10 cm) and furrow (0 – 10 cm)

	CO_3^{2-}	Mg	Fe	Al	Si	Ca	P	S
Unit	ppm	%	%	%	%	%	%	ppm
Berm (0-10 cm)	159.7 (8.9)§	2.18 (0.02)*	4.36 (0.01)*	5.27 (0.03)*	21.38 (0.09)*	2.86 (0.02)	0.18 (0.004)	1142.3 (67.4)*
Furrow (0-10 cm)	239.3 (47)§	2.48 (0.03)*	4.43 (0.03)*	5.51 (0.04)*	21.97 (0.13)*	2.86 (0.02)	0.17 (0.003)	890.1 (36.5)*

* Significantly different at p <0.01. Values in parentheses indicated the standard error of the mean. §Sample size too small for statistical comparison

A2.2 Drone images of field site

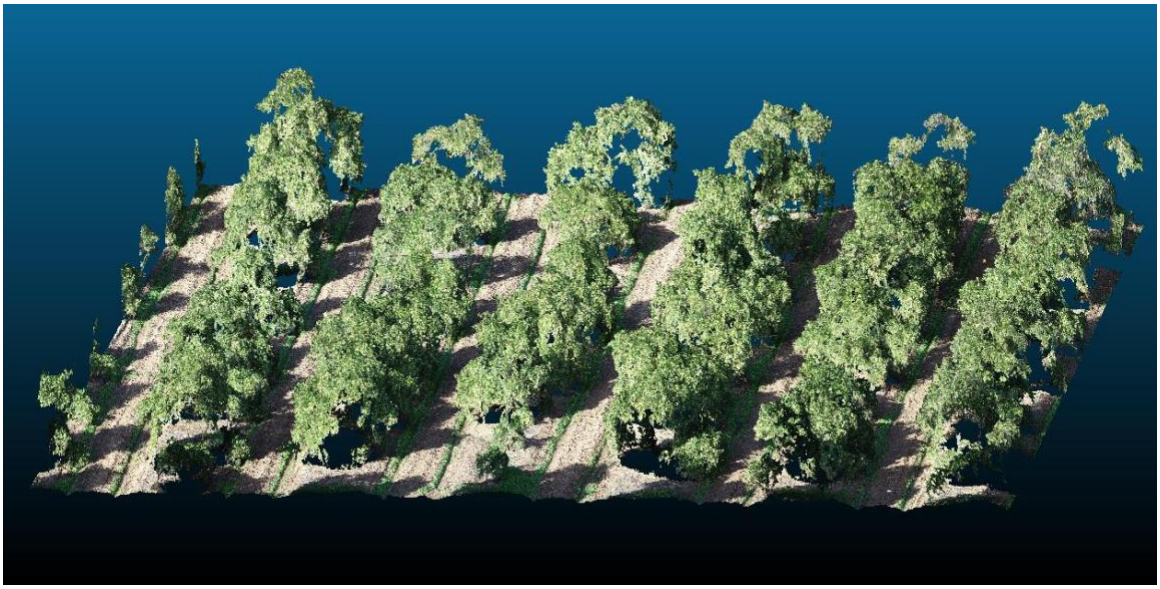

Figure A2.2.1: Drone image (North to West) of a small sample area of the entire field site. Drone flight imagery was taken on 12/4/18 in the wet season just before furrow was tilled to remove weed growth.

Figure A.2.2.2 Drone image (view to Southeast) of a small sample area of the entire field site. Drone flight imagery was taken on 12/4/18 in the wet season just before furrow was tilled to remove weed growth.

Figure A2.2.3: Drone image (view to North) of the entire orchard. Drone flight imagery was taken on 12/4/18 in the wet season just before furrow was tilled to remove weed growth.

A2.3 Annual trends (Z-score) of furrow and berm (0-10 cm)

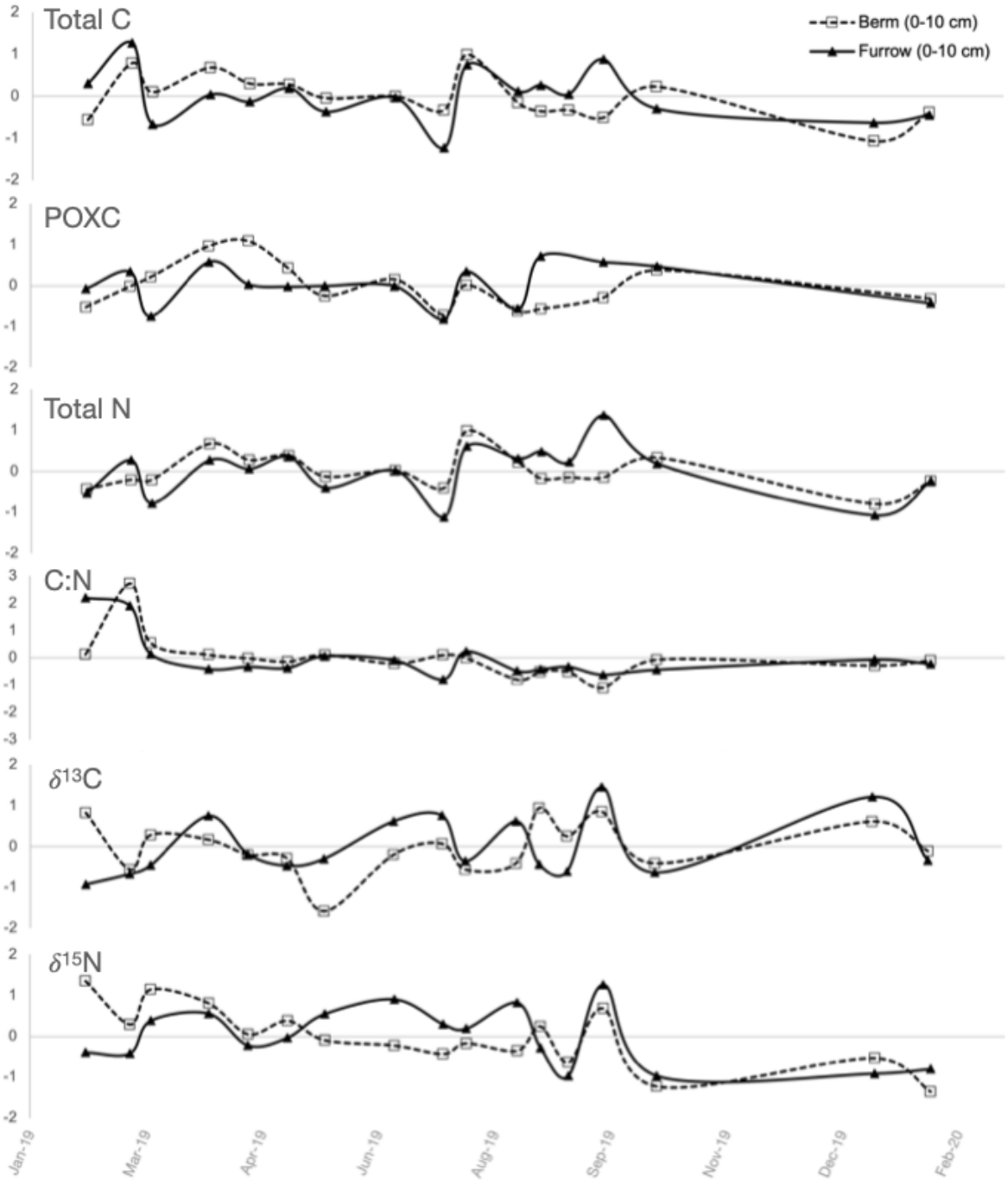

Figure A2.3: The standardized trends by the annual mean, where 0 is the mean annual average and positive values represent an increase in that time points average, where 1 is 1 standard deviation from the annual mean.

A2.4 POXC deviation from the annual mean

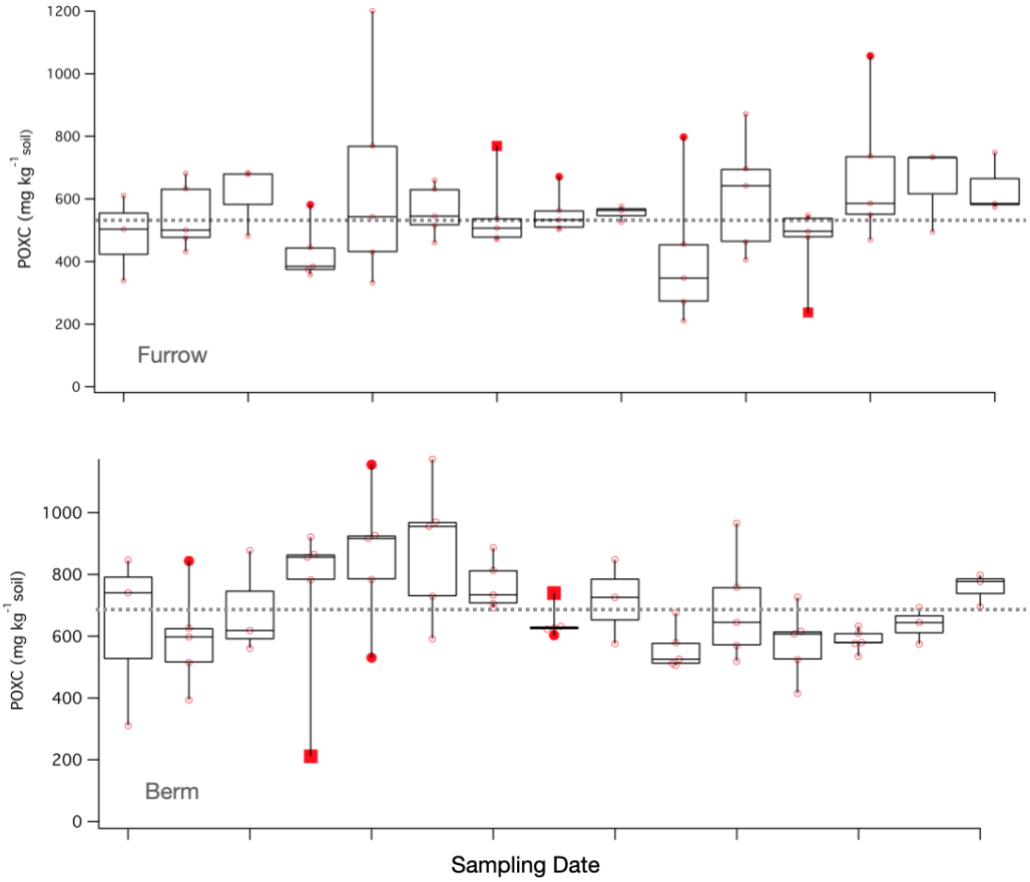

Figure A2.4: Box plots of the measured spread in POXC in the furrow (TOP) and berm (BOTTOM). The dotted line is the measured annual average, and the individual boxes are listed by date, however sampling time points were not equally spaced but are listed in order of date from left to right.

Appendix 3: Appendix to Gas Flux Changes Brought on by Shifting Irrigation Strategy in a Legacy Furrow Irrigated Soil

A3.1 Schematic of intact soil cores experiment

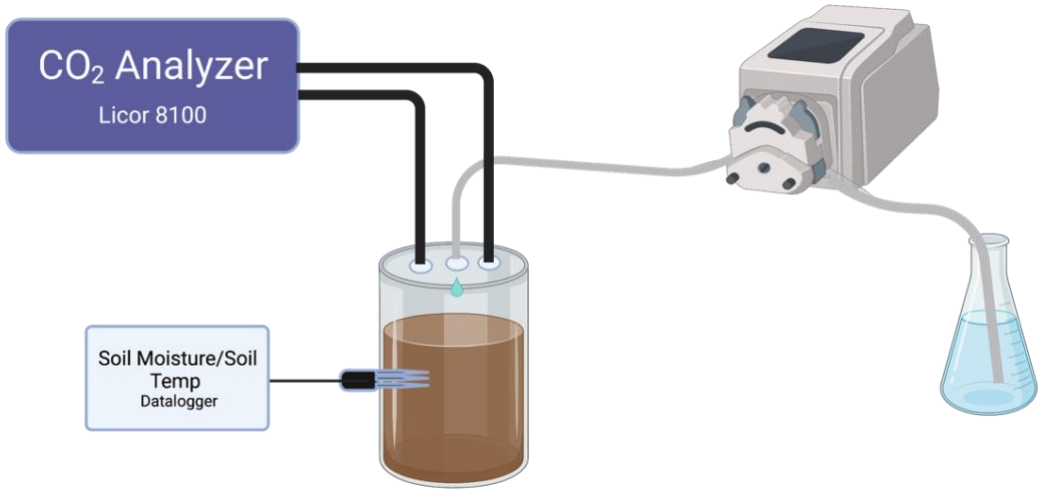

Figure A3.1: The general schematic of the intact soil cores and the simulated irrigation done in the lab. Please note, a transparent visual was used to show where the soil moisture sensors were placed, however, white PVC tubing with drain caps were utilized.

A3.2 Soil moisture comparison between furrow and berm (10 cm depth)

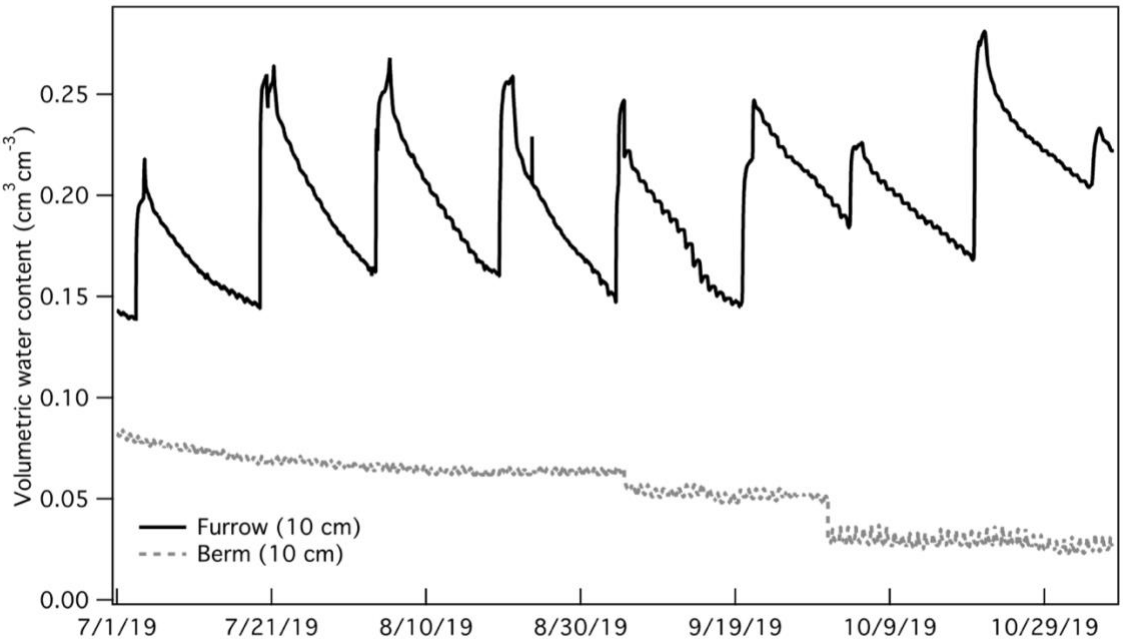

Figure A3.2: The soil moisture trends in the furrow and berm in the field. Data shown are averages (n=3) of sensors are a depth of 10 cm within the berm and furrow. Intact cores were taken in July 2019 for the first set of experiments and in November 2019 for the second.

A3.3 Wet-up experiment in berm soils in the field

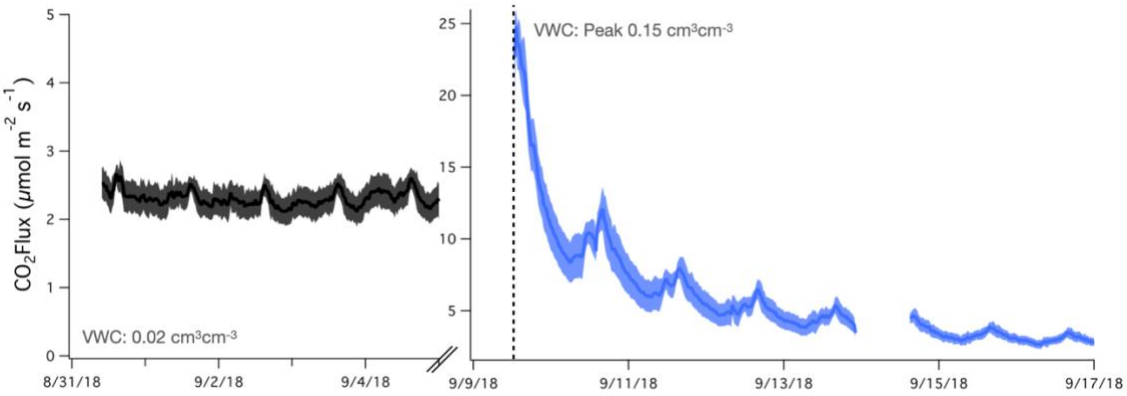

Figure A3.3: An in-situ wet up experiment at the furrow irrigated field site within the berm. (Left) The CO_2 flux of triplicate soil respiration chambers when berm soils are dry (0.02 cm^3cm^{-3}). (Right) The CO_2 flux of the same soil after water was manually added to each soil collar to reach a VWC of 0.15 cm^3cm^{-3}) which resulted in a 11 times greater magnitude flux.